STEREOTACTIC BODY RADIATION THERAPY FOR LIVER TUMORS

Alejandra Méndez Romero

ISBN: 978-94-6169-017-3

Layout and print: Optima Grafische Communicatie, Rotterdam

Cover design: Juan Manuel Abelleira Ronqete (photo: Cabo Vilán), Henrie van der Est, and Hans Joosten.

Copyright © 2011 by A. Méndez Romero. All rights reserved. No part of this book may be reproduced, stored in a retrieval system or transmitted in any form or by any means, without prior permission of the author.

The publication of this thesis was financially supported by Accuray.

STEROTACTIC BODY RADIATION THERAPY FOR LIVER TUMORS

Stereotactische radiotherapie voor lever tumoren

Proefschrift

ter verkrijging van de graad van doctor aan de
Erasmus Universiteit Rotterdam
op gezag van de
rector magnificus
Prof.dr. H.G. Schmidt
en volgens besluit van het College voor Promoties.
De openbare verdedigen zal plaatsvinden op
vrijdag 4 maart 2011 om 11:00 uur

door

Alejandra María Méndez Romero

geboren te Melide (La Coruña), Spanje

ERASMUS UNIVERSITEIT ROTTERDAM

PROMOTIECOMMISSIE

Promotoren:	Prof.dr. P.C. Levendag
	Prof.dr. B.J.M. Heijmen
Overige leden:	Prof.dr. J.L.C.M. van Saase
	Prof.dr. M. Høyer
	Prof.dr. L.A. Dawson
Copromotor:	Dr. C. Verhoef

Para Rob, mis padres y mis hermanos, Cris y Tono
Para mis padrinos Faustino y Anuncia y mis tios, Gemma, Rolando y Maruxa
Aan mijn patiënten en hun families

CONTENTS

Chapter 1	Introduction	*9*
Chapter 2	Stereotactic body radiation therapy for primary and metastatic liver tumors: A single institution phase I-II study	*19*
Chapter 3	Quality of life after stereotactic body radiation therapy for primary and metastatic liver tumors	*33*
Chapter 4	Computer optimization of noncoplanar beam setups improves stereotactic treatment of liver tumors	*45*
Chapter 5	Stereotactic body radiation therapy for liver tumors: impact of daily setup corrections and day-to-day anatomic variations on dose in target and organs at risk	*63*
Chapter 6	Stereotactic body radiation therapy for colorectal liver metastases	*81*
Chapter 7	Comparison of macroscopic pathology measurements with magnetic resonance imaging and assessment of microscopic pathology extension for colorectal liver metastases	*93*
Chapter 8	General discussion and future directions	*111*
Chapter 9	Summary / Samenvatting	*125*
List of publications		*131*
Acknowledgements		*133*
Curriculum vitae		*137*
PhD Portfolio Summary		*139*

1

INTRODUCTION

INTRODUCTION

Treatment options for liver metastases

As a common deposit for tumor cells, the liver is second only to the lymph nodes as a site of metastatic disease (1, 2). Unfortunately, by the time patients present with liver metastases there is usually evidence of the systemic spread of the disease, and patients can not longer be considered as candidates for surgery or other local ablative treatments.

Because the liver is the first major organ reached by venous blood draining from the intestinal tract, it is the most common site of metastatic disease in cancers of the large intestine (2). It is involved in as many as 50-70% of colorectal cancer patients who develop metastatic disease, in approximately half of whom it is the only site of recurrence (3).

While the role of local treatments such as surgery and radiofrequency ablation (RFA) is relatively well defined for colorectal metastases, their indications and benefits are less clear in metastases from other tumor types (2, 4). However, due to concomitant medical diseases or to poor anatomical location or performance status, few patients with colorectal liver metastases are considered eligible for resection (5, 6).

For those patients who are not candidates for surgery, RFA is emerging as an alternative curative option. But while RFA is the commonest used non-surgical technique for local therapy of colorectal liver metastases, it can be hampered by various problems involving the location of the tumors within the liver, particularly those adjacent to the large hepatic vessels (7). Although large blood vessels adjacent to a tumor are not likely to be injured during an ablation, the blood flow acts like a heat sink, making it more difficult to heat the portion of the tumor directly adjacent to the blood vessel.

Ablation of tumors located near the portal vein pedicles is also associated with increased complications, as RFA in this area can cause main injury to a major bile duct, resulting in biliary stricture. Similarly, due to the risk of thermal injury to adjacent organs, subcapsular tumors are also problematic (8). Another point of concern is the chance of incomplete ablation in tumors over 3 cm (9). Although larger tumors can be treated by overlapping ablations, the likelihood of incomplete ablation seems to increase as tumor size increases (10-13). To introduce a new "bipolar" system that may provide better local control than the conventional "monopolar" system when treating larger lesions, several modifications of the needle electrodes have been developed to improve the coagulative capacity of the probes (14).

The positive effects of chemotherapy are well documented for patients with advanced colorectal cancer, whether or not the disease is confined to the liver (15). Due to their improved efficacy, modern chemotherapy regimes such as FOLFOX, FOLFIRI or XELOX combined with bevacizumab can make unresectable disease resectable (16, 17).

Treatment options for hepatocellular carcinoma

Primary liver cancer, particularly hepatocelular carcinoma (HCC), is a major health problem worldwide (18). In 80% of cases, HCC develops in cirrhotic livers. In Western countries, infection with the hepatitis C virus is the main risk factor, together with other causes of cirrhosis, such as alcohol (19, 20). The presence of underlying cirrhosis is important, as it interferes with the treatment options and also influences survival. Several authors have endorsed the staging and treatment algorithm of HCC from the Barcelona Clinic Liver Cancer Group as the best tool for management (Figure 1) (21).

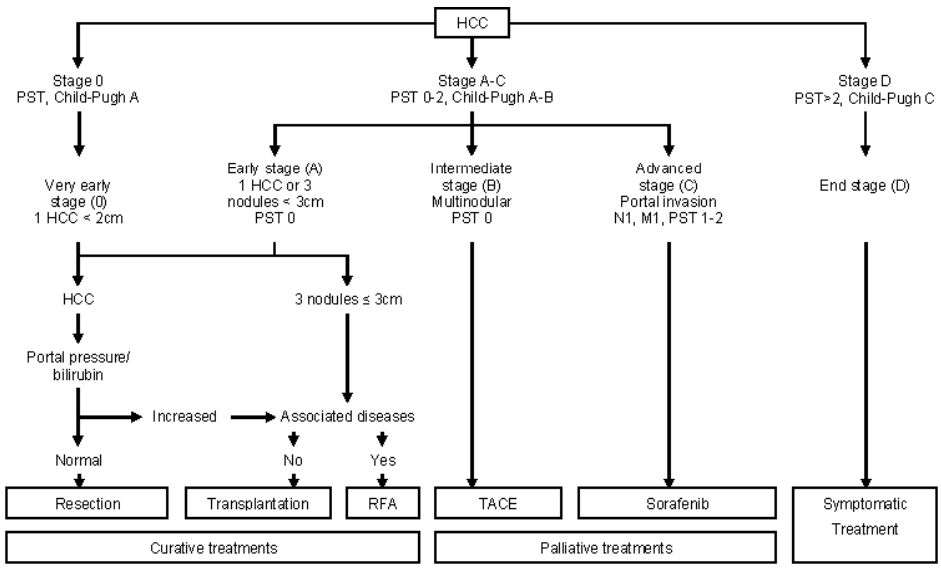

Fig. 1. Barcelona Clinic Liver Cancer staging system and treatment allocation. PST=performance status. N1=lymph node involvement. M1=metastatic spread. RFA=radiofrequency ablation. TACE=transarterial chemoembolisation. (From Bruix J *et al. http://www.aasld.org/practiceguidelines/.* Reproduced and modified with permission of the author).

Hepatic resection has been the primary treatment for HCC in selected patients with limited disease; it is preferred for HCC patients with non-cirrhotic livers or selected patients with Child-Pugh A cirrhosis. Unlike liver transplantation, it does not treat the underlying cirrhosis present in the remnant liver. Tumor recurrence is also greater after resection (22). Candidates for liver transplantation are preferably those with cirrhosis and a tumor that complies with the Milan criteria (single tumor <5 cm or 1-3 tumors each of <3 cm). Liver transplantation reduces the risk of recurrence and *de novo* HCC in the remnant liver, and reestablishes a normal liver function.

Because most HCC patients are not amenable to resection or liver transplantation, RFA has emerged as an effective treatment option for patients who are not eligible for surgery. It can also be used as a bridge for patients who are waiting for liver transplan-

tation. As with the treatment of liver metastases, RFA is limited by the location of the tumor in the liver, and possibly by the tumor size (9, 22-24). In a randomized study, RFA has shown to be significantly superior to PEI with respect to local recurrence-free survival rates for small HCC (25).

Patients with tumors at an intermediate stage (large or multifocal tumors without vascular invasion or extrahepatic disease, well preserved liver function, and absence of symptoms) are the best candidates for transarterial chemoembolization (TACE) (21, 26, 27). What makes TACE relatively safe is the liver-unique vascular supply from the portal vein, whereas HCC is supplied almost entirely by branches of the hepatic artery (23). Although TACE is the preferred treatment for palliation of HCC, it may be used to downstage a tumor prior to resection or RFA, or as a bridge to liver transplantation.

Patients with locally advanced HCC who are not candidates for a local therapy modality, or those with metastatic disease and Child-Pugh A cirrhosis, can benefit from Sorafenib, a multikinase inhibitor with antiproliferative and antiangiogenic activity (28, 29). Although it has been suggested that patients with Child-Pugh B cirrhosis up to 7 points might benefit from Sorafenib, further data is needed to confirm its safety and benefit in patients with poorer liver function (21, 29). Combinations of local therapies with Sorafenib are currently being investigated (30, 31).

Growing evidence suggests that radioembolization with ^{90}Ytrium is a safe and effective modality for treating HCC and liver metastases; to date its results have been promising. Possible indications may be bridging or downstaging to transplantation or resection, as well as palliation in patients with multifocal disease (32-35).

Stereotactic body radiation therapy for liver tumors

External beam radiotherapy had been considered to have a very limited role in the treatment of liver tumors. This is due to the evidence that conventional fractionation could safely treat the whole liver in doses of up to only 30 Gy, and that such doses could lead only to the short-term palliation of symptoms (36, 37). The technical development of 3D conformal radiotherapy in the 1980s renewed interest in the treatment of primary and metastatic liver tumors.

In the 1990s, new strategies were developed for treating liver tumors with radiotherapy alone or in combination with hepatic arterial chemotherapy (38, 39). This work was done mainly by two groups, in Michigan and Stockholm, who demonstrated that the delivery of high doses of radiation to limited volumes of the liver had promising results in terms of local control and survival at an acceptable toxicity. To adapt the principles of intracranial radiosurgery for tumors in the body, the Karolinska group developed a stereotactic body frame (SBF) which was used for patient fixation and precise tumor localization during planning and treatment (Figure 2).

Fig. 2. Stereotactic body frame (dummy patient).

The treatment was delivered in one to four treatment fractions (40). To determine the reproducibility of the target in the stereotactic system for the first patients, computer tomography (CT) examinations were performed. These measurements showed that a margin of 5mm in the transversal plane and 10mm in the cranial-caudal direction around the tumor compensated for 95% of the tumor deviations from the planning CT in the axial plane, and for 89% in the cranial-caudal plane (41).

The treatment was delivered using a conformal technique in which several coplanar or noncoplanar stationary beams created a steep gradient of dose falloff at the interface between tumor and normal tissues (40). Generally, a heterogeneous dose distribution within the planning target volume (PTV) was used, in which the central parts of the PTV received a dose almost 50% higher than the dose prescribed for the periphery. The first rationale behind this method was to minimize the dose delivered to the normal tissues outside the target. The second rationale was to overcome the radioresistance caused by hypoxia, which is presumably present mainly in the central areas of the tumors. Thus, for a given dose at the periphery, an increase in dose to the central parts of the PTV would increase the therapeutic ratio (42).

Over the following decade, this concept of stereotactic radiotherapy was further developed at several other centers. In Europe, two German groups successfully continued developing the stereotactic method for liver tumors (43, 44). The Michigan group also studied the factors influencing the liver toxicity associated with radiotherapy or radiation-induced liver disease. Their findings suggested that, due to the presence of preexisting cirrhosis or hepatitis, the liver of most patients with HCC had a lower tolerance to radiation than the liver of patients with metastases (45).

Methods that use a small number of fractions with a high degree of precision to deliver a high dose of radiotherapy to a target in the body are now known as stereotactic body radiation therapy (SBRT) (46). Generally, this treatment option for primary (mainly HCC) and metastatic liver tumors is offered as an ablative radical local treatment for patients who are not eligible for surgery or RFA.

Recently, technical advances have been introduced to implement stereotactic treatments. They include frequent imaging during the course of radiotherapy to correct for the day-to-day variation in tumor position (image-guided radiotherapy), and advances in radiotherapy planning (IMRT and adaptive radiotherapy).

Aims and outline of the thesis

Over recent years, several groups have reported their experience with regard to feasibility and clinical outcomes in the emerging field of stereotactic body radiation therapy (SBRT) for liver tumors. However, nothing was known about the impact of the treatment in the patient's quality of life; very little was known about the effect of the daily tumor setup corrections on the organs at risk and about the correlation between imaging and pathology or the microscopic extension for liver metastases. There was also very little literature that sought to improve the quality of the treatment by comparing different treatment planning strategies. Similarly, there was no completely separate analysis within the liver metastases group that reported specifically for the metastases of colorectal primary only.

The aim of this thesis was thus to assess the clinical outcomes of SBRT for liver tumors at our institution, and to investigate both the quality of SBRT and potential methods for its improvement.

In Chapter 2 we present a phase I-II study conducted at our clinic on SBRT for HCC and liver metastases. We report feasibility and local control results. In Chapter 3 we investigated the impact of the treatment on the patients' quality of life.

Chapter 4 explores our use of an automated optimization method developed in house for beam orientation and weight selection (Cycle) to improve stereotactic treatments.

Chapter 5 measures the impact of our daily tumor-based setup corrections on the dose delivered to the target volume and the organs at risk during SBRT.

Chapter 6 analyzes our long-term results on local control, survival and toxicity of patients treated with SBRT for colorectal liver metastases.

Chapter 7 studies the correlation between MRI and pathology tumor dimensions, and establishes the microscopic tumor extension of colorectal liver metastases.

Chapter 8 is a general discussion in which we forecast future developments in the field of SBRT for liver tumors.

Chapter 9 is a short summary that includes the studies described in this thesis.

REFERENCES

1. Kavolius J, Fong Y, Blumgart LH. Surgical resection of metastatic liver tumors. *Surg Oncol Clin N Am* 1996; 5:337-352.
2. McCarter MD, Fong Y. Metastatic liver tumors. *Semin Surg Oncol* 2000; 19:177-188.
3. Poston GJ. Surgical strategies for colorectal liver metastases. *Surg Oncol* 2004; 13:125-136.
4. Lermite E, Marzano E, Chereau E*, et al.* Surgical resection of liver metastases from breast cancer. *Surg Oncol* 2010; 19:e79-e84.
5. Kulaylat MN, Gibbs JF. Regional treatment of colorectal liver metastasis. *J Surg Oncol* 2010; 101:693-698.
6. Yoon SS, Tanabe KK. Surgical treatment and other regional treatments for colorectal cancer liver metastases. *Oncologist* 1999; 4:197-208.
7. Stang A, Fischbach R, Teichmann W*, et al.* A systematic review on the clinical benefit and role of radiofrequency ablation as treatment of colorectal liver metastases. *Eur J Cancer* 2009; 45:1748-1756.
8. Wong SL, Mangu PB, Choti MA*, et al.* American Society of Clinical Oncology 2009 clinical evidence review on radiofrequency ablation of hepatic metastases from colorectal cancer. *J Clin Oncol* 2010; 28:493-508.
9. de Meijer V, Verhoef C, Kuiper JW*, et al.* Radiofrequency ablation in patients with primary and secondary hepatic malignancies. *J Gastrointest Surg* 2006; 10:960-973.
10. Dodd GD, III, Frank MS, Aribandi M*, et al.* Radiofrequency thermal ablation: computer analysis of the size of the thermal injury created by overlapping ablations. *AJR Am J Roentgenol* 2001; 177:777-782.
11. Kosari K, Gomes M, Hunter D*, et al.* Local, intrahepatic, and systemic recurrence patterns after radiofrequency ablation of hepatic malignancies. *J Gastrointest Surg* 2002; 6:255-263.
12. Solbiati L, Livraghi T, Goldberg SN*, et al.* Percutaneous radio-frequency ablation of hepatic metastases from colorectal cancer: long-term results in 117 patients. *Radiology* 2001; 221:159-166.
13. van Duijnhoven FH, Jansen MC, Junggeburt JM*, et al.* Factors influencing the local failure rate of radiofrequency ablation of colorectal liver metastases. *Ann Surg Oncol* 2006; 13:651-658.
14. Meijerink MR, Van Den TP, Van Tilborg AA*, et al.* Radiofrequency ablation of large size liver tumours using novel plan-parallel expandable bipolar electrodes: Initial clinical experience. *Eur J Radiol* 2009.
15. Glimelius B. Chemotherapy of colorectal cancer liver metastases. *Eur J Cancer* 2003; 1, suppl 6:173-180.
16. Kneuertz PJ, Maithel SK, Staley CA*, et al.* Chemotherapy-Associated Liver Injury: Impact on Surgical Management of Colorectal Cancer Liver Metastases. *Ann Surg Oncol* 2010.
17. van Cutsem E., Rivera F, Berry S*, et al.* Safety and efficacy of first-line bevacizumab with FOLFOX, XELOX, FOLFIRI and fluoropyrimidines in metastatic colorectal cancer: the BEAT study. *Ann Oncol* 2009; 20:1842-1847.
18. Hoshida Y, Toffanin S, Lachenmayer A*, et al.* Molecular classification and novel targets in hepatocellular carcinoma: recent advancements. *Semin Liver Dis* 2010; 30:35-51.
19. Llovet JM, Beaugrand M. Hepatocellular carcinoma: present status and future prospects. *J Hepatol* 2003; 38 Suppl 1:S136-S149.
20. Pons F, Varela M, Llovet JM. Staging systems in hepatocellular carcinoma. *HPB (Oxford)* 2005; 7:35-41.

21. Bruix J, Llovet JM. Major achievements in hepatocellular carcinoma. *Lancet* 2009; 373:614-616.
22. Jarnagin W, Chapman WC, Curley S*, et al.* Surgical treatment of hepatocellular carcinoma: expert consensus statement. *HPB (Oxford)* 2010; 12:302-310.
23. Georgiades CS, Hong K, Geschwind JF. Radiofrequency ablation and chemoembolization for hepatocellular carcinoma. *Cancer J* 2008; 14:117-122.
24. Higgins H, Berger DL. RFA for liver tumors: does it really work? *Oncologist* 2006; 11:801-808.
25. Lencioni RA, Allgaier HP, Cioni D*, et al.* Small hepatocellular carcinoma in cirrhosis: randomized comparison of radio-frequency thermal ablation versus percutaneous ethanol injection. *Radiology* 2003; 228:235-240.
26. Llovet JM, Real MI, Montana X*, et al.* Arterial embolisation or chemoembolisation versus symptomatic treatment in patients with unresectable hepatocellular carcinoma: a randomised controlled trial. *Lancet* 2002; 359:1734-1739.
27. Schwarz RE, Abou-Alfa GK, Geschwind JF*, et al.* Nonoperative therapies for combined modality treatment of hepatocellular cancer: expert consensus statement. *HPB (Oxford)* 2010; 12:313-320.
28. Cheng AL, Kang YK, Chen Z*, et al.* Efficacy and safety of sorafenib in patients in the Asia-Pacific region with advanced hepatocellular carcinoma: a phase III randomised, double-blind, placebo-controlled trial. *Lancet Oncol* 2009; 10:25-34.
29. Llovet JM, Ricci S, Mazzaferro V*, et al.* Sorafenib in advanced hepatocellular carcinoma. *N Engl J Med* 2008; 359:378-390.
30. Hoffmann K, Glimm H, Radeleff B*, et al.* Prospective, randomized, double-blind, multi-center, Phase III clinical study on transarterial chemoembolization (TACE) combined with Sorafenib versus TACE plus placebo in patients with hepatocellular cancer before liver transplantation - HeiLivCa [ISRCTN24081794]. *BMC Cancer* 2008; 8:349.
31. Horgan AM, Dawson LA, Swaminath A*, et al.* Sorafenib and Radiation Therapy for the Treatment of Advanced Hepatocellular Carcinoma. *J Gastrointest Cancer* 2010.
32. Kennedy A, Nag S, Salem R*, et al.* Recommendations for radioembolization of hepatic malignancies using yttrium-90 microsphere brachytherapy: a consensus panel report from the radioembolization brachytherapy oncology consortium. *Int J Radiat Oncol Biol Phys* 2007; 68:13-23.
33. Kennedy AS, Salem R. Radioembolization (yttrium-90 microspheres) for primary and metastatic hepatic malignancies. *Cancer J* 2010; 16:163-175.
34. Kulik LM, Carr BI, Mulcahy MF*, et al.* Safety and efficacy of 90Y radiotherapy for hepatocellular carcinoma with and without portal vein thrombosis. *Hepatology* 2008; 47:71-81.
35. Salem R, Lewandowski RJ, Mulcahy MF*, et al.* Radioembolization for hepatocellular carcinoma using Yttrium-90 microspheres: a comprehensive report of long-term outcomes. *Gastroenterology* 2010; 138:52-64.
36. Borgelt BB, Gelber R, Brady LW*, et al.* The palliation of hepatic metastases: results of the Radiation Therapy Oncology Group pilot study. *Int J Radiat Oncol Biol Phys* 1981; 7:587-591.
37. Emami B, Lyman J, Brown A*, et al.* Tolerance of normal tissue to therapeutic irradiation. *Int J Radiat Oncol Biol Phys* 1991; 21:109-122.
38. Lax I, Blomgren H, Naslund I*, et al.* Stereotactic radiotherapy of malignancies in the abdomen. Methodological aspects. *Acta Oncol* 1994; 33:677-683.
39. McGinn CJ, Ten Haken RK, Ensminger WD*, et al.* Treatment of intrahepatic cancers with radiation doses based on a normal tissue complication probability model. *J Clin Oncol* 1998; 16:2246-2252.

40. Blomgren H, Lax I, Göranson H*, et al.* Radiosurgery for Tumors in the Body: Clinical Experience Using a New Method. *Journal of Radiosurgery* 1998; 1:63-74.
41. Blomgren H, Lax I, Naslund I*, et al.* Stereotactic high dose fraction radiation therapy of extracranial tumors using an accelerator. Clinical experience of the first thirty-one patients. *Acta Oncol* 1995; 34:861-870.
42. Lax I, Blomgren H, Larson DA*, et al.* Extracranial Stereotactic Radiosurgery of Localized Targets. *Journal of Radiosurgery* 1998; 1:135-148.
43. Herfarth KK, Debus J, Lohr F*, et al.* Stereotactic single-dose radiation therapy of liver tumors: results of a phase I/II trial. *J Clin Oncol* 2001; 19:164-170.
44. Wulf J, Hadinger U, Oppitz U*, et al.* Stereotactic radiotherapy of targets in the lung and liver. *Strahlenther Onkol* 2001; 177:645-655.
45. Dawson LA, Normolle D, Balter JM*, et al.* Analysis of radiation-induced liver disease using the Lyman NTCP model. *Int J Radiat Oncol Biol Phys* 2002; 53:810-821.
46. Potters L, Steinberg M, Rose C*, et al.* American Society for Therapeutic Radiology and Oncology and American College of Radiology practice guideline for the performance of stereotactic body radiation therapy. *Int J Radiat Oncol Biol Phys* 2004; 60:1026-1032.

2

STEREOTACTIC BODY RADIATION THERAPY FOR PRIMARY AND METASTATIC LIVERTUMORS: A SINGLE INSTITUTION PHASE I-II STUDY

Alejandra Méndez Romero, Wouter Wunderink, Shahid M. Hussain,
Jacco A. De Pooter, Ben J. M. Heijmen, Peter J. C. M. Nowak,
Joost J. Nuyttens, Rene P. Brandwijk, Cornelis Verhoef,
Jan N. M. IJzermans, and Peter C. Levendag

Acta Oncologica, 2006; 45: 831-837

ABSTRACT

The feasibility, toxicity and tumor response of stereotactic body radiation therapy (SBRT) for treatment of primary and metastastic liver tumors was investigated. From October 2002 until June 2006, 25 patients not suitable for other local treatments were entered in the study. In total 45 lesions were treated, 34 metastases and 11 hepatocellular carcinoma (HCC). Median follow-up was 12.9 months (range 0.5-31). Median lesion size was 3.2 cm (range 0.5-7.2) and median volume 22.2 cm^3 (range 1.1-322). Patients with metastases, HCC without cirrhosis, and HCC < 4cm with cirrhosis were mostly treated with 3 x 12.5 Gy. Patients with HCC ≥ 4cm and cirrhosis received 5 x 5 Gy or 3 x 10 Gy. The prescription isodose was 65%. Acute toxicity was scored following the Common Toxicity Criteria and late toxicity with the SOMA/LENT classification. Local failures were observed in two HCC and two metastases. Local control rates at 1 and 2 years for the whole group were 94% and 82%. Acute toxicity grade ≥ 3 was seen in four patients; one HCC patient with Child B developed a liver failure together with an infection and died (grade 5), two metastases patients presented elevation of gamma glutamyl transferase (grade 3) and another asthenia (grade 3). Late toxicity was observed in one metastases patient who developed a portal hypertension syndrome with melena (grade 3). SBRT was feasible, with acceptable toxicity and encouraging local control. Optimal dose-fractionation schemes for HCC with cirrhosis have to be found. Extreme caution should be used for patients with Child B because of a high toxicity risk.

Acknowledgements: The authors would like to thank P.T.N. Pattynama M.D., Ph.D. and S. Dwarkasing, M.D., for their valuable contributions.

INTRODUCTION

Hepatocellular carcinoma (HCC) and colorectal cancer are among the five most common causes of cancer mortality in the world (1). As many as 50-70% of patients diagnosed of colorectal cancer will present liver involvement during follow-up, being the only site of recurrence in half of these patients (2). Surgery is accepted as a potentially curative option with survival rates at 5 years of 50-70% for early diagnosed HCC, and 25-35% for liver metastases when disease is confined to the liver (2-5). However, the majority of patients are not eligible for surgery because of liver function impairment, diminished liver function capacity after several resections, location of the lesion in centrally located segments or concomitant medical diseases (4-6). For patients who are not suitable for surgery, other local treatment methods, especially radiofrequency ablation (RFA) are emerging as alternative curative options but, the proximity of the lesion to the gall bladder or main vessels, the subdiaphragmatic location, or the presence of a non-echogenic lesion (for ultrasound-guided RFA) constitute major problems to apply this treatment (7). Radiotherapy, alone or in combination with transarterial chemoembolization has become a potential new treatment option for primary and metastatic liver tumors around the world (8-10). Stereotactic body radiation therapy (SBRT) has no strict restrictions regarding lesion location, and offers the possibility of a high precision non-invasive treatment, using small margins (11). The aim of this paper was to assess feasibility, toxicity and tumor response of SBRT as a new local treatment modality for primary and metastatic liver tumors in our patient population.

MATERIALS AND METHODS

Patient characteristics

Patients included were those with primary or metastatic tumors confined to the liver, and not eligible for surgery or other local treatment (RFA). The Karnofsky index was at least 80%. The Child-Pugh grade for HCC patients was A-B. With the maximum lesion size allowed being 7 cm, a maximum of three lesions was acceptable for the protocol. Tables 1 and 2 summarize the patient characteristics of this study. From October 2002 until June 2006, eight patients were treated for 11 primary liver tumors (HCC) and 17 patients for 34 metastases. Median age was 63 years (range 37-81). Gender distribution was five females, 20 males. Median tumor size was 3.2 cm (range 0.5-7.2 cm) and median tumor volume 22.2 cm^3 (range 1.1-322). All patients with primary tumors, except one, had cirrhotic livers. In contrast, in the metastases group, only one patient had liver function impairment with signs of portal hypertension (cardial and esophageal varices). Probably, this was due to portal vein thrombosis developed after previous radiotherapy performed elsewhere because of other liver metastases.

Table 1. HCC Patient characteristics

Patient HCC	Cirrhosis Child-Pugh grade	Vascular invasion	Lesion number	Lesion size (cm)	Liver segment	Treatment
1	A	Yes (PVT)	1	3.5	6	3x12.5Gy
2	A	Yes	1 2, 3	7.2 0.5, 0.5	2 2, 2	5x5Gy* 5x5Gy
3	A	No	1	6.1	1	5x5Gy
4	A	No	1	4.5	6	5x5Gy
5	B	No	1, 2	1.6, 1.3	3, 6	3x12.5Gy
6	B	Yes (PVT)	1	4.5	7	3x10Gy
7	A	No	1	2.2	7	3x12.5Gy
8	No	No	1	6	8	3x12.5Gy

PVT : portal vein thrombosis. * Patient 2 developed 2 new lesions (2,3) in the same segment close to the initially treated lesion. Although there was not a relapse of the lesion 1 (still 5.6 cm diameter) there was a simultaneous re-treatment with 5 x 5 Gy of the first lesion.

Table 2. Liver metastases. Patient characteristics

Patient Metastases	Primary tumor	Lesion number	Lesion size (cm)	Liver segment	Treatment
1	Colorectal	1	Microscopic rest	7	3x10Gy
2	Colorectal	1	4.0	4	3x12.5Gy
3	Colorectal	1, 2	3.7, 1.3	7, 7	3x12.5Gy
4	Lung	1, 2	1.5, 0.5	7, 7	3x12.5Gy
5	Colorectal	1 2, 3	2.7 1.6, 1.3	8 8, 8	3x12.5Gy 3x12.5Gy
6	Colorectal	1, 2, 3 4, 5	2.8, 2.0, 1.0 1.5, 1.6	4a, 4a, 4a 2, 3	3x10Gy 3x12.5Gy
7	Colorectal	1	2.3	1	3x12.5Gy
8	Breast	1, 2 , 3, 4*	1.4, 1.2, 1.0, 2.1	4a, 6, 8, 8	3x12.5Gy
9	Colorectal	1, 2	3.9, 1.5	1, 8	3x12.5Gy
10	Colorectal	1	6.2	4a	3x12.5Gy
11	Colorectal	1, 2, 3	6, 3.9, 3.2	2, 4, 4	3x10Gy
12	Colorectal	1, 2	2.8, 0.7	1, 3	3x12.5Gy
13	Colorectal	1, 2	4.1, 0.8	7, 7	3x12.5Gy
14	Colorectal	1	2.4	1	3x12.5Gy
15	Carcinoid	1	3.2	4	3x12.5Gy
16	Colorectal	1	2.7	4	3x12.5Gy
17	Colorectal	1, 2	3.3, 1.0	1, 7	3x12.5Gy

*Lesions 3-4 were very close to each other and considered as one target.

Dose-fractionation schemes

The dose was prescribed at the 65% isodose that surrounded the PTV. Patients with liver metastases, HCC without cirrhosis, and HCC < 4 cm and cirrhosis were mostly treated with 3 fractions of 12.5 Gy. Three patients with liver metastases have been treated with 3 fractions of 10 Gy. One patient because of the presence of only micro-

scopic disease (after non-radical microscopic surgery), another patient because of the small bowel in the high dose area, and the third one because of the amount of normal liver involved in the high dose region. For patients with HCC ≥ 4 cm and cirrhosis, treatment consisted initially, for the first 3 patients, on 5 fractions of 5 Gy (5 x 5 Gy). Because no grade 3-4 toxicity was observed but a local failure was evidenced in two of them very close after treatment (see below), retreatment was performed using 3 fractions of 8 Gy without evidence of severe toxicity. These two patients were considered as a failure for the actuarial local control calculations. The dose was increased for the last patient to 3 fractions of 10 Gy. Treatment fractions were delivered every second day. Overall treatment time was 5-6 days for 3 fractions and 10 days for 5 fractions.

Treatment preparation and execution

For SBRT patients were positioned in the Elekta Stereotactic Body Frame (SBF) (Elekta Oncology Systems, Stockholm, Sweden) with maximum tolerable abdominal compression to reduce respiratory tumor motion. All patients had a planning, an arterial and a venous contrast CT scan. The rim of contrast enhancement was taken as boundary of the clinical target volume (CTV) and was delineated on the arterial and venous contrast CT scans and summed to construct the definitive 3-D CTV. The tumor delineations were reviewed by an experienced radiologist (S. M. Hussain/ S. Dwarkasing). Initially, the applied PTV margin was based on the Karolinska experience (5-10 mm) (12). Currently, implanted gold fiducials and fluoroscopy are used to assess residual tumor motion in all directions and margins are individualized.

Treatment plans (Fig. 1A and 1B) were generated with the Cadplan treatment planning system (Varian Oncology Systems, Palo Alto, CA) with 4-10 coplanar and noncoplanar beams. The following normal tissue constraints were used (13): for normal liver $D_{33\%} < 21$ Gy, $D_{50\%} < 15$ Gy, for bowel, duodenum, stomach and esophagus $D_{5cc} < 21$ Gy, for spinal cord $D_{max} < 15$ Gy and for kidney $D_{33\%} < 15$ Gy.

The treatments were delivered with a Siemens Primus linear accelerator (Siemens Oncology Systems, Concord, CA). Just prior to each treatment fraction a contrast CT scan was acquired to assess tumor motion and bony anatomy displacements in the SBF. Also, electronic portal images were used to exclude movements of the patient (bony anatomy) in the SBF during transport from the CT scanner to the linear accelerator and to verify applied SBF setup corrections, in case of detected tumor displacements in the SBF at the CT scanner.

Follow-up and definition of local failure

All patients had a multiphase gadolinium enhanced liver MRI scan, a liver function test, and tumor marker assessment between 4 and 6 weeks prior to treatment planning, and at 1, 2, 3 months after treatment and periodically every 3 months during

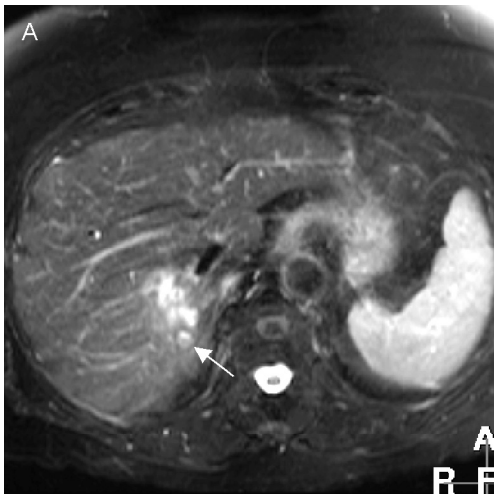

Fig. 1A. T2-weighted MR image shows one hyperintense metastasis in segment 7 with a small satellite lesion (arrow).

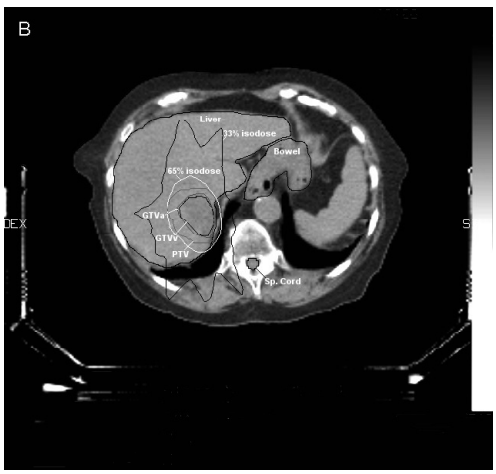

Fig. 1B. CT-planning showing the delineations corresponding to the two liver metastases in segment 7, both included in one target, the GTV arterial and venous phase, the organs at risk (liver, bowel and spinal cord), the PTV surrounded by the 65% isodose and the 33% isodose.

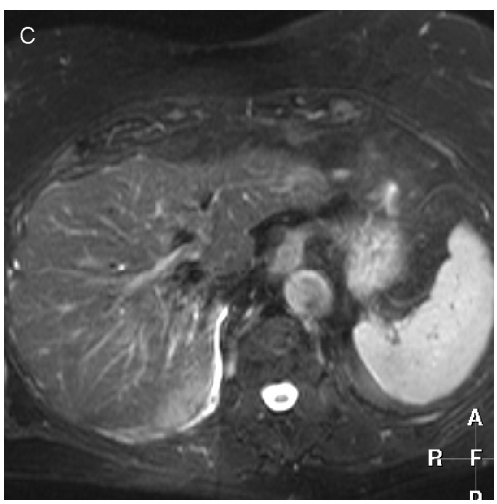

Fig. 1C. T2-weighted MR image shows complete remission with morphological parenchymal changes due to radiation hepatitis 21 months after treatment.

the first 2 years, and every 6 months thereafter. The tumor size was evaluated on a MRI axial reconstruction and the volumes with the contrast CT scan delineations. Local failure was defined as increase in tumor size and/or steady increase of tumor marker values above normal, without evidence of new intra- or extrahepatic lesions at any point during the follow-up. Median follow-up for local control was 12.9 months (range 0.5-31).

Toxicity evaluation

Acute toxicity was evaluated during the first 3 months after treatment with the Common Toxicity Criteria (CTC), version 2.0 of the National Cancer Institute. The SOMA/LENT grading system was used to score the late toxicity. Radiation induced liver disease (RILD) was defined as, anicteric ascites and elevation of alkaline phosphatase levels to at least two fold increase above the pretreatment values in absence of tumor progression, classic (14), or hepatic toxicity grade 3 or higher according to the CTC also in absence of tumor progression, non-classic (15,16).

Statistics

To assess local control and survival, Kaplan-Meier curves were generated with SPSS, version 11.5.

This retrospectively analyzed phase I-II study was approved by the Ethical Commission of Erasmus MC and all patients have given their written consent.

RESULTS

Local control

Local failure was observed in four out of 45 lesions in four patients (2 HCC, 2 metastases). One HCC patient presented a steady increase of AFP 7 months after treatment without increase in tumor size but with an active rest lesion on a PET scan. The other HCC patient showed an in field regrowth after initial decrease of lesion size and elevated AFP 4 months posttreatment. These two patients were treated with 5 x 5 Gy. Two metastases patients presented an in field regrowth after an initial complete remission with an increase of the CEA level at 31 and 21 months after treatment. Both patients were treated with 3 x 12.5 Gy. An example to illustrate a complete remission is shown in Figure 1C.

The actuarial one and two year local control rates were 94% and 82% for the whole group and 100% and 86% for the metastases group, respectively (Fig. 2). For the HCC the one year and twenty-two months local control probability were 75%

(maximum follow-up of a HCC in local control is 22 months). Crude local control rates for liver metastases and HCC were 94% and 82%, respectively.

Actuarial overall survival rates at one and two years (Fig. 3) were 82% and 54% for the whole group; 85% and 62% for the metastases group, and 75% and 40% for HCC patients.

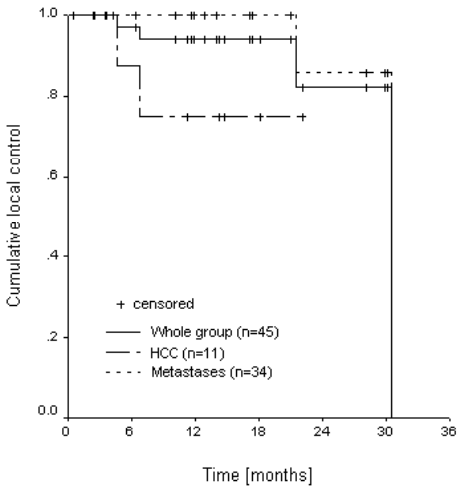

Fig. 2. Actuarial local control function. The curve corresponding to the whole group and liver metastases drops at the end until zero because the patient with largest follow-up (31 months) presented a local failure.

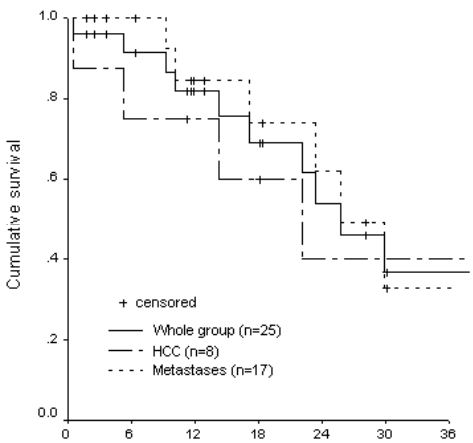

Fig. 3. Actuarial survival function.

Toxicity

Changes in the liver function parameters grade 1-2, were present in all the patients except one (grade 0) in the first 3 months after treatment. Within the HCC group, one episode of RILD classic and non-classic was observed. Two weeks after treatment, a Child B patient presented hepatic toxicity grade 4 with signs of decompensated portal hypertension, bleeding from esophageal varices, and fever from a urinary infection.

The patient died within the first month after treatment and the toxicity was evaluated as grade 5. Two patients presented ascites grade 2 with less than two fold increased alkaline phosphatase and hepatic toxicity (CTC) less than grade 3, responding well to temporary diuretic medication. No late toxicity was found. In the metastases group, two episodes of RILD non-classic were found in the first 3 months after treatment. Two patients presented an elevation of gamma glutamyl transpherase (GGT) grade 3. In one case the increase was isolated, without any symptom or parallel increase of other liver function parameters. In the other, an increase of the other liver parameters and asthenia (both grade 2) was observed. One patient developed asthenia grade 3 with hepatic toxicity grade 2 during the first month after treatment and recovered spontaneously during the second month. Also, one episode of ascites grade 2 with less than two times increase of alkaline phosphatase was observed in one patient after being treated three times with radiotherapy (last two in our center) and previously with surgery. Late toxicity could also be present in this patient because of the development of a portal hypertension syndrome with one melena episode that was evaluated as SOMA grade 3. No esophagus, stomach, bowel or kidney toxicity was found.

DISCUSSION

Local control whole group

Our results, with local control rates of 94% and 82% at 1 and 2 years, respectively, are in accordance with those published from similar studies in the literature (Table 3) (9, 13, 17-20). The better local control compared to Wulf *et al*. (13) and Shefter *et al*. (19) can perhaps be explained by the higher doses used in the present study. Herfarth *et al*., in a recent publication (21), have reported results of 70 patients, 35 of the first phase I/II trial (18) (4 primary tumors, 51 metastases) and 35 treated after the trial was closed (51 metastases, mainly colorectal). Actuarial local control rates were 66% at 18 months and 60% at 2 years. The lower results in comparison with those from the first 35 patients were due to a poor local control rate of the colorectal metastases group (see metastases section).

Separate comparisons for HCC and metastases are difficult to perform, as most studies don't make this separation in their analysis.

Table 3. Comparison of local control and survival between studies using hypofractionated radiotherapy

Author	Lesions (p)/(lm)	Dose-fractionation scheme (prescription isodose)	Median follow-up moths	(%) Actuarial local control 1, 2 years	(%) Actuarial survival 1, 2 years
Blomgren	18/20	1-3x5-15Gy(p) (65%)	Mean 12	NRP*	NRP#
		2-4x10-20Gy (lm) (65%)	Mean 9.6	NRP*	NRP#
Wulf	1/23	3x10Gy (65%)	9	76, 61	71, 43
Herfath	4/102	1x20-26Gy (80%)	Mean 14.9	66¶, 60	76, 55
Wada	6/5	3x15Gy (90-100%)	19.3	NRP, 71.2	NRP, NRP
Schefter	1/15	3x7-10Gy (80-90%)	10.1	47(at10.1m), NRP	NRP, NRP
Fuss	1/17	3-6x6-12Gy (NRP)	6.5	94, NRC	80, NRC
Kavanagh	0/NRPμ	1x20Gy (80-90%)		100, 93%	NRP, NRP
Present study	11/34	3-5x5-12.5Gy (p) (65%)	12.9	94, 82 (wg)	82, 54 (wg)
		3x10-12.5Gy (lm) (65%)		75, 75§	75, 40
				100, 86	85, 62

(p): primary tumors (HCC/ cholangiocarcinoma). (lm): liver metatases. (wg): whole group.
NRP: not reported. NRC: not reached.
*Crude local control at last follow-up: 100% for HCC and 95% for liver metastases. #Mean survival 13.4m for HCC and mean 17.8m for liver metastases. ¶At 18 months. μ36 treated patients § At 22 months.

Local control HCC

Blomgren *et al*. (9) reported a crude local control at last follow-up (median 12 months) of 100%. Our result of 80% crude local control at one year is lower but this needs further consideration. All tumors in the present study treated with 3 x 12.5 Gy stayed in local control. The difference with the results from Blomgren *et al*. is due to our poor local control achieved for large tumors with cirrhosis, probably because of the too low total dose delivered (5 x 5 Gy). A clear dose effect relationship for HCC has been established in the literature by Dawson *et al*. and Park *et al*. (10, 22); eventually the combination with a large size, as demonstrated by Wada *et al*. (20) could have influenced the low local control rate.

Local control metastases

Kavanagh *et al*. observed local control rates of 100% and 93% at 1 and 2 years, in 36 liver metastases patients treated with 3 fractions of 20 Gy (pers. comm.). Probably, the delivered higher doses have decreased the local failure rate in comparison with our study. Herfarth *et al*. (21) performed a separate analysis considering only the metastases patients. They observed that colorectal metastases presented a poorer local control than those with other histology (45% vs. 91% after 18 months), especially for those treated previously with systemic chemotherapy, that could have selected radioresistant cells. We observed better local control rates even with a population including mainly colorectal metastases (27 of 34 lesions). It might be possible that our patients were treated less with chemotherapy and this could explain the observed difference.

Toxicity whole group

Comparison with other groups is difficult because of different or not mentioned scoring systems used to report toxicity. However, the data from the literature (9,13,18-20) seem to suggest that published toxicity for the whole group is lower than in our study.

Toxicity HCC

Cheng *et al*. and Jiang *et al*. (15, 16) have demonstrated that patients with cirrhosis Child-Pugh grade B have a high risk to develop toxicity (RILD). As well, Cheng *et al*. conclude that hepatitis B virus (HBV) was also associated with higher susceptibility for RILD but the mean liver dose and the V_{30Gy} (percentage of normal liver volume that received a radiation dose > 30 Gy) were not statistical significantly correlated. This is in agreement with our experience. We had two patients with Child-Pugh B that also carried HBV. One who developed tumor progression and could therefore not be evaluated for toxicity. The other patient presented fever two weeks after treatment, due to an infection, with signs of increased portal hypertension and RILD, progressing to liver failure and death. Although it is known that in cirrhotic patients a liver decompensation can be associated with infections, possibly the radiation induced edema increased the portal pressure and the subsequent bleeding contributed to deteriorate the unstable liver function. This patient had a V_{30Gy} of 6% and the mean and the median liver dose were also low, 8.6 and 3.4 Gy (converted to 2 Gy per fraction with $\alpha/\beta = 2$). HCC with cirrhosis Child-Pugh A and patients without cirrhosis, regardless of size, didn't show any toxicity grade ≥ 3. Possibly, the absence of severe liver function impairment makes them less susceptible to develop complications.

Toxicity metastases

Within the metastases group, we observed grade 3 hepatic toxicity in two patients based on an increased GGT. The published phase I trial from the Colorado and Indiana groups (23) showed that for metastases, escalating the dose until 60 Gy delivered in 3 fractions was possible, without reaching the maximum tolerated dose for grade 3-4 toxicity. In this study, at least 35% of normal liver, or 700 ml, estimating a normal liver volume of 2000 ml, had to receive a total dose less than 15 Gy. Analysis of the dose-volume histogram of the two patients with hepatic toxicity showed that 53% and 60% of the normal liver received 15 Gy or less corresponding to 638 and 639 ml, respectively. The first patient was treated because of two targets and the second one had a small liver volume after previous operations. The patient with asthenia grade 3 was treated with chemotherapy and resection prior to radiotherapy what could have influenced the development of more constitutional symptoms.

CONCLUSIONS

SBRT was feasible, with an acceptable toxicity and encouraging local control, especially for liver metastases. More studies including larger numbers of patients are necessary to verify these results and to find optimal dose-fractionation schemes for HCC patients with cirrhotic livers. If patients with Child-Pugh B are considered for treatment extreme caution should be used because of the high risk to develop toxicity.

REFERENCES

1. Llovet JM, Burroughs A, Bruix J. Hepatocellular carcinoma. *Lancet* 2003 Dec 6;362(9399):1907-17.
2. Poston GJ. Surgical strategies for colorectal liver metastases. *Surg Oncol* 2004 Aug;13:125-36.
3. Llovet JM. Updated treatment approach to hepatocellular carcinoma. *J Gastroenterol* 2005 Mar;40:225-35.
4. Verhoef C, Visser O, de Man RA, de Wilt JH, IJzermans JN, Janssen-Heijnen ML. Hepatocellular carcinoma in the Netherlands incidence, treatment and survival patterns. *Eur J Cancer* 2004 Jul;40:1530-8.
5. Yoon SS, Tanabe KK. Surgical treatment and other regional treatments for colorectal cancer liver metastases. Oncologist 1999;4:197-208.
6. Llovet JM, Beaugrand M. Hepatocellular carcinoma: present status and future prospects. *J Hepatol* 2003;38 (Supplement 1):S136-S149.
7. Decadt B, Siriwardena AK. Radiofrequency ablation of liver tumours: systematic review. *Lancet Oncol* 2004 Sep;5:550-60.
8. Blomgren H, Lax I, Naslund I, Svanstrom R. Stereotactic high dose fraction radiation therapy of extracranial tumors using an accelerator. Clinical experience of the first thirty-one patients. *Acta Oncol* 1995;34:861-70.
9. Blomgren H, Lax I, Göranson H, Kraepelien T. Radiosurgery for Tumors in the Body: Clinical Experience Using a New Method. *Journal of Radiosurgery* 1998;1:63-74.
10. Dawson LA, McGinn CJ, Normolle D, Ten Haken RK, Walker S, Ensminger W, *et al.* Escalated focal liver radiation and concurrent hepatic artery fluorodeoxyuridine for unresectable intrahepatic malignancies. *J Clin Oncol* 2000 Jun;18:2210-8.
11. Lax I, Blomgren H, Larson D, Naslund I. Extracranial Stereotactic Radiosurgery of Localized Targets. *Journal of Radiosurgery* 1998;1:135-48.
12. Lax I, Blomgren H, Naslund I, Svanstrom R. Stereotactic radiotherapy of malignancies in the abdomen. Methodological aspects. *Acta Oncol* 1994;33:677-83.
13. Wulf J, Hadinger U, Oppitz U, Thiele W, Ness-Dourdoumas R, Flentje M. Stereotactic radiotherapy of targets in the lung and liver. *Strahlenther Onkol* 2001 Dec;177:645-55.
14. Dawson LA, Normolle D, Balter JM, McGinn CJ, Lawrence TS, Ten Haken RK. Analysis of radiation-induced liver disease using the Lyman NTCP model. *Int J Radiat Oncol Biol Phys* 2002 Jul 15;53:810-21.
15. Cheng JC, Wu JK, Lee PC, Liu HS, Jian JJ, Lin YM, *et al.* Biologic susceptibility of hepatocellular carcinoma patients treated with radiotherapy to radiation-induced liver disease. *Int J Radiat Oncol Biol Phys* 2004 Dec 1;60:1502-9.
16. Jiang GL, Liang SX, Zhu XD, Fu XL, Lu HF. Radiation-Induced Liver Disease in Three-Dimensional Conformal Radiotherapy for Primary Liver Carcinoma. [abstract] *Int J Radiat Oncol Biol Phys* 2004 Sep;60(supplement 1):S 413.
17. Fuss M, Thomas CR, Jr. Stereotactic body radiation therapy: an ablative treatment option for primary and secondary liver tumors. *Ann Surg Oncol* 2004 Feb;11:130-8.
18. Herfarth KK, Debus J, Lohr F, Bahner ML, Rhein B, Fritz P, *et al.* Stereotactic single-dose radiation therapy of liver tumors: results of a phase I/II trial. *J Clin Oncol* 2001 Jan 1;19:164-70.
19. Schefter T, Gaspar LE, Kavanagh BD, Ceronsky N, feiner A, Stuhr K. Hypofractionated Extracranial Stereotactic Radiotherapy for liver tumors. [abstract] *Int J Radiat Oncol Biol Phys* 2003 Oct;57, (supplement 1):S282.

20. Wada H, Takai Y, Nemoto K, Yamada S. Univariate analysis of factors correlated with tumor control probability of three-dimensional conformal hypofractionated high-dose radiotherapy for small pulmonary or hepatic tumors. *Int J Radiat Oncol Biol Phys* 2004 Mar 15;58:1114-20.
21. Herfarth KK, Debus J. Stereotactic radiation therapy for liver metastases. Chirurg 2005 Jun;76:564-9.
22. Park HC, Seong J, Han KH, Chon CY, Moon YM, Suh CO. Dose-response relationship in local radiotherapy for hepatocellular carcinoma. *Int J Radiat Oncol Biol Phys* 2002 Sep 1;54:150-5.
23. Schefter TE, Kavanagh BD, Timmerman RD, Cardenes HR, Baron A, Gaspar LE. A phase I trial of stereotactic body radiation therapy (SBRT) for liver metastases. *Int J Radiat Oncol Biol Phys* 2005 Aug 1;62:1371-8.

3

QUALITY OF LIFE AFTER STEREOTACTIC BODY RADIATION THERAPY FOR PRIMARY AND METASTATIC LIVER TUMORS

Alejandra Méndez Romero, Wouter Wunderink, Rob M. van Os,
Peter J. C. M. Nowak, Ben J. M. Heijmen,
Joost J. Nuyttens, Rene P. Brandwijk, Cornelis Verhoef,
Jan N. M. IJzermans, and Peter C. Levendag

Int. J. Radiation Oncology Biol. Phys., Vol. 70, No. 5, pp. 1447-1452, 2008

ABSTRACT

Purpose: Stereotactic body radiation therapy (SBRT) provides a high local control rate for primary and metastatic liver tumors. The aim of this study is to assess the impact of this treatment on the patient's quality of life. This is the first report on quality of life associated to liver SBRT.

Methods and Materials: From October 2002 until March 2007, a total of 28 patients not suitable for other local treatments and with a Karnofsky performance status of at least 80%, were entered in a Phase I-II study of SBRT for liver tumors. Quality of life was a secondary end point. Two generic quality of life instruments were investigated, EuroQol-5D (EQ-5D) and EuroQoL-Visual Analogue Scale (EQ-5D VAS) , in addition, a disease-specific questionnaire, the European Organization for Research and Treatment of Cancer Core Quality of Life Questionnaire (EORTC QLQ C-30). The points of measurement were directly before, and 1, 3 and 6 months after treatment. Mean scores and SDs were calculated. Statistical analysis was performed using paired-samples *t*-test and Student *t*-test.

Results: The calculated EQ-5D index, EQ-5D VAS, and QLQ c-30 global health status showed that the mean quality of life of the patient group was not significantly influenced by the treatment with SBRT; if anything, a tendency towards improvement was found.

Conclusions: Stereotactic body radiation therapy combines a high local control rate, by delivering a high dose per fraction, with no significant change in quality of life. Multicenter studies including larger numbers of patients are recommended and under development.

Acknowledgments: The authors thank Elly Stolk, Ph.D., and Rob A. de Man, M.D., Ph.D., for their valuable contributions.

INTRODUCTION

Clinical studies on the effect of stereotactic body radiation therapy (SBRT) included local control, survival and toxicity. However, this outcome did not measure the influence of the treatment on the quality of life of patients. Quality of life is an important health parameter and provides useful information to clinicians and patients about the impact of a treatment on the health status. SBRT is an emerging local treatment option for patients with intrahepatic malignancies not eligible for surgery or radiofrequency ablation (RFA). Several reports showed high local control rates with acceptable toxicity associated to this treatment (1-4). To achieve these favorable local response rates, high radiation doses in a small number of fractions are delivered. Application of high-precision patient positioning (rigid) and control of the respiratory liver motion (5-7) may have an impact on the patient's well being during the treatment and on the subsequent quality-of-life evaluation.

The aim of the present study is to assess, prospectively, the impact of SBRT on the quality of life of patients with primary and metastatic liver tumors. To our knowledge, this is the first report of quality of life associated to hypofractionated stereotactic liver treatments.

METHODS AND MATERIALS

Patients characteristics

From October 2002 to March 2007, a total 28 patients were entered in a phase I-II study on SBRT for liver tumors, approved by the Ethical Commission of Erasmus MC and in accordance with the Declaration of Helsinki. All patients gave their written consent. Results on local control, survival, and toxicity were reported recently (3). Quality-of-life assessment was a secondary endpoint of this study. Patients included were those with a diagnosis of liver metastases or hepatocellular carcinoma (HCC), who were not candidates for other local treatments, including surgery and RFA. Liver cirrhosis assessment was suggested by the case history (hepatitis virus B infection, hepatitis virus C infection and alcohol abuse) and was performed by studying the typical aspects defining cirrhosis on computed tomography and magnetic resonance imaging. Portal hypertension splenomegaly was determined by means of imaging techniques and the presence of esophageal varices by gastroscopy. Patients with a diagnosis of liver metastases had no typical aspects of cirrhosis on computed tomography or magnetic resonance imaging. Karnofsky index was at least 80%. Patient and tumor characteristics are presented in Table 1.

Table 1. Patient and tumor characteristics

Gender	
Male	23
Female	5
Median age (years)	68 (37-81)
Patient diagnosis	
Liver metastases	19
HCC	9
Primary site of metastases	
Colorectal	17
Lung	1
Breast	1
Cirrhosis (all within HCC group)	
Child- Pugh grade A	6
Child- Pugh grade B	2
Previous treatments	
Surgery	12
Ethanol injection	2
RFA	6
Chemotherapy	10
No. of lesions treated	
Liver metastases	38
HCC	11
Median lesion size (cm)	3.0 (0.5-7)
Median lesion volume (cc)	54.5 (1.03-322.5)

HCC = hepatocellular carcinoma.

Treatment

Details on tumor delineation, patient setup, methodology used for liver motion control, treatment planning, treatment accuracy, margins and treatment delivery, have been previously published (3, 7). Briefly, patients were positioned in the Elekta stereotactic body frame (Elekta Oncology Systems, Stockholm, Sweden) with maximum tolerable abdominal compression to decrease respiratory tumor motion for planning and treatment purposes. Patients with metastases, HCC without cirrhosis, and HCC less than 4 cm with cirrhosis were treated mostly with 3 x 12.5 Gy. Patients with HCC of 4 cm or larger and cirrhosis received 5 x 5 or 3 x 10 Gy. The prescription isodose was 65%. Treatment plans were generated with the Cadplan treatment planning system (Varian Oncology Systems, Palo Alto, CA) with a median of eight coplanar and noncoplanar beams (range 4-10 beams). Acute toxicity was evaluated during the first 3 months after treatment by using the Common Toxicity Criteria, version 2.0, of the National Cancer Institute. The Subjective, Objective, Management and Analytic Scales/ Late Effects of Normal Tissue (SOMA/LENT) grading system was used to score the late toxicity (3).

Quality of life instruments

The effect of SBRT on quality of life was studied by using two generic quality of life instruments, the EuroQol-5D (EQ-5D) and the EuroQoL-visual analogue scale (EQ-5D VAS), in addition to a disease-specific questionnaire, the European Organization for Research and Treatment of Cancer Core Quality of Life Questionnaire (EORTC QLQ C-30). Patients completed these three instruments at home using a validated Dutch translation. Measurements obtained with these questionnaires were meant to describe what the patient has experienced as a result of the treatment intervention, and to supplement traditional measures of health (3, 8).

The EQ-5D is a standardized instrument for use as a measure of health outcome applicable to a wide range of health conditions and treatments. It was developed by a multidisciplinary international group (the EuroQoL Group), (9, 10) as a generic questionnaire comprising five domains: mobility, self-care, usual activities, pain/discomfort and anxiety/depression. Each question has three response categories: 1, indicates no problems; 2, some or moderate problems; and 3, inability or extreme problems. Responses to the items are combined to give a descriptive health-related quality-of-life state (11). The EQ-5D VAS is a sixth item added to the other EQ-5D domains to give a global evaluation of the health state using a VAS ranging from 0 (worst imaginable health state) to 100 (best imaginable health state) (12). The QLQ C-30 (version 1.0) is a reliable and validated instrument developed by the EORTC to evaluate the quality of life of patients with cancer in multicultural clinical research settings (13). It is a 30-item questionnaire composed of multi-item scales and single items. It incorporates five functional scales (physical, role, cognitive, emotional and social), three symptom scales (fatigue, pain and nausea and vomiting) and a global health and quality-of-life scale. The remaining single items assess additional symptoms commonly reported by patients with cancer (dyspnea, appetite loss, sleep disturbance constipation and diarrhea) as well as the perceived financial impact of the disease and treatment. All scales and single items have a score range of 0-100. A high score for a functional scale represents a high/healthy level of functioning. A high score for the global health status represents a high quality of life. However, a high score for a symptom item represents a high level of symptomatology/problems.

Time points for assessing quality of life

Published reports on liver SBRT showed that treatment-related effects were expected mainly within the first 6 months after treatment (1-4, 14). Based on this observation, our main goal was to get most of the quality-of-life questionnaires completed and returned within 1 month before treatment (baseline), and at 1, 3 and 6 months after treatment. Additional information on quality-of-life data was registered every 3 months during the first year and every 6 months thereafter. Patients with evidence

of disease progression during follow-up were referred to other departments, and no further quality-of-life information was requested to prevent bias caused by other treatment modalities or the effect of the disease.

For those patients treated more than once, we assumed that the treatment was not finalized until the last course was completed. This means that the selected measure times started before the first treatment (baseline) and were resumed, according to the schedule, after the last treatment was delivered.

Statistical analysis

Mean scores and SDs were calculated for the EQ-5D index, the EQ-5D VAS and all the EORTC scales. Comparisons with the EQ-5D index obtained from a general Dutch population and with the QLQ C-30 global health status from a general Norwegian population were performed. Statistical analysis was carried out with the statistical program SPSS version 12.0 (SPSS Inc., Chicago, IL). Paired-samples *t*-test and Student *t*-test were carried out. The level of statistical significance was considered $p < 0.05$ for all the calculations.

RESULTS

Data collection

Twenty-eight treated patients were considered candidates to be included in this study. One patient with residence outside The Netherlands was excluded because of lack of adequate follow-up. In addition, 1 patient did not want to participate in the study. From the remaining 26 patients, 25 pretreatment forms were submitted. One questionnaire was missing.

One month after treatment, 1 patient died (possibly treatment-related death) and 1 patient did not return the form (missing). From 25 patients available for follow-up, 24 forms were returned.

At 3 months, 1 patient was transferred to another department because of disease progression, 2 patients did not respond because they were on holidays outside the country and they had not taken the questionnaires, and 5 forms were missing. From 24 patients available for follow-up, 17 forms were returned for analysis.

At 6 months, 4 more patients were referred to other departments because of disease progression. The remaining 20 patients available for data submission completed and returned the instruments.

After 6 months, the number of collected forms decreased rapidly. At 9 months, only eight forms were returned and two were missing. At 12 months, seven forms were collected. At 18, 24 and 30 months only three, three and two forms were returned,

respectively. At these times, most patients underwent chemotherapy because of disease progression.

In all cases, when the patient responded, all three questionnaires, the EQ-5D, EQ-5D VAS and EORTC QLQ C-30, were completed.

Quality of life analysis

An overview of the quality-of-life domains at different time is listed in Table 2.

Mean values corresponding to the EQ-5D index, EQ-VAS score and C-30 global health status increased after treatment compared with the baseline (Fig. 1). However, no statistical significance was evidenced when paired *t*-tests between baseline values and those obtained at 1, 3 and 6 months after treatment were performed. Mean values corresponding to symptom-specific domains seemed to increase after treatment (presence of more intense symptoms). Except for fatigue at 1 month (p = 0.004), paired t-tests comparing functional and symptom items at baseline and after treatment did not show a statistical significant difference.

Table 2. Mean values and standard deviations of EQ-5D health state index, EQ-5D VAS score, EORTC QLQ C-30 global health status and C-30 functional and symptoms scales

	Baseline (n = 25)		+1 Month (n = 24)			+3 Month (n = 17)			+6 Month (n = 20)		
	Mean	SD	Mean	SD	p	Mean	SD	p	Mean	SD	p
EQ-5D health state index	0.79	0.21	0.81	0.17	0.85	0.80	0.17	0.84	0.81	0.24	0.69
EQ-5D VAS score	69.2	16.1	70.8	15.0	1.00	72.9	16.5	0.54	71.3	16.8	0.71
C-30 global health status	50.3	21.0	55.2	17.0	0.51	60.8	20.1	0.12	55.0	19.4	0.58
Functional scales											
Physical Functioning	72.0	20.0	70.0	21.3	0.18	70.6	18.9	0.38	75.0	18.2	0.66
Role Functioning	68.0	31.9	68.8	28.8	1.00	73.5	25.7	0.08	77.5	25.5	0.66
Emotional Functioning	74.6	22.0	77.4	20.6	0.40	78.9	22.6	0.29	82.9	15.9	0.19
Cognitive Functioning	80.0	25.0	81.3	19.8	1.00	87.3	23.2	0.72	86.7	15.9	0.17
Social Functioning	82.0	26.3	84.0	25.3	0.60	81.4	23.5	0.77	90.0	13.7	0.81
Symptom scale/item											
Fatigue	26.2	22.6	34.3	24.1	<0.01	28.1	17.6	0.53	29.4	19.5	0.20
Nausea & Vomiting	5.3	12.5	4.2	8.9	0.78	4.9	9.8	0.77	7.5	12.7	1.00
Pain	16.0	21.2	16.7	22.5	1.00	16.7	20.6	0.54	20.6	28.8	0.61
Dyspnea	16.0	23.8	22.2	27.2	0.26	21.6	23.4	0.18	20.0	22.7	1.00
Insomnia	20.0	27.2	20.9	30.8	0.66	25.6	32.4	0.49	25.2	32.4	0.37
Appetite loss	8.0	17.4	8.3	17.7	0.57	15.7	26.6	0.06	13.3	22.7	0.18
Constipation	5.3	20.8	6.9	19.6	0.71	3.9	16.2	0.33	8.3	23.9	1.00
Diarrhea	9.3	18.1	4.2	11.3	0.66	3.9	11.1	0.58	6.7	13.7	1.00
Financial difficulties	6.7	19.2	6.9	24.0	1.00	9.8	28.3	1.00	5.0	16.3	1.00

All p-values were obtained using paired-samples t-test between baseline and 1, 3 and 6 months after treatment.
Abbreviations: EQ-5D=EuroQoL-5D, EQ-5D VAS=EuroQoL Visual Analogue Scale, EORTC QLQ C-30=European Organization for Research and Treatment of Cancer Core Quality of Life Questionnaire.

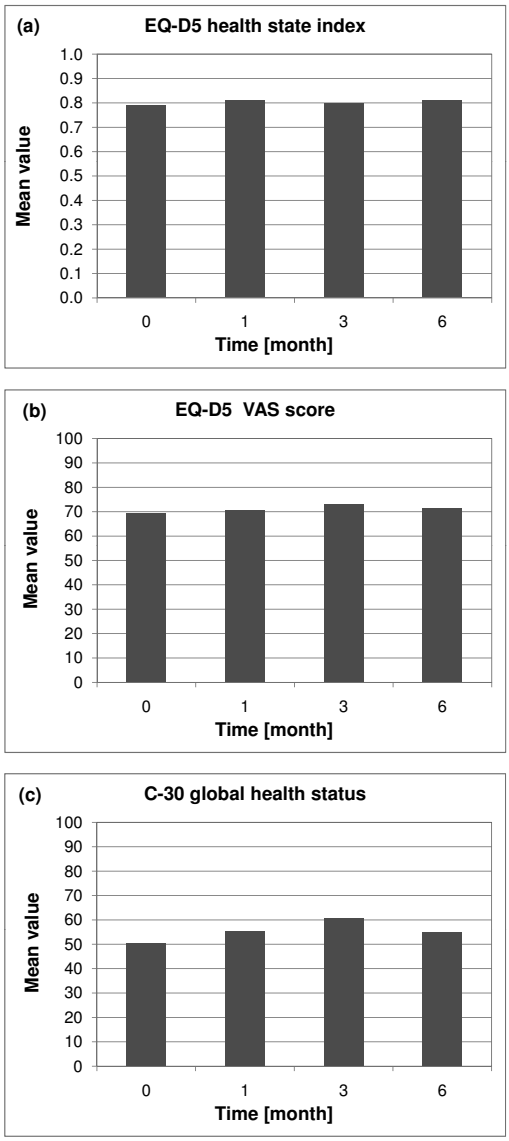

Fig. 1. Mean values of the (a) EuroQoL (EQ-5D) health state index, (b) EuroQoL-Visual Analogue Scale (EQ-5D VAS) score, and (c) European Organization for Research and Treatment of Cancer Core Quality-of-Life Questionnaire (EORTC QLQ C-30) global health status.

Comparison with baseline values of a general population

A statistically significant difference ($p = 0.014$) was found by using Student *t*-test between the baseline EQ-5D index from our group and the EQ-5D of a general Dutch population group between 60-69 years (mean 0.86 years; SD 0.20 years; E.A. Stolk, personal communication, January 2007). Comparison with the EORTC global health status obtained from a general Norwegian population group between 60-69 years, (mean age for male group 73.6 years; for female group, 69.4 years) and assuming the same SD, (not reported) also showed a statistically significant difference ($p < 0.001$) (15).

DISCUSSION

Stereotactic body radiation therapy applied to primary and metastatic liver tumors showed a high local control rate. Our aim was to investigate whether this positive effect was achieved without quality-of-life impairment. Our results show that quality of life did not deteriorate despite the delivered high-fraction doses.

Based on the health-related quality-of-life conceptual model proposed by Wilson and Cleary (8), we analyzed quality of life at several levels: general health perceptions, functioning and symptoms. General health perceptions were measured by using the EQ-5D health state index, EQ-5D VAS score and QLQ C-30 global health status index. They constitute our primary result. Although mean values obtained at baseline were lower than in the general population, they remained quite stable after treatment. Functional and symptom status were evaluated by using the EORTC C-30 functional and symptom domains, respectively. Mean values corresponding to functional domains were also stable after treatment compared with baseline. Mean values corresponding to symptom domains, showed slightly higher scores after treatment, although only fatigue at 1 month resulted in a significant difference compared with baseline. This fact did not affect the subjective evaluation of quality of life.

The purpose of the study was specifically to evaluate the impact of the treatment on the quality of life of the patients by means of quality-of-life questionnaires. We believe we obtained high response rate; 96% before treatment, and 96%, 70% and 100% at 1, 3 and 6 months after treatment respectively. One has to realize that patients were only studied in case of response or stable disease. That is, if disease progression was detected, patients were excluded from further analysis to avoid bias from other treatments or from the effect of the disease.

To test robustness of our results, we compared our findings with the literature. Clinical studies that have analyzed the impact of local liver treatments on quality of life are scarce. Moreover, the fact that different groups were administrated different instruments to measure quality of life, which makes comparison almost impossible.

We compared the EQ-5D health state index and EORTC QLQ C-30 global health status between available data obtained from general population samples and our patient group. The aim was to investigate whether the baseline scores of our group were similar to those of the general population. As expected, EQ-5D scores in our group were significantly lower than those obtained in a sample from the general Dutch population. In addition, comparison with the EORTC QLQ C-30 global health status obtained from a general Norwegian population (15) showed the same result. These observations possibly reflect the impact of disease and treatments on the patient's life regardless of a readjustment process (discussed next).

Langehoff *et al*. (16) analyzed quality of life after surgical treatment in three groups of patients with colorectal liver metastases. The first group underwent the planned

resection of metastases or was treated with local tumor ablation if resection alone was not possible. The second group was found to have inoperable disease at laparotomy and underwent exploratory laparotomy only (no resection or local ablative therapy with curative intent was possible). The third group consisted of patients referred for surgery, but judged to have inoperable disease and therefore not scheduled for surgery. This last group was included as a control group. The same three quality-of-life instruments as applied in our study were administered; the EQ-5D, the EQ-5D VAS; and the EORTC QLQ C-30. Quality-of-life data before the intervention and at 2 weeks, 3 and 6 months after that were reported. Although the EQ-5D baseline is more or less similar to our group, they found, contrary to us, EORTC scales similar to norm scores obtained from the general population. They suggested that these high scores might be caused by a reframing process. Reframing (17) is described as an integral part of patient's adaptation to disease and treatment and is related to the patient's ability to adjust to the limitations of disease and treatment. A potential explanation may be that regardless of a reframing process, the outcome reflected that the patients referred for SBRT had already experienced an extensive treatment armamentarium, including (several) liver resections or RFA procedures and different chemotherapy schemes. An evident decrease of global health status and functional scales was found by Langehoff *et al*. (16), together with an increase in symptoms scales at 2 weeks after the operation for Groups 1 and 2 that returned to baseline at 3 months for Group 1 and at 6 months for Group 2. Our data did not show a decrease in quality of life directly after treatment. Within the symptoms domain, fatigue was the only item that showed a statistical significant difference (at 1 month), and might be associated with the treatment effect. Contrary to Group 3 of Langehoff *et al*. (16), with decreased scores at 6 months in absence of treatment, remarkably, after SBRT, we found no significant decrease of quality-of-life domains 6 months after treatment. This suggests that SBRT, as surgery or RFA, may help to maintain the patient's quality of life.

Wietzke-Braun *et al*. (18) analyzed to the impact of ultrasound-guided laser interstitial thermotherapy on quality of life in patients with unresectable liver metastases from primary colorectal cancer. The administered questionnaire was the EORTC QLQ C-30, and the times for evaluation were before treatment, and at 1 week, 1 month and 6 months after the intervention. In agreement with our findings, they also reported no significant change in functional scales or global health status after treatment. A significant increase in symptoms regarding pain was detected. They suggest that this might be related to the local incision and insertion of the catheter. Contrary to the significant increase in fatigue only during the first month after SBRT, increased pain after ultrasound-guided laser interstitial thermotherapy reached statistical significance not only 1 week after treatment but also 6 months after that.

Our study presents the main limitation of the small number of patients. Therefore, the positive findings reported here need confirmation in a larger study. The North European Liver Tumor Group is preparing a Phase III randomized trial for liver metastases, comparing RFA with SBRT. Data will be collected from 300 patients to analyze recurrence-free survival as a primary end point, and quality of life as a secondary end point.

CONCLUSIONS

Data from this study show that apart from the high local control rate, SBRT was also associated with a constant quality of life, maintaining the pretreatment level in the 6 months after the treatment period. Obviously, despite the delivered high doses, there is no posttreatment decrease in quality of life related to unavoidable exposure of healthy tissues. Possibly, the obtained local control resulting from the high doses may even prevent a decrease in quality of life. Currently, in Europe, a large study is being prepared that will provide data to validate these findings.

REFERENCES

1. Hoyer M, Roed H, Traberg HA, *et al*. Phase II study on stereotactic body radiotherapy of colorectal metastases. *Acta Oncol* 2006;45:823-830.
2. Kavanagh BD, Schefter TE, Cardenes HR, *et al*. Interim analysis of a prospective phase I/II trial of SBRT for liver metastases. *Acta Oncol* 2006; 45:848-855.
3. Méndez Romero A, Wunderink W, Hussain SM, *et al.* Stereotactic body radiation therapy for primary and metastatic liver tumors: A single institution phase i-ii study. *Acta Oncol* 2006;45:831-837.
4. Wulf J, Guckenberger M, Haedinger U, *et al*. Stereotactic radiotherapy of primary liver cancer and hepatic metastases. *Acta Oncol* 2006;45:838-847.
5. Dawson LA, Brock KK, Kazanjian S, *et al*. The reproducibility of organ position using active breathing control (ABC) during liver radiotherapy. *Int J Radiat Oncol Biol Phys* 2001;51:1410-1421.
6. Lax I, Blomgren H, Naslund I, *et al*. Stereotactic radiotherapy of malignancies in the abdomen. Methodological aspects. *Acta Oncol* 1994; 33:677-683.
7. Wunderink W, Romero AM, Osorio EM, *et al.* Target coverage in image-guided stereotactic body radiotherapy of liver tumors. *Int J Radiat Oncol Biol Phys* 2007;68:282-290.
8. Wilson IB, Cleary PD. Linking clinical variables with health-related quality of life. A conceptual model of patient outcomes. *JAMA* 1995;273:59-65.
9. EuroQol--a new facility for the measurement of health-related quality of life. The EuroQol Group. *Health Policy* 1990;16:199-208.
10. http://www.euroqol.org
11. Jenkinson C, Gray A, Doll H, *et al.* Evaluation of index and profile measures of health status in a randomized controlled trial. Comparison of the Medical Outcomes Study 36-Item Short Form Health Survey, EuroQol, and disease specific measures. *Med Care* 1997;35:1109-1118.
12. Essink-Bot ML, Krabbe PF, Bonsel GJ, *et al.* An empirical comparison of four generic health status measures. The Nottingham Health Profile, the Medical Outcomes Study 36-item Short-Form Health Survey, the COOP/WONCA charts, and the EuroQol instrument. *Med Care* 1997; 35:522-537.
13. Aaronson NK, Ahmedzai S, Bergman B, *et al.* The European Organization for Research and Treatment of Cancer QLQ-C30: a quality-of-life instrument for use in international clinical trials in oncology. *J Natl Cancer Inst* 1993; 85:365-376.
14. Herfarth KK, Debus J, Lohr F, *et al.* Stereotactic single-dose radiation therapy of liver tumors: results of a phase I/II trial. *J Clin Oncol* 2001; 19:164-170.
15. Hjermstad MJ, Fayers PM, Bjordal K, *et al.* Health-related quality of life in the general Norwegian population assessed by the European Organization for Research and Treatment of Cancer Core Quality-of-Life Questionnaire: the QLQ=C30 (+ 3). *J Clin Oncol* 1998;16:1188-1196.
16. Langenhoff BS, Krabbe PF, Peerenboom L, *et al.* Quality of life after surgical treatment of colorectal liver metastases. *Br J Surg* 2006;93:1007-1014.
17. Bernhard J, Hurny C, Maibach R, *et al.* Quality of life as subjective experience: reframing of perception in patients with colon cancer undergoing radical resection with or without adjuvant chemotherapy. Swiss Group for Clinical Cancer Research (SAKK). *Ann Oncol* 1999;10:775-782.
18. Wietzke-Braun P, Schindler C, Raddatz D, *et al.* Quality of life and outcome of ultrasound-guided laser interstitial thermo-therapy for non-resectable liver metastases of colorectal cancer. *Eur J Gastroenterol Hepatol* 2004; 16:389-395.

4

COMPUTER OPTIMIZATION OF NONCOPLANAR BEAM SETUPS IMPROVES STEREOTACTIC TREATMENT OF LIVER TUMORS

Jacco A. de Pooter, Alejandra Méndez Romero, Wim P. A. Jansen, Pascal R. M. Storchi, Evert Woudstra, Peter C. Levendag, and Ben J. M. Heijmen

Int. J. Radiation Oncology Biol. Phys., Vol 66, No. 3, pp. 913-922, 2006

ABSTRACT

Purpose: To investigate whether computer-optimized fully noncoplanar beam setups may improve treatment plans for the stereotactic treatment of liver tumors.

Methods: An algorithm for automated beam orientation and weight selection (Cycle) was extended for noncoplanar stereotactic treatments. For 8 liver patients previously treated in our clinic using a prescription isodose of 65%, Cycle was used to generate noncoplanar and coplanar plans with the highest achievable minimum planning target volume (PTV) dose for the clinically delivered isocenter and mean liver doses, while not violating the clinically applied hard planning constraints. The clinical, and the optimized coplanar and noncoplanar plans were compared, with respect to $D_{PTV,99\%}$, the dose received by 99% of the PTV, the PTV generalized equivalent uniform dose (*gEUD*) and the compliance with the clinical constraints.

Results: For each patient, the ratio between $D_{PTV,99\%}$ and D_{isoc}, and the $gEUD_{-5}$ and $gEUD_{-20}$ values of the optimized noncoplanar plan were higher than for the clinical plan with an average increase of respectively 18.8% (range 7.8-24.0%), 6.4 Gy (range 3.4-11.8 Gy) and 10.3 Gy (range 6.7-12.5). $D_{PTV,99\%}/D_{isoc}$, $gEUD_{-5}$ and $gEUD_{-20}$ of the optimized noncoplanar plan was always higher than for the optimized coplanar plan with an average increase of respectively 4.5% (range 0.2-9.7%), 2.7 Gy (range 0.6-9.7 Gy) and 3.4 Gy (range 0.6-9.9 Gy). All plans were within the imposed hard constraints. On average, the organs at risk were better spared with the optimized noncoplanar plan than with the optimized coplanar plan and the clinical plan.

Conclusions: The use of automatically generated, fully noncoplanar beam setups results in plans that are favorable compared to coplanar techniques. Because of the automation, we found that the planning workload can be decreased from 1 to 2 days to 1 to 2 h.

INTRODUCTION

The number of patients with metastatic or primary liver tumors treated with external beam radiotherapy is increasing. Often the patients treated with this modality can not be operated on or treated with another local modality such as radio frequency ablation, or percutaneous ethanol injection therapy.

In some institutes, hypofractionated stereotactic radiotherapy is used (1-6), applying a stereotactic body frame (SBF) with abdominal compression for reduction of respiratory tumor motion. In 2002, using the Elekta SBF (Elekta AB, Stockholm, Sweden), this type of treatment has been started in our clinic, for metastatic and hepatocellular carcinoma (HCC) lesions. Patients accepted for treatment cannot be treated with surgery or other local treatments such as radiofrequency ablation or percutaneous ethanol injection. The maximum allowed diameter of the lesion is 6 cm. With the patient positioned in the SBF, arterial and venous contrast computed tomography (CT) scans are made for tumor definition as well as a planning CT scan for contouring of the organs at risk (OAR). Delineated tumors in the arterial and venous CT scans are summed to construct the definitive clinical target volume (CTV). To determine the required CTV-to-planning target volume (PTV) margin, the residual respiratory tumor motion, is assessed with fluoroscopy at a conventional simulator using implanted fiducials. The patients are treated mostly with three fractions of 10-12.5 Gy (depending on disease type and tumor size), prescribed at the 65% isodose, that closely surrounds the PTV. This inhomogeneous dose concept is based on the work of Lax *et al*. (7). They showed that for a constant dose at the periphery of the PTV, a 50% increase in the target center dose can be obtained, compared with a homogeneous dose concept, without a substantial increase of dose to the normal tissue. To irradiate liver tumors, most clinics use three-dimensional conformal therapy with a set of manually selected beam directions and forward treatment planning. Generally, coplanar beam directions are used, whereas in some cases, noncoplanar setups have been applied (8, 9). Thomas *et al*. (10) investigated for a group of patients whether manually chosen noncoplanar beam setups (i.e., with noncoplanar and coplanar directions) are more favorable for intensity-modulated radiation therapy treatment of liver tumors. They concluded that for the group of patients with a tumor close to an OAR, the noncoplanar setup improved the treatment plan. For the other patients, the plans with a noncoplanar beam setup were as good as those with a seven beam equidistant coplanar setup or as those using the beam setup of the clinical plan.

In this article, we have investigated the benefit of noncoplanar beam setups for hypofractionated, stereotactic treatment of liver tumors, using automated beam direction selection from a large set of coplanar and noncoplanar input directions. For this purpose, our in-house developed beam direction selection algorithm, Cycle (11,12), was extended for handling of stereotactic (inhomogeneous) PTV dose distributions

including an option for beam shape optimization. For 8 liver patients previously treated in our clinic using a prescription isodose of 65%, Cycle was used to generate noncoplanar and coplanar plans with the highest achievable minimum PTV doses for the clinically delivered isocenter and mean liver doses. The clinically applied hard planning constraints were also used for the automated plan generation. The clinical, and the optimized coplanar and noncoplanar plans were compared, with respect to $D_{PTV,99\%}$, the dose received by 99% of the PTV, the PTV generalized equivalent uniform dose (*gEUD*), and the distance from the applied constraint levels.

METHODS AND MATERIALS

Description of liver plans

In clinical practice, the liver treatment plans were designed by a dosimetrist using forward trial-and-error planning. Both coplanar and noncoplanar beams (open or wedged) could be selected. For practical reasons not more than 10 different directions were allowed in a plan. The dose (3 x 10 Gy or 3 x 12.5 Gy) was prescribed to the 65% isodose level. The clinical treatment plans for the 8 patients in this study consisted of five to nine coplanar beams. In addition, in Case 8, three noncoplanar beams were used. The workload of the manual treatment plan generation was 1-2 days. The delineated OAR with their clinical constraints are summarized in Table 1. Because the tumor location was heterogeneous among the patient group, not all OARs were always relevant for all patients.

Short description of Cycle algorithm

The general principles of the Cycle algorithm for automated beam orientation and weight selection have been described in detail by Woudstra *et al*. (11-14). Here, a summary is given with the focus on some extensions. The algorithm aims at generating a treatment plan with the prescribed tumor dose (isocenter), whereas not exceeding the imposed hard constraints. The algorithm starts with an empty plan. Sequentially (Fig. 1), new beams are added to the plan by selection from a large set of potential input directions based on a score function.

The selection of beams stops, if the selected beams result in a plan that can be scaled to the prescribed PTV dose without violation of any constraint level (the plan generation is successful), or if no more beams can be added without violation of one of the constraints, or if the number of allowed directions is reached. In the last 2 cases a new plan generation is started with automatically adjusted penalty factors in the score function (11, 12).

Table 1. Applied constraints in the iterative optimization of the minimum PTV dose

Structure	Constraint	Constraint parameter
PTV	$D_{PTV,rel} < D^{tol}_{PTV,rel}$ (n)	N.A.
Normal liver	$D_{mean} < D_{mean,clinical}$	N.A.
Normal liver	$D_{50\%}$ <15 Gy	$D_{50\%}$/15
Normal liver	$D_{33\%}$ <21 Gy	$D_{33\%}$/21
Spinal cord	D_{max} <15 Gy	D_{max}/15
Bowel, duodenum, stomach, esophagus, heart, aorta.	D_{5CC} <21 Gy	D_{5CC} /21
Kidney's	$D_{33\%}$ <15 Gy	$D_{33\%}$/15
R_1	D_{max}	N.A.
R_2	D_{max} <20 Gy	N.A.

NA = not applicable; PTV = planning target volume.

$D^{tol}_{PTV,rel}$ (n) is the applied constraint level in iteration n on the relative PTV dose inhomogeneity. In the iterative procedure, $D_{PTV,rel}$ is minimized by repeated runs of Cycle with decreasing values of $D^{tol}_{PTV,rel}$ (see text). $D_{a\%}$ indicates that a% of the volume receives a dose of at least $D_{a\%}$ and D_{aCC} indicates that *a CC* receives a dose of at least D_{aCC}. Structures R_1 and R_2 and the maximum tolerated dose in R_1 are defined in the text. The constraint parameters, C_j , for OAR constraints, j, are required for calculation of the *DIP* (eq. 2).

Strictly speaking, by itself, Cycle is not an optimization algorithm; its aim is generation of an acceptable plan (i.e. attaining the prescribed dose without exceeding the constraints). The score function is used to build such an acceptable plan and not to define and generate the "best" plan. However, in an iterative loop, the algorithm may indeed be used to optimize a plan parameter (14). In this study, such a procedure was used to maximize the minimum PTV dose (see below, section "Maximizing the minimum PTV dose").

Beam shape optimization

Usually beam direction optimization for three-dimensional conformal radiotherapy is performed with a fixed field/segment shape for each of the beam directions in the initial set (11-15). Often the beams' eye view (BEV) projection of the target and an additional margin for the penumbra is used for the determination of the field shape (11, 16).

In this article, we study stereotactic treatments with highly inhomogeneous PTV dose distributions that are very sensitive to the selected beam sizes. Because each selected beam passes through the liver, each beam contributes to the mean liver dose. The contribution of an individual beam is approximately proportional to the liver volume incorporated by that beam, which is proportional to the area of the field of that beam. On average, the fields have a diameter in the order of about 5 cm. An addition or subtraction of a margin of 0.5 cm from the field shape, may therefore increase/reduce the field area by about 30%.

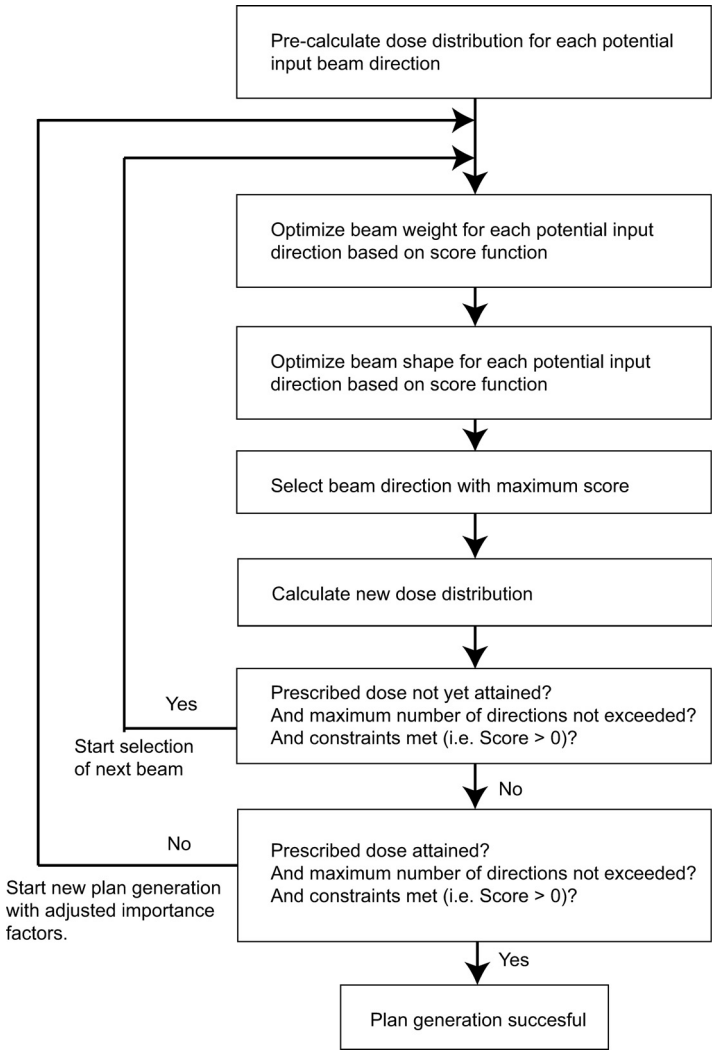

Fig. 1. Schematic diagram of the Cycle algorithm.

Therefore an extension was made to the Cycle algorithm, to enable optimization of the field shape for each input direction. First, an initial field shape is made, based on the BEV projection of the target (without penumbra margin). With this shape the beam weight is optimized. After that, the algorithm tries to further increase the score by expanding or reducing the margin in small steps (2 mm), in four independent perpendicular directions (+x, -x, +y, -y). Each step requires a recalculation of the off-axis dose distribution of the beam. A beam direction can be selected multiple times. In general, each time it will be selected with a different shape and weight; therefore, a plan can have multiple segments per beam direction.

Input beam directions

For the coplanar plans, Cycle used 72 input beam directions evenly distributed in the axial plane. For the noncoplanar plans, the input beam directions were distributed in separate sets of 36 or 72 beam directions. The beam directions in each set have the same angle with the axial plane, α, and they are evenly distributed with an equal separation in θ (see Fig. 2). For $\alpha = 0$ (i.e. the axial plane), the same 72 input beam directions were used as for the coplanar plans. For sets with other α values (i.e. for the noncoplanar input beams), 36 input beam directions were used.

Increments in α of 10° were used. The upper and lower α were determined manually, using the BEV (see Table 2). The set of noncoplanar beam directions with the α_{up} or α_{low} is the set with the highest $|\alpha|$ for which none of the beams enters through the upper (cranial) or lower (caudal) CT slice, i.e. α_{up} and α_{low} were determined by the cranialcaudal extent of the CT scan. If the separation between α_{up} or α_{low} and the nearest set of input directions was $\geq 5°$, an extra set of input beam directions was defined for α_{up} or α_{low}.

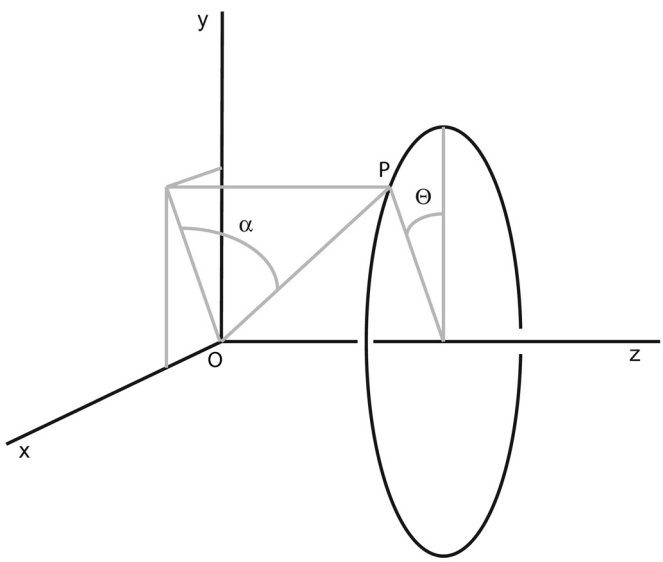

Fig. 2. Patient coordinate system and angles α, θ for definition of the input noncoplanar beam directions. O is the isocenter and, z is the cranialcaudal direction of the patient. OP is an example of a beam direction. α is the angle of the *xy*-plane (axial plane) with OP.

Maximizing the minimum PTV dose

In the procedure to maximize the minimum PTV dose, the isocenter dose in the clinical plan was used as the prescribed dose for the PTV, D^{pre}_{PTV}. The minimum PTV dose was then optimized in an iterative procedure, by minimizing the relative PTV dose inho-

Table 2. Patient characteristics, the prescribed dose for the clinical plans (65 % isodose), the α_{low} and α_{up} defining the sets of input beam directions and, the number of input directions for the noncoplanar plan

Case	V_{PTV} (CC)	V_{liver} (CC)	Prescription dose (Gy)	α_{low}	α_{up}	No. of input beam directions
1	74.5	1271.0	3 x12.5	-30	5	216
2	113.4	1228.0	3 x12.5	-30	19	252
3	121.4	768.3	3 x12.5	-30	10	216
4	105.9	1869.0	3 x12.5	-30	5	216
5	211.8	1601.0	3 x10.0	-20	10	180
6	46.9	1011.0	3 x10.0	-30	20	252
7	111.2	985.9	5 x 5.0	-9	9	144
8	264.7	1632.0	3 x12.5	-28	10	216

mogeneity, $D_{PTV,rel} = (D_{isoc}/D_{PTV,min})/D_{isoc}$ (see Table 1). In first instance, for the constraint on the relative PTV dose inhomogeneity, $D^{tol}_{PTV,rel}$, the level of the clinical plan was used (35%). If Cycle succeeded in generating a plan, the $D^{tol}_{PTV,rel}$ level was decreased with a step of 1%. This was repeated until plan generation was no longer successful (i.e. D^{pre}_{PTV} could not be attained without a constraint violation). As mentioned previously, the allowed maximum number of beam directions in the clinical plans was 10. To generate clinically acceptable plans, and for a straightforward comparison with the manually created clinical plans, the allowed number of beam orientations in the Cycle plans was also limited to 10. Apart from the $D^{tol}_{PTV,rel}$ constraint, generation of plans was always subject to the constraints in Table 1. To end up with a probability on liver complication for the optimized plans equal to or lower than the clinical plan, the mean dose constraint on the normal liver volume (i.e. the entire liver minus the CTV) was set to the clinically achieved mean normal liver dose value (17).

For Cases 5-7, the clinical plan had a relatively low prescribed dose (Table 2). For these patients, in a second step, an attempt was made to escalate the absolute isocenter PTV dose. This was again done in an iterative way, by increasing the prescribed isocenter dose while keeping the relative PTV dose inhomogeneity constraint, $D^{tol}_{PTV,rel}$, constant. For $D^{tol}_{PTV,rel}$, the value used in the last iteration of the optimization procedure for the minimum PTV dose (see previous) was used. The iterative procedure was stopped if further isocenter dose increase was prevented by a constraint violation.

Nonorgan-specific regions in normal tissue

Apart from organ based constraints (e.g. for the kidneys) for automated plan generation, two other regions were defined in the normal tissue by expansions of the PTV (expansion 1 is the PTV plus a 2.0 cm margin, expansion 2 is the PTV plus a 5.0 cm margin). Region R_1, was all tissue outside expansion 1 and inside expansion 2. Region R_2, was all tissue outside expansion 2. For each region a maximum dose constraint was imposed (Table 1). The constraint on R_1 aims at conformality of the dose distribution

to the target volume, whereas the constraint on R_2 avoids hot spots far away from the target volume. The value for the constraint on R_1 was chosen 5-10 Gy lower than the minimum PTV dose level. The exact value of this constraint was chosen in such a way, that it was not a limiting constraint for maximizing the minimum PTV dose. If, during the optimization process, a plan generation failed because of violating this constraint, the constraint level was relaxed. For R_2, a maximum dose constraint of 20 Gy was used for each patient (Table 1).

Plan comparison

As described previously, the main goal of the iterative use of Cycle was to maximize the minimum dose in the PTV, whereas not exceeding the clinically delivered mean liver dose and without violation of the other clinical constraints. In this study, the ratio between $D_{PTV,99\%}$, the minimum dose received by 99% of the PTV, and D_{isoc}, the isocenter dose, was used for evaluation of the plans. Also the *gEUD* of the PTV was evaluated using the following formula (18),

$$gEUD_a = \left(\frac{1}{N} \sum_{i=1}^{N} D_i^a \right)^{1/a} \tag{1}$$

With N the number of dose points, D_i. The a parameter (a < 0) represents the aggressiveness of the tumor, with an increased aggressiveness for more negative α values. In this study the *gEUD* was calculated with α values of -5 and -20 (10). Potentially, an improved $D_{PTV,99\%}$ value for a constant mean normal liver dose could be accomplished at the cost of a closer approach of other constraint levels. To evaluate this, the distance from ideal plan (*DIP*), as defined by Woudstra *et al*. (12), was calculated for each plan.

$$DIP = \sqrt{\sum_{j=1}^{M} \frac{C_j^2}{M}} \tag{2}$$

In which C_j are the OAR constraint parameters as mentioned in Table 1. *M* is the number of OAR constraints. For the optimized plans the maximum doses delivered to regions R_1 and R_2 in the normal tissue were also evaluated. For plan evaluation, the maximum dose in R_1 was subtracted from $D_{PTV,99\%}$. This value represents the minimum dose gradient between the PTV and region R_1.

RESULTS

PTV: Optimized noncoplanar plan vs. clinical plan

The results for the PTV of the clinical, the coplanar and the noncoplanar plans are summarized in Tables 3 and 4.

For each case, $D_{PTV,99\%}/D_{isoc}$ and the $gEUD_{-5}$ and $gEUD_{-20}$ values were substantially higher for the optimized noncoplanar plan than for the clinical plan. For $D_{PTV,99\%}/D_{isoc}$ the average increase was 18.8% (range 7.8 - 24.0%). The average increase for $gEUD_{-5}$ and $gEUD_{-20}$ was respectively 6.4 Gy (range 3.4 - 11.8 Gy) and 10.3 Gy (range 6.7 - 12.5 Gy) (Table 4). In Fig. 3, the dose-volume histograms of the normal liver volume and the PTV are plotted for Case 2. The increase in PTV dose is clearly visible. The high dose volume in the normal liver is slightly higher for the optimized plans, because of the increase in minimum PTV dose. This increase is however compensated by a smaller normal liver volume receiving a low dose, to end up with the same mean liver dose.

Table 3. $D_{PTV,99\%}/D_{isoc}$ for the clinical and the optimized coplanar and noncoplanar plans

Case	Clinical	Coplanar	Noncoplanar
1	61.0%	82.3%	85.0%
2	63.2%	76.6%	83.3%
3	70.4%	84.1%	88.4%
4	67.7%	80.0%	87.2%
5	69.1%	87.4%	87.6%
6	83,1%	87.9%	90.9%
7	61.6%	74.6%	84.3%
8	70.5%	88.6%	90.1%
Mean	68.3%	82.7%	87.2%

Table 4. $gEUD_{-5}$ and $gEUD_{-20}$ values for the clinical and the optimized coplanar and noncoplanar plans

	a = -5			a = -20		
Case	Clinical	Coplanar	Noncoplanar	Clinical	Coplanar	Noncoplanar
1	48.2	51.9	53.1	43.7	50.4	52.1
2	46.5	50.6	53.1	40.5	48.1	52.0
3	49.1	54.3	55.7	43.7	53.2	55.2
4	48.9	52.4	54.4	43.5	50.9	53.9
5	39.9	46.9	47.5	35.8	46.3	46.9
6	44.4	46.6	56.2	43.4	46.0	55.9
7	31.1	32.9	34.5	27.0	31.0	33.7
8	49.4	51.5	54.3	43.5	50.2	53.5
Mean	44.7	48.4	51.1	40.1	47.0	50.4

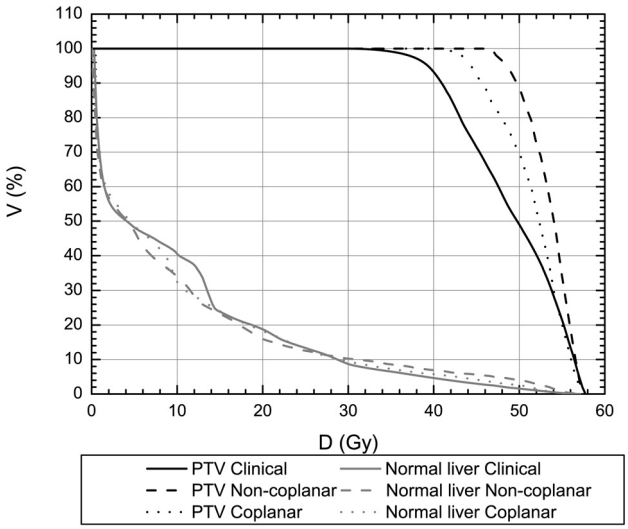

Fig. 3. DVHs of the dose distributions in the PTV and the normal liver for the clinical plan and the optimized noncoplanar and coplanar plans of Case 2.

PTV: Coplanar vs. noncoplanar plan

In each case, the optimized noncoplanar plan was better than the optimized coplanar plan (Tables 3 and 4). The increase in $D_{PTV,99\%}/D_{isoc}$ was on average 4.5% (range 0.2 - 9.7%). The average increase in $gEUD_{-5}$ and $gEUD_{-20}$ was respectively 2.7 Gy (range 0.6 - 9.7 Gy) and 3.4 Gy (range 0.6 - 9.9 Gy) (Table 4). The total number of selected beam directions was 10 for all of the optimized plans except for 1 case which had nine directions for the noncoplanar plan. The average ratio between the number of segments and the number of beam directions in a plan was 2.0 (range 1.4 - 3.1) for the noncoplanar plans, and 2.7 (range 1.8 - 3.9) for the coplanar plans.

Resulting dose distributions of Case 2 are shown in Fig. 4. Because of the close proximity of the heart, the aorta and the esophagus to the target as well as the eccentric position of the target in the liver, this case was rather complicated. In the slice 2 cm cranial from the isocenter slice, the increased dose homogeneity for the noncoplanar plan can be seen from the 45-Gy isodose, which is at the edge of the PTV for the noncoplanar plan (Fig. 4b) and inside the PTV for the coplanar plan (Fig. 4d).

PTV: dose escalation

For Cases 5-7, it was tried to escalate the isocenter dose with a constant PTV inhomogeneity as described previously. Escalation succeeded for the Cases 5 and 6. The increase in D_{isoc} with respect to the clinical plan was 3.5 Gy and 2.9 Gy for respectively the noncoplanar plan and the coplanar plan of Case 5 and 11.0 Gy and 1.5 Gy for, respectively, the noncoplanar plan and the coplanar plan of Case 6. For the noncoplanar plan of Case 6, the iteration procedure for minimization of the relative PTV dose inhomogeneity (first step, see section Maximizing the minimum PTV dose) was

stopped after the 90% PTV dose homogeneity level was reached, which was not the highest achievable homogeneity level. This explains the large increase in D_{isoc}. The liver volume in Case 7 was relatively small (Table 2), and the PTV was situated in the center of the liver. For Cases 5 and 6, the PTV was located at the edge of the liver. In the latter cases, beams could be selected that involved a rather small volume of normal liver, whereas in Case 7 this was not possible.

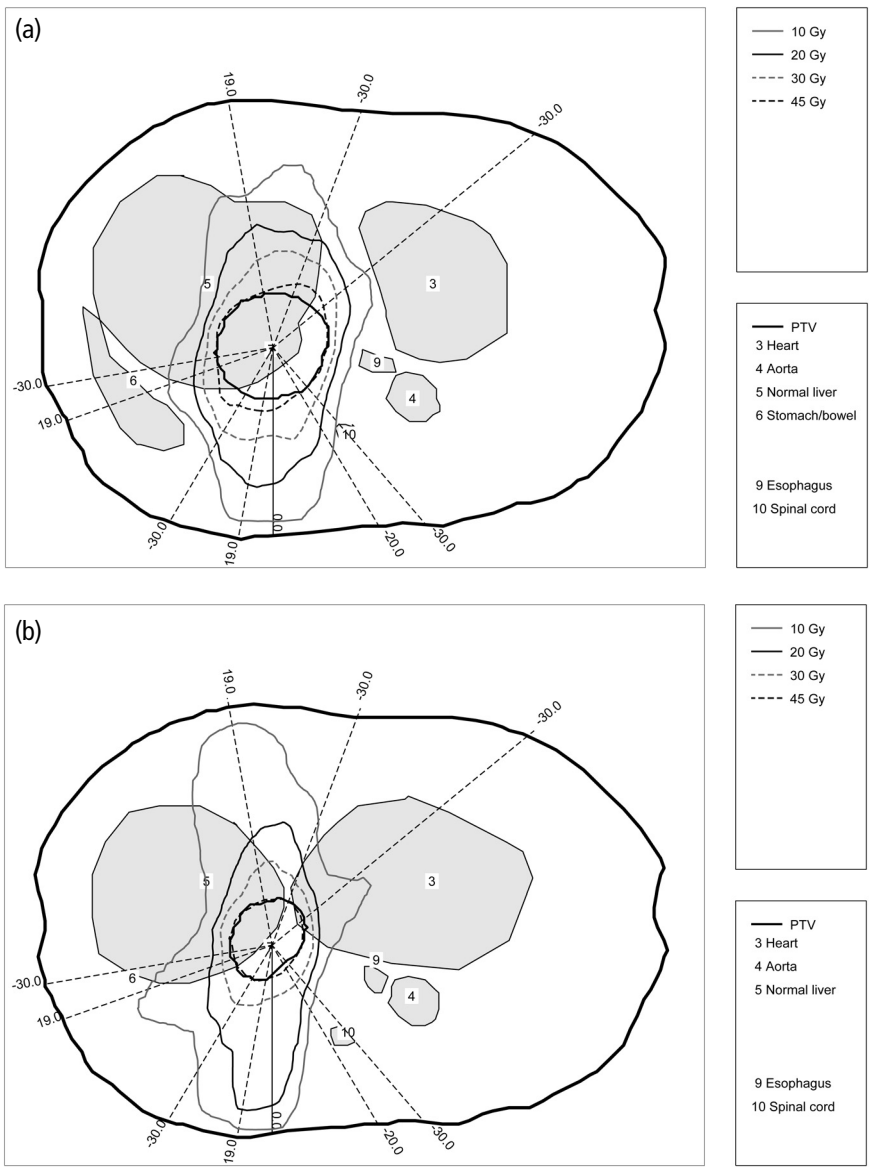

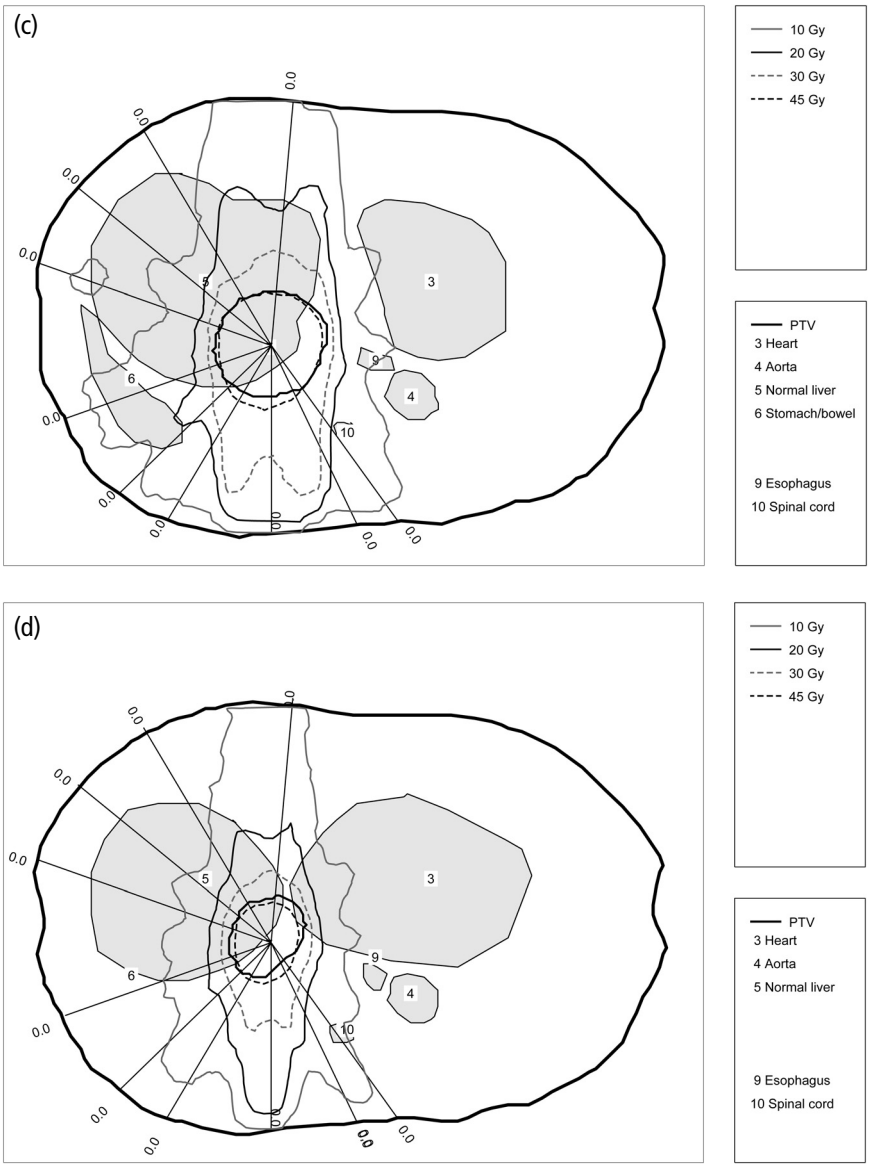

Fig. 4. Dose distributions for Case 2 for the noncoplanar plan (a and b) and the coplanar plan (c and d) for the isocenter slice (a and c) and a slice 2-cm cranial from the isocenter (b and d). The dashed lines are the projections of the beam axis of the noncoplanar beam directions in the axial slices, the solid lines are the beam axis of the coplanar beam directions. The labels indicate the angle, α, between the beam axis and the axial slices.

Normal tissues

As aimed for, all optimized plans delivered the clinically prescribed isocenter dose with the same mean liver dose as for the clinical plan, without violation of the normal

tissue constraints. The mean liver dose constraint was the limiting constraint for further increase of the minimum PTV dose in each case. In Table 5, the clinical plan and the optimized coplanar and noncoplanar plans are compared with respect to the maximum doses in the regions R_1 and R_2. In 6 of the 8 cases, the optimized coplanar plans have a higher difference between $D_{PTV,99\%}$ and the maximum dose in R_1, than the clinical plans. In 7 of the 8 cases, the optimized noncoplanar plans have a higher $D_{PTV,99\%}$ - $D_{R1,max}$, than the optimized coplanar plans. In 6 of the 8 cases the maximum dose in R_2 is lower for the optimized coplanar plan than for the clinical plan. In 6 of the 8 cases the maximum dose in R_2 is lower for the noncoplanar plan than for the coplanar plan.

The *DIP* was calculated for each case as explained in the Methods section. The average *DIP* of the optimized noncoplanar plans was both lower than the *DIP* for the clinical plans, and lower than the *DIP* for the optimized coplanar plans (Table 6). Tables 3-6 illustrate that noncoplanar beam setups allow the highest minimum PTV doses, and $gEUD_{-5}$ and $gEUD_{-20}$ values, while avoiding most approaching OAR constraint levels.

Table 5. Comparison between the noncoplanar, coplanar, and the clinical plans with respect to the maximum dose delivered to the normal tissue regions R_1 and R_2

	$D_{PTV,99\%}$ - $D_{R1,max}$			$D_{R2,max}$		
Case	Clinical	Coplanar	Noncoplanar	Clinical	Coplanar	Noncoplanar
1	8.2	6.3	14.7	19.6	19.2	17.9
2	3.4	4.5	11.8	22.1	20.0	15.6
3	1.1	21.1	22.3	21.3	18.8	17.3
4	5.3	20.3	18.1	26.3	17.8	19.1
5	3.3	7.6	8.6	12.2	19.8	19.2
6	8.5	12.5	16.4	21.4	19.2	19.0
7	6.0	5.3	7.7	13.1	13.3	14.3
8	-0.1	1.5	8.0	24.7	19.9	18.7

Table 6. Distance from ideal plan for the optimized coplanar and noncoplanar plans and the clinical plan

Case	Noncoplanar	Coplanar	Clinical
1	0.025	0.115	0.094
2	0.224	0.264	0.254
3	0.257	0.292	0.293
4	0.223	0.255	0.205
5	0.169	0.160	0.161
6	0.159	0.213	0.246
7	0.175	0.137	0.155
8	0.240	0.243	0.231
Mean	0.184	0.210	0.205

DISCUSSION

Automatically optimized beam selection for the stereotactic treatment of liver tumors results in increased $D_{PTV,99\%}$ values compared to the clinical plan, for the same isocenter and mean normal liver doses, without violation of the clinical constraints, and even avoiding best approaching these constraints. For noncoplanar beam setups the improvement in $D_{PTV,99\%}$ is higher than for coplanar beam setups. Automatically selected noncoplanar beam setups also have a higher dose gradient between the PTV and the normal tissue region R_1 than the automatically selected coplanar beam setups, and on average, a lower *DIP* than the coplanar plans.

A plan produced by Cycle has an optimal number of beams, in the sense that Cycle stops adding beams when the prescribed dose is attained. In this study, the number of selected beam directions was dependent on how strict the relative PTV dose inhomogeneity constraint,$D^{tol}_{PTV,rel}$, was set. In the first steps of the iterative optimization procedure, when $D^{tol}_{PTV,rel}$ was not very strict (see Maximizing the minimum PTV dose), the number of selected beam directions was usually lower than 10. With the $D^{tol}_{PTV,rel}$ constraint becoming more strict, the number of selected directions increased, until the maximum number of allowed beams per plan (i.e., 10) was reached. Unlike the number of beam directions, the number of segments was not limited in the plan optimization. It was demonstrated that in a coplanar plan the average number of beam segments per beam orientation was substantially higher than for the noncoplanar plan (2.7 vs. 2.0).

Except for 1 case, the number of beam directions for the plans generated by Cycle was 10. With regard to the required treatment time, this might be a high number, especially for noncoplanar cases because of the need for couch rotation. However, the treatment is given in only three fractions. So the relative effect of the high number of beams on the treatment time is much less than for a treatment with a conventional fractionation scheme. For most cases all selected directions are noncoplanar directions. Cases 5 and 8 had respectively six and seven noncoplanar directions in the beam setup of the noncoplanar plan. These two cases had the lowest improvement in $D_{PTV,99\%}$, (Table 3).

Thomas *et al*. (10) also investigated the use of noncoplanar beams for treatment of liver tumors, comparing three intensity-modulated radition therapy plans, each with a different beam setup. One setup contained noncoplanar directions, one setup used the directions applied in the clinical plan, and one setup used seven equidistant coplanar directions. They saw that the noncoplanar beam setup was only favorable in cases where the PTV incorporated another OAR besides the liver. In our study we see a clear advantage of applying noncoplanar directions in the beam setup for each case. A reason for these different observations might be that in our study the noncoplanar beam directions are computer optimized for each individual patient, which is not the

case in the study by Thomas *et al*. Moreover, in our study relatively small tumors are considered with small CTV-PTV margins, resulting from the abdominal compression, treated with stereotactic (inhomogeneous) PTV dose distributions.The maximum calculation time for a plan with Cycle (allowing 10 restarts with adjusted penalty factors) on a workstation with an Intel Xeon 3.2 *GHz* processor was 2 h for a noncoplanar plan. For coplanar planning this calculation time was reduced by a factor of three.

In this study, we have assumed that the probability of liver complications is correlated with the mean normal liver dose, as found by Dawson *et al*. (17). Recently, Cheng *et al*. (19) showed for the treatment of primary tumors, that for hepatitis B virus carriers or Child Pugh grade B, this probability might be more correlated with the high dose delivered to the normal liver. Separate analysis would be required to assess the advantage of noncoplanar beam setups for these cases.

For all patients, the tumor was located in the upper part of the set of CT slices. Therefore, for 6/8 patients, α_{up} was not larger than 10° (Table 2), so only one set of noncoplanar directions entering the patient from the cranial direction could be defined. Despite the small angles between these noncoplanar directions and the axial plane, the noncoplanar plans are better than the coplanar plans for these 6 patients. A larger improvement may be expected if a larger part of the patient in the cranial direction is scanned.

Here, we have investigated the use of computer-optimized noncoplanar beam setups to improve the PTV dose distribution for liver tumors treated with stereotactic radiotherapy. It was decided to aim at an increase in the minimum PTV dose in order to better approach the homogeneous PTV dose distribution in conventional radiotherapy. Cycle would also have allowed escalation of the isocenter dose while keeping the dose inhomogeneity constant, or escalation of the PTV *gEUD*. The choice to focus on elevation of the minimum PTV dose is in line with recent findings of Wulf *et al*. (20) who found that in stereotactic treatment of lung tumors the dose at the PTV margin was the only significant variable for local control. Integration of Cycle in the commercial treatment planning system XIO (CMS, Inc., St. Louis, MO) is being investigated.

CONCLUSIONS

The use of automatically optimized noncoplanar beam setups for stereotactic treatment of liver tumors results in treatment plans with improved PTV coverage and reduced dose delivery to healthy tissues. Compared with manual forward planning, the planning time can be reduced from 1-2 days to 2 h at maximum.

REFERENCES

1. Hadinger U, Thiele W, Wulf J. Extracranial stereotactic radiotherapy: evaluation of PTV coverage and dose conformity. *Z Med Phys* 2002;12:221-229.
2. Wulf J, Hadinger U, Oppitz U, *et al.* Stereotactic radiotherapy for primary lung cancer and pulmonary metastases: a noninvasive treatment approach in medically inoperable patients. *Int J Radiat Oncol Biol Phys* 2004;60:186-196.
3. Wulf J, Hadinger U, Oppitz U, *et al.* Impact of target reproducibility on tumor dose in stereotactic radiotherapy of targets in the lung and liver. *Radiother Oncol* 2003;66:141-150.
4. Wulf J, Hadinger U, Oppitz U, *et al.* Stereotactic radiotherapy of targets in the lung and liver. *Strahlenther Onkol* 2001;177:645-655.
5. Schefter TE, Kavanagh BD, Timmerman RD, *et al.* A phase I trial of stereotactic body radiation therapy (SBRT) for liver metastases. *Int J Radiat Oncol Biol Phys* 2005;62:1371-1378.
6. Timmerman RD, Kavanagh BD. Stereotactic body radiation therapy. *Curr Probl Cancer* 2005;29:120-157.
7. Lax I. Target dose versus extratarget dose in stereotactic radiosurgery. *Acta Oncol* 1993;32:453-457.
8. Park W, Lim dH, Paik SW, *et al.* Local radiotherapy for patients with unresectable hepatocellular carcinoma. *Int J Radiat Oncol Biol Phys* 2005;61:1143-1150.
9. Ten Haken RK, Balter JM, Marsh LH, *et al.* Potential benefits of eliminating planning target volume expansions for patient breathing in the treatment of liver tumors. *Int J Radiat Oncol Biol Phys* 1997;38:613-617.
10. Thomas E, Chapet O, Kessler ML, *et al.* Benefit of using biologic parameters (EUD and NTCP) in IMRT optimization for treatment of intrahepatic tumors. Int J Radiat Oncol Biol Phys 2005;62:571-578.
11. Woudstra E, Storchi PR. Constrained treatment planning using sequential beam selection. *Phys Med Biol* 2000;45:2133-2149.
12. Woudstra E, Heijmen BJM. Automated beam angle and weight selection in radiotherapy treatment planning applied to pancreas tumors. *Int J Radiat Oncol Biol Phys* 2003;56:878-888.
13. Woudstra E, Heijmen BJM, Storchi PR. A comparison of an algorithm for automated sequential beam orientations selection with exhaustive search and simulated annealing. Submitted. 2006.
14. Woudstra E, Heijmen BJ, Storchi PR. Automated selection of beam orientations and segmented intensity-modulated radiotherapy (IMRT) for treatment of oesophagus tumors. *Radiother Oncol* 2005;77:254-261.
15. Beaulieu F, Beaulieu L, Tremblay D, *et al.* Simultaneous optimization of beam orientations, wedge filters and field weights for inverse planning with anatomy-based MLC fields. *Med Phys* 2004;31:1546-1557.
16. Beaulieu F, Beaulieu L, Tremblay D, *et al.* Automatic generation of anatomy-based MLC fields in aperture-based IMRT. *Med Phys* 2004;31:1539-1545.
17. Dawson LA, Normolle D, Balter JM, *et al.* Analysis of radiation-induced liver disease using the Lyman NTCP model. *Int J Radiat Oncol Biol Phys* 2002;53:810-821.
18. Niemierko A. A generalized concept of equivalent uniform dose (EUD) [Abstract]. *Med Phys* 1999;26:1100.
19. Cheng JC, Wu JK, Lee PC, *et al.* Biologic susceptibility of hepatocellular carcinoma patients treated with radiotherapy to radiation-induced liver disease. *Int J Radiat Oncol Biol Phys* 2004;60:1502-1509.

20. Wulf J, Baier K, Mueller G, *et al.* Dose-response in stereotactic irradiation of lung tumors. *Radiother Oncol* 2005;77:83-87.

STEREOTACTIC BODY RADIATION THERAPY FOR LIVER TUMORS: IMPACT OF DAILY SETUP CORRECTIONS AND DAY-TO-DAY ANATOMIC VARIATIONS ON DOSE IN TARGET AND ORGANS AT RISK

Alejandra Méndez Romero, Roel Th. Zinkstok, Wouter Wunderink,
Rob M. van Os, Hans Joosten, Yvette Seppenwoolde,
Peter J. C. M. Nowak, Rene P. Brandwijk, Cornelis Verhoef,
Jan N. M. IJzermans, Peter C. Levendag, and Ben J. M. Heijmen

Int. J. Radiation Oncology Biol. Phys., Vol 75, No. 4, pp. 1201-1208, 2009

ABSTRACT

Purpose: To assess day-to-day differences between planned and delivered target volume (TV) and organs-at-risk (OAR) dose distributions in liver stereotactic body radiation therapy (SBRT), and to investigate the dosimetric impact of setup corrections.

Methods and Materials: For 14 patients previously treated with SBRT, the planning CT scan and three treatment scans (one for each fraction) were included in this study. For each treatment scan, two dose distributions were calculated: one using the planned setup for the body frame (no correction), and one using the clinically applied (corrected) setup derived from measured tumor displacements. Per scan, the two dose distributions were mutually compared, and the clinically delivered distribution was compared with planning. Doses were recalculated in equivalent 2-Gy fraction doses. Statistical analysis was performed with the linear mixed model.

Results: With setup corrections, the mean loss in TV coverage relative to planning was 1.7%, compared to 6.8% without corrections. For calculated equivalent uniform doses, these figures were 2.3% and 15.5%, respectively. As for the TV, mean deviations of delivered OAR doses from planning were small (between -0.4 and +0.3 Gy), but the spread was much larger for the OARs. In contrast to the TV, the mean impact of setup corrections on realized OAR doses was close to zero, with large positive and negative exceptions.

Conclusions: Daily correction of the treatment setup is required to obtain adequate TV coverage. Because of day-to-day patient anatomy changes, large deviations in OAR doses from planning did occur. On average, setup corrections had no impact on these doses. Development of new procedures for image guidance and adaptive protocols is warranted.

Acknowledgments: The authors thank Evert Woudstra, Ph.D., Jeroen B. van de Kamer Ph.D., and Koos Zwinderman Ph.D., for their valuable contributions.

INTRODUCTION

Stereotactic body radiation therapy (SBRT) for liver tumors has demonstrated a high local control rate with an acceptable toxicity (1-5). Because large radiation doses are delivered in a few fractions, high precision is required in tumor volume definition, daily setup, and dose delivery to guarantee accurate targeting and low toxicity. Precision in dose delivery is affected by anatomical changes in the liver and organs at risk, such as variable filling, peristalsis, cardiac, and (residual) respiratory motion (6, 7). Day-to-day changes in the liver position may impair target coverage in SBRT, as reported by several groups (5, 8-10). Therefore, the tumor position is commonly verified with CT-guided treatment procedures to adjust, if necessary, the treatment setup before dose delivery (10). Methods to reduce, control, or track the respiratory motion have been developed, and are routinely used in SBRT (7, 11-14).

For SBRT of liver tumors, little is known about the impact of the daily varying, nonrigid patient anatomy and patient rotations on doses delivered to organs at risk (OARs). Even in image-guided treatments, optimal sparing of OARs according to the treatment plan is not guaranteed, because setup corrections are fully based on measured tumor displacements. Changes in OAR positions and shapes are not explicitly accounted for in these procedures. Moreover, also with corrected tumor setups, differences in radiological path lengths between planning and treatment, resulting from patient anatomy variations or rotations, may jeopardize target dose distributions.

The purpose of this study is to determine day-to-day dose deviations in the target volume (TV) and OARs for SBRT of liver tumors, and to assess the impact of daily tumor setup corrections on these deviations. For a group of 14 patients, two dose distributions were retrospectively calculated for each of the three treatment scans: one using the planned setup for the body frame (no correction), and one using the clinically applied (corrected) setup. Per scan, the two dose distributions were mutually compared, and the clinically delivered distribution was also compared with the planning.

METHODS AND MATERIALS

Patients

This study included 14 patients entered in a phase I-II study, with a total of 23 liver metastases, consecutively treated in our institution between April 2003 and November 2006 (3). The patients were discussed in a multidisciplinary liver tumor board, and were not considered eligible for other local treatments, including surgery (due to limited remnant or co-morbidity) or radiofrequency ablation (due to unfavorable location). Patient and tumor characteristics are presented in Table 1.

Table 1. Demographics

Patient	Gender	Age (y)	Primary tumor	Tumor number	Tumor size	Tumor volume (cc)	Liver segment	Liver volume
1	Male	70	Colorectal	1, 2	3.9, 1.5	53.4, 14.3	1, 8	1162.3
2	Male	75	Colorectal	1	2.8	76.2	8	1469.7
3	Female	56	Lung	1, 2	1.5, 0.5	7.2	7, 7	1251.4
4	Male	81	Colorectal	1	6.2	112.7	4	1765.8
5	Male	70	Colorectal	1	2.3	26	1	1292.7
6	Male	44	Colorectal	1, 2	2.8, 0.7	53.8, 3.2	1, 3	2412.1
7	Male	70	Colorectal	1	4.7	183.5	4	2907.1
8	Male	53	Colorectal	1, 2	4.1, 0.8	32, 8.7	7, 7	1166.6
9	Male	79	Colorectal	1, 2, 3	4.9,3.7,1.2	84.9,58.4	8,6,6	2060.7
10	Female	63	Carcinoid	1	3.2	31.1	4	1095.1
11	Male	58	Colorectal	1	2.4	13.8	1	1690.3
12	Male	72	Colorectal	1, 2	3.3, 1.0	43.1, 12.2	1, 7	2190.3
13	Male	52	Colorectal	1, 2, 3	6, 3.9, 3.2	64.4, 17.4, 9.8	2, 4, 4	2343.3
14	Female	55	Colorectal	1	3.4	35.8	4	1647.8

* Due to the close proximity of the tumors, they were considered as one volume for treatment purposes.

Treatment preparation

During (planning) CT scan acquisitions and treatments, patients were positioned in a stereotactic body frame (SBF) (Elekta Instrument AB, Stockholm, Sweden) with abdominal compression to reduce respiratory tumor motion. A large-volume planning CT scan, and two contrast-enhanced CT scans in arterial and venous phases were acquired for treatment preparation. The planning CT was matched with the contrast CT scans by registering the SBF's position indicators included in the sidewalls (10). The tumor was delineated in both contrast-enhanced CT scans, after which the contoured volumes were joined to construct the composite clinical target volume (CTV). For each patient an MRI scan was available to assist tumor delineations. The planning target volume (PTV) was constructed from the composite CTV, initially using margins adopted from the Karolinska experience (13). The margins were individualized once fiducial markers were implanted in the patients' livers, enabling measurement of residual breathing motion with a video fluoroscopy system (7). OARs were delineated in the planning CT scan.

Treatment was planned in 3 fractions, prescribing 12.5 Gy per fraction on the 65% reference isodose surrounding the PTV (1 patient received 3 fractions of 10 Gy because of a limited liver volume). The PTV coverage aimed for was ≥95%. OAR constraints as used for treatment planning adopted from Wulf *et al*. (3, 15) are presented in Table 2. OAR and PTV constraints were carefully followed during the design of the treatment plan. However, violations were occasionally accepted if not all constraints could practically be met. Treatment plans were designed using the Cadplan treatment-planning

system (Varian Oncology Systems, Palo Alto, CA) using a median of 8 (range 4-10) coplanar and noncoplanar beams.

Table 2. Dose constraints for the OARs in absolute dose per fraction, and recalculated as EQD_2

OAR	Absolute dose (Gy)	EQD_2 (Gy)
Duodenum D_{5cc}	7.0	13.4
Heart D_{5cc}	7.0	14.8
Kidneys $D_{33\%}$	5.0	8.3
Liver $D_{33\%}$	7.0	14.0
Liver $D_{50\%}$	5.0	8.0
Esophagus D_{5cc}	7.0	13.4
Spinal cord D_{max}	5.0	8.8
Stomach D_{5cc}	7.0	13.4

OAR = organ at risk; EQD_2 = equivalent 2-Gy fraction.

Treatment execution

On each treatment day, prior to dose delivery, a contrast-enhanced CT scan was acquired to establish the position of the tumor in the SBF. In this so-called treatment CT the physician delineated the CTV (treatment CTV). The treatment CT was matched with the planning CT by registering the SBF position indicators as previously described, such that the treatment CTV could be projected on the planning CT. If the CTV appeared to have moved from the CTV position in the planning CT scan, a treatment isocenter correction was derived to realign the CTV with the original treatment plan. The correction was determined by projecting the PTV and treatment CTV contours in three orthogonal planes to measure distances between the contours. The planned coordinates for SBF setup at the treatment unit were then updated to establish the correction (shift) in the treatment isocenter. Details of the treatment procedures have been described by Méndez Romero *et al*. (3) and Wunderink *et al*.(10).

Calculated dose distributions

For each treatment CT, two treatments were simulated by calculating their dose distributions: one treatment using the planned body frame setup (Tp), and one treatment using the corrected setup (Tc), as delivered in clinical practice. The beam configuration with respect to the treatment isocenter was copied from the treatment plan and was identical in both treatment configurations; for the corrected setup, the position of the treatment isocenter was displaced according to the measured tumor displacement. The two configurations Tp and Tc, and the planning configuration, P, are schematically summarized in Figure 1. All calculations were performed with the planning system also used for plan design.

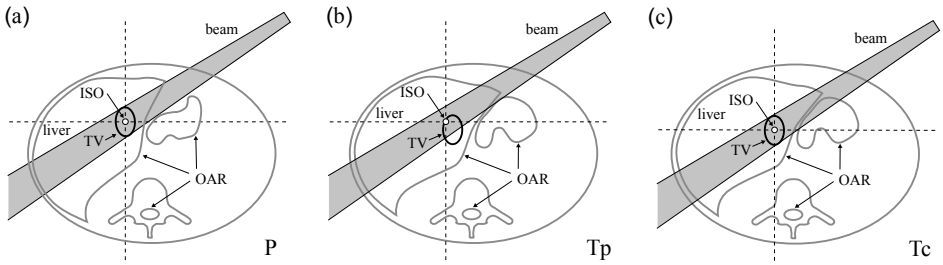

Fig. 1. Schematic explanation of treatment configurations Tp and Tc. (a) Planning CT scan with a single beam. (b) Treatment scan with the isocenter according to planning (Tp setup), the beam partially misses the target. (c) The same treatment scan, but with a corrected isocenter and corresponding beam set-up (Tc set-up). Abbreviations: TV = target volume, OAR = organ at risk, ISO = treatment isocenter.

TV dose assessments and comparisons

To avoid effects of tumor delineation uncertainties, the TV in each treatment CT was a copy of the PTV in the corresponding planning CT. For corrected setups, PTVs were positioned in the treatment scans by applying a shift in accordance with the displaced treatment isocenter (previous paragraph). As a result, for each corrected setup, all beam projections encompassed the PTV as in the planning situation (Fig. 1). Observed differences in target doses between a corrected setup and planning are then attributed to anatomical differences in the healthy tissues surrounding the target (radiological path length differences), and to (small) uncertainties in the applied procedures.

Target dose distributions were evaluated using TV coverages (percentage of the TV within the 12.5-Gy isodose volume), and calculated generalized equivalent uniform dose values (gEUD) with volume parameters a = -5 and a = -10 (16-19). Because of the high similarity of conclusions to be drawn from the a = -5 and a = -10 analyses, results are only shown for a = -5. For patients with more than one lesion (Table 1), the analyses were performed for the composite TV.

OAR dose assessments and comparisons

For each simulated dose distribution, the following OAR dose parameters, (as also used for plan design; see above), were evaluated: liver $D_{33\%}$, liver $D_{50\%}$, bowel, duodenum, stomach and esophagus D_{5cc}, spinal cord D_{max}, kidneys $D_{33\%}$, and heart D_{5cc}. For the parameter assessments, OARs were additionally contoured in all treatment CT scans. Despite the limited span of some treatment CT scans, for the serial OARs, the relevant regions (exposed to the high doses) were always included. In most treatment CT scans the caudal aspect of the kidneys was not completely included, requiring the following procedure to establish the dose parameters for these parallel organs. After registering the kidneys in the planning and a treatment scan, the kidneys in the treatment scan were completed by adding missing contours from the planning scan. Because the missing contours were to be placed outside the original scanned

volume, the treatment CT was first extended with additional slices that were copies of the most caudal slice. In a similar way, additional slices were added to the volume boundaries if required in the treatment simulation to obtain representative radiological path lengths.

For all analyses, OAR dose parameters were converted into equivalent 2-Gy fraction doses (EQD_2), using:

$$EQD_2 = D\frac{d + (\alpha / \beta)}{2 + (\alpha / \beta)} \quad (1)$$

where EQD_2 is the dose in 2-Gy fractions that is biologically equivalent to a total dose D given with a fraction size of *d* gray (20, 21). For liver we applied an α/β value of 3.0 Gy; for stomach, duodenum and esophagus 3.5 Gy; for spinal cord 2.0 Gy; for heart 2.5 Gy, and for kidneys 2.5 Gy (21). The OAR constraint doses used for planning and converted to EQD_2 are presented in Table 2. In the remainder of this paper, OAR doses refer to EQD_2 values.

Statistics

For the descriptive statistics, established dose parameters for P, Tp and Tc were handled as separate measurements to give an overview of the actual data. To test the difference of the dose parameters or the chance of falsely rejecting the null hypothesis, "no difference" (p value), the linear mixed model was used, and correlation was assumed between the observations. The linear mixed model was selected because it can properly account for correlation between repeated measurements. The level of statistical significance was considered $\alpha = 0.05$ for all tests. Statistical analyses were performed using SPSS software, version 16.0 (SPSS Inc., Chicago, IL).

RESULTS

Target volume

Distributions of measured tumor displacements in the 42 treatment fractions relative to planning were 2.1, 4.0, and 1.5 mm (1 SD), for the lateral, superior-inferior, and anterior-posterior directions, respectively. Figure 2a shows for all treatment fractions the length of the three-dimensional setup error and differences in target coverage with planning if no corrections would have occurred (Tp-P), and for the actual treatment with setup corrections (Tc-P). Distances between corresponding Tc-P and Tp-P data points in Figure 2a represent improvements in TV coverage resulting from the performed CT-guided tumor setup corrections. The planned mean target coverage for

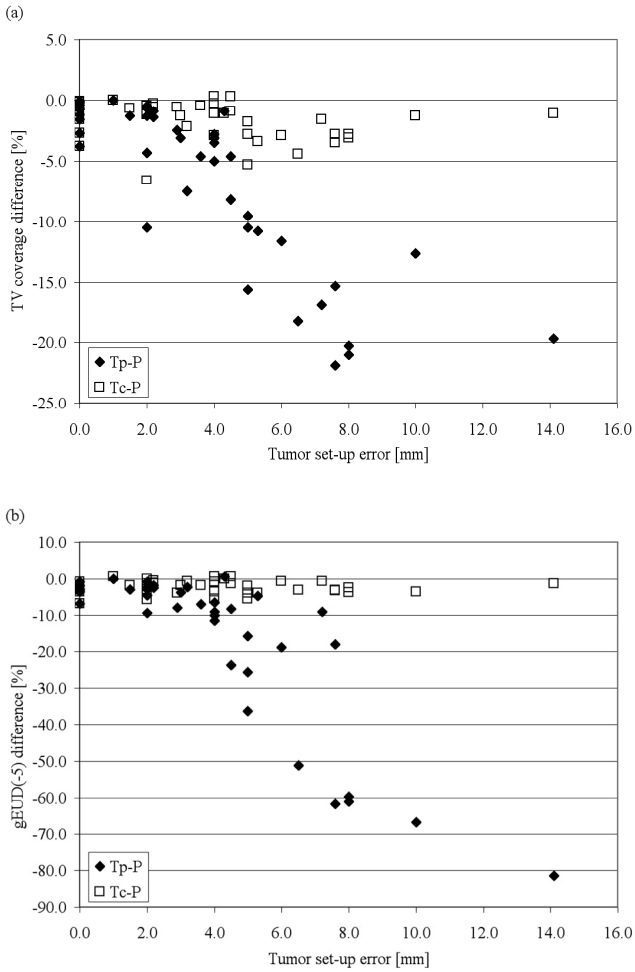

Fig. 2. Deviations in (a) TV coverage and (b) generalized equivalent uniform dose (gEUD) (-5) from planning before (Tp-P) and after (Tc-P) tumor setup corrections.

the 42 fractions was 97.2%. Without setup corrections this would have decreased by 6.8% to 90.4%. With the clinically applied CT guidance, the mean coverage was 95.5%, a reduction of 1.7% compared to planning (Figs. 3a and 4a). Patients 3, 11, and 14 had mean tumor setup errors in the three fractions of 7.9, 5.5, and 5.0 mm, respectively. Without corrections this would have resulted in mean target coverage losses of 21.1%, 14.9%, and 12.0%, respectively. Due to applied corrections, the reductions were limited to 2.9%, 4.4%, and 2.2%. All 42 setup corrections, but 1 resulted in improved target coverage. The difference between Tc and Tp for this exception was only -0.2Gy. Ninety-five percent of treatment fractions had a realized coverage after correction (slightly) lower than or equal to the planned coverage (p = 0.001, Table 3).

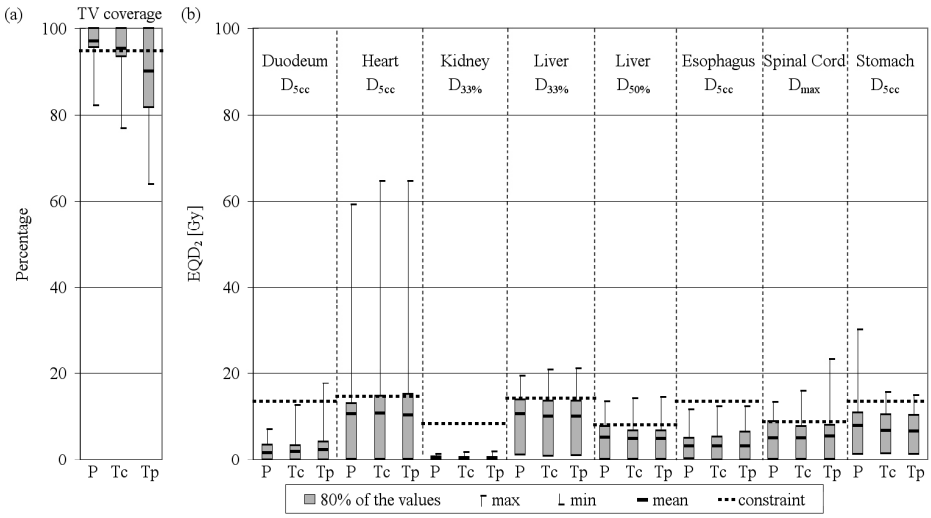

Fig. 3. Summarized planning and treatment dose distribution parameters. Summaries for planning (P), corrected treatment simulations (Tc), and noncorrected treatment simulations (Tp) for (a) the target volume, and (b) organs at risk.

Table 3. Probability (p) values resulting from a linear mixed model, comparing dose distribution parameters in the simulated actual treatments (with setup corrections) with corresponding planned parameters (Tc vs. P), and comparing differences between setup correction and no correction (Tc vs. Tp)

Dose distribution parameter	Tc vs. Tp (p)	Tc vs. P (p)
Duodenum D_{5cc}	0.478	0.087
Heart D_{5cc}	0.313	0.464
Kidneys $D_{33\%}$	0.630	0.788
Liver $D_{33\%}$	0.952	0.023
Liver $D_{50\%}$	0.781	0.015
Esophagus D_{5cc}	1.000	0.769
Spinal cord D_{max}	0.090	0.377
Stomach D_{5cc}	0.157	0.480
TV* coverage	0.002	0.001

*$p < 0.05$

Without corrections, 45% of fractions would have had a TV coverage lower than 95%. With the applied corrections this was reduced to 24% (Fig. 5a). In the absence of corrections, 31% of fractions would have suffered from a coverage reduction relative to planning of 10% or more. With corrections, coverage reductions larger than 10% could be fully avoided.

Figure 2b shows for individual fractions, drops in gEUD(-5) that would have resulted from treatment with uncorrected tumor setup errors (Tp-P), and reductions in these gEUD(-5) losses with the applied setup corrections (compare with Fig. 2a). The mean planned fraction gEUD(-5) was 15.6 Gy (10-90% percentile range: 13.1-17.0 Gy). Without corrections, the mean gEUD(-5) for treatment would have been reduced

by 15.5% relative to planning (10% and 90% percentile values: -59% and -2%); 52% of fractions would have suffered from a calculated gEUD loss of 5% or more. Performed corrections limited the gEUD reductions to an average of –2.3% (10% and 90% percentile values: -4% and 0%), with only 10% of fractions having a gEUD loss (slightly) larger than 5%.

Organs at risk

OAR dose distribution parameters for planning (P) and the noncorrected (Tp) and corrected (Tc) treatment simulations are summarized in Figure 3b. Figure 4b contains Tc-P and Tc-Tp summaries. *p* values are presented in Table 3 (see also Discussion). Mean increases in OAR doses during treatment, relative to planning, (positive mean values for Tc-P in Fig. 4b) were all below 0.3 Gy. However, notwithstanding applied corrections, for some treatment fractions there were substantial deviations from planning. For example, in Fraction 1, Patient 1 had a duodenum D_{5cc} of 12.5 Gy, whereas the planning showed 1.3 Gy; in Fraction 1, Patient 6 had a heart dose of 22.7 Gy, whereas the planning indicated 12.1 Gy; and Patient 4 had a stomach dose of 15.4Gy in Fraction 3, compared with a planned dose of 8.8 Gy. On the other hand, there were also important decreases in realized OAR doses relative to planning. For example, Patient 1 had a planned stomach dose of 29.9 Gy, whereas doses of 6.8, 7.0 and 6.4 Gy were calculated for the three treatment scans (with corrected tumor setup errors of 4, 10 and 0 mm, respectively).

For the various OARs, the numbers of fractions with constraint adherence and constraint violation in the planning (P) and treatment simulations (Tc and Tp) are

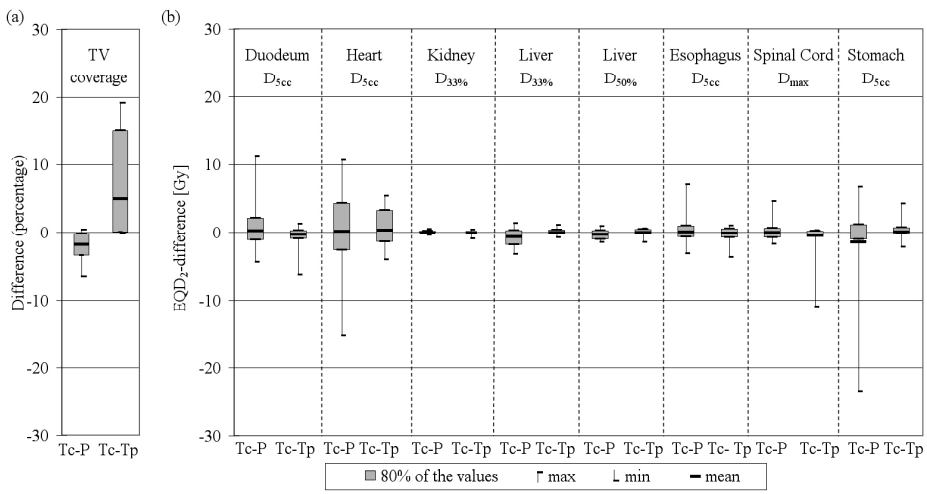

Fig. 4. Changes in dose distribution parameters for (a) target volume (TV), and (b) organs at risk. Tc-P = differences between simulated actual treatment and planning; Tc-Tp = changes related to tumor setup corrections.

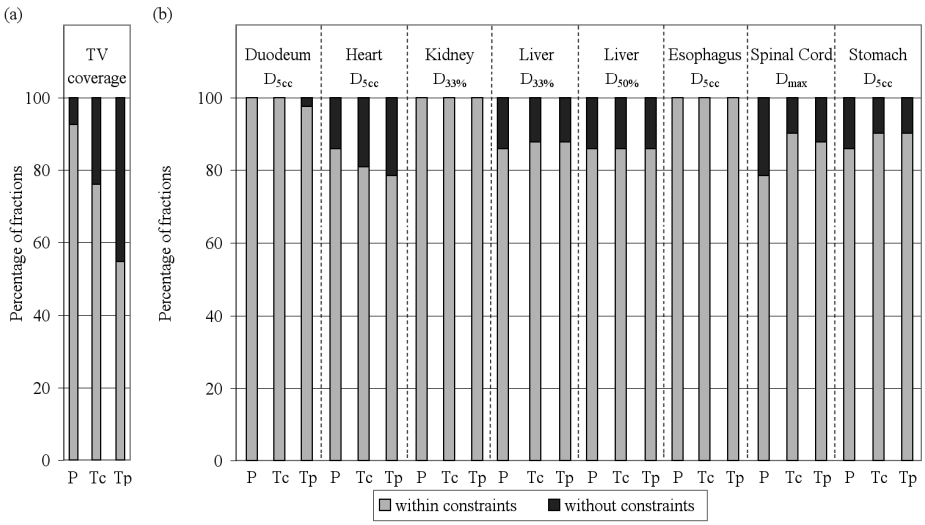

Fig. 5. Constraint violations. Percentage of fractions within and without the planning constraints for (a) the target volume (TV), and (b) the organs at risk for the treatment plans (P), corrected treatment simulations (Tc), and noncorrected treatment simulations (Tp).

presented in Figure 5b. It confirms that the impact of setup corrections on OARs was not as consistent as for the TV (compare Tc and Tp in Fig. 5b). For 7 patients, all OARs were planned within the constraints. From these patients, 1 had constraint violations in both the Tc and Tp treatment simulations. From the 7 patients with constraint violations in the planning, 1 patient was fully within the constraints in Tc, although above constraints in Tp.

The Tc-Tp data in Figure 4b show that for all OAR dose distribution parameters the mean impact of correction was between -0.4 and +0.3 Gy. However, also here there were important deviations in individual patient fractions, both positive and negative. For example, because of the applied tumor setup correction, the duodenum dose of patient 1 in Fraction 1 went down from 17.5 to 12.5 Gy (still far above the planned value of 1.3 Gy; see above), and in Fraction 2 it decreased from 9.6 to 3.3 Gy; for Patient 6, tumor setup correction in Fraction 2 resulted in an increase in heart dose from 15.8 to 19.2 Gy, compared to no correction. Both the residual deviations in OAR dose distribution parameters from planning after tumor setup corrections (Tc-P, Fig.6a), and the impact of CT guidance on parameter deviations (Tc-Tp, Fig. 6b) are independent of the magnitude of the corrected tumor setup error. The latter finding is in strong contrast with observations for the TV (compare with Figs. 2 and 6).

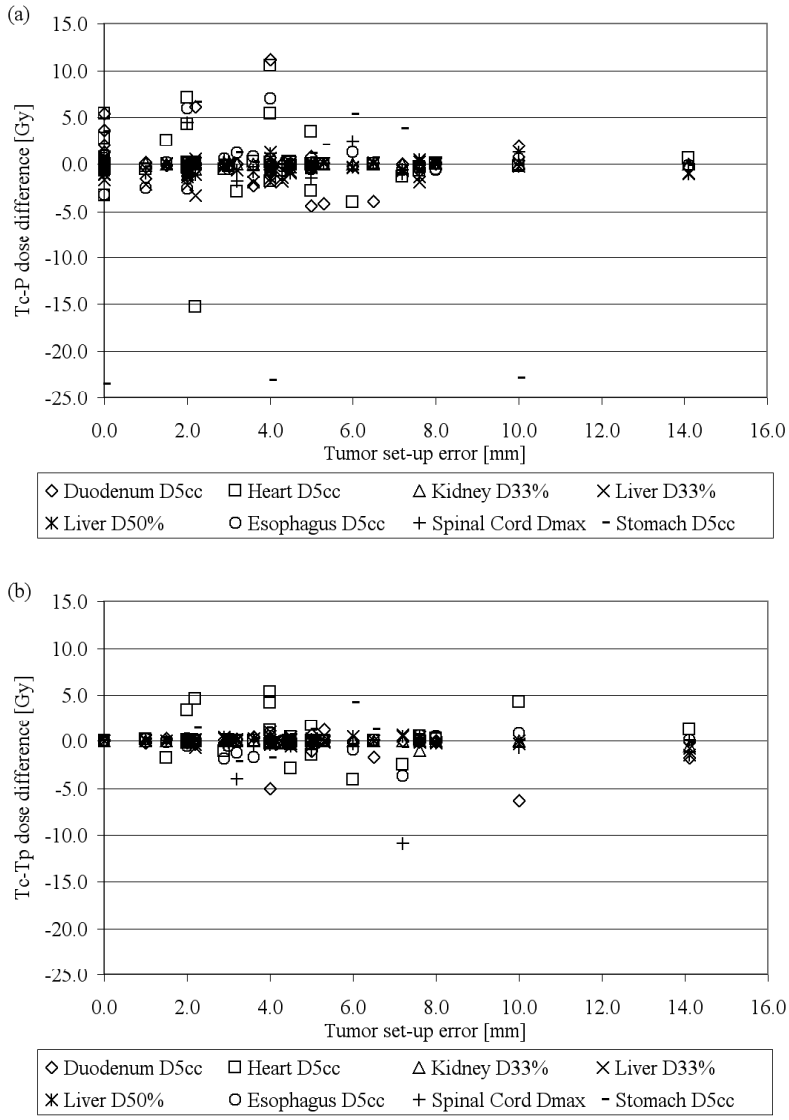

Fig. 6. Differences between realized organ-at-risk dose distribution parameters (applying corrections) and (a) planned parameters (Tc-P), and (b) parameters that would have occurred without corrections (Tc-Tp).

DISCUSSION

Setup corrections were of major importance for adequate TV irradiation, especially in fractions with detected large tumor setup errors (Figs. 2a, 2b, 4a, and 5a). However, 95% of treatment fractions had a realized coverage after correction (slightly) lower than or equal to the planned coverage ($p = 0.001$, mean deviation –1.7%). In addition realized gEUD values were on average lower than planned (-2.3%). With the high

planned target coverages (97.2% on average), for most points in the target edge, the planned dose is higher than or equal to the prescribed 12.5 Gy, and an increase here in dose relative to planning does not impact the TV coverage parameter. For these points, the parameter is only sensitive to negative dose deviations that may yield a drop in coverage. An increase in coverage compared to planning can only occur with enhanced treatment doses in the low percentage of points with a planned dose lower than 12.5 Gy. As a consequence, deviations of treatment dose distributions relative to planning are most likely to result in a TV coverage reduction, as was also observed in practice (above). By its nature, gEUD(-5) is most sensitive to dose reductions in the TV, yielding lower values. Consequently, when positive and negative target dose deviations are equally distributed during treatments, treatment gEUD(-5) values are mostly lower than planned. This might explain the observed mean gEUD(-5) loss of 2.3%.

As explained in Methods and Materials, differences from planning in the calculated realized target dose distributions cannot be attributed to tumor delineation variations. On the other hand, radiological path length differences between the planning and treatment CT scans may explain the differences. Additionally, we have found that the procedures for positioning beams around the TV in treatment CT scans may introduce errors of up to 1 mm, resulting in some extra dosimetrical uncertainty. Hence, the observed mean differences in TV coverage and gEUD(-5) between planning and treatment of -1.7% and -2.3%, respectively, are upper limits for the mean impact of radiological path length variations on these parameters, originating from day-to-day, non-rigid patient anatomy variations or rotations.Obviously, the impact of radiological path length variations on TV dose delivery was much smaller than the impact of setup errors, if not corrected (Figs. 2a and 2b).

As presented in Results, for all OAR dose distribution parameters, the mean difference between correction (Tc) and nocorrection (Tp) was within –0.4 and +0.3 Gy. For the Liver $D_{33\%}$ and $D_{50\%}$, the mean differences between actual treatment and planning (Tc-P) were –0.6 and –0.3 Gy, respectively, and during treatment these parameters were significantly lower than planned (Table 3). No explanation has been found for this benefit.

Reporting on clinically observed toxicity was not specifically the aim of this study. Results of 11 of the 14 patients have been previously reported (3). In the other 3 patients, we did not find any toxicity of Grade 3, 4 or 5. Although occasionally high doses above OAR constraints were delivered, in none of the 14 patients, severe toxicity, such as perforation, cardiac insufficiency or neurological symptoms, observed. Many OAR dose-volume histograms showed a tail towards the high doses, suggesting that only a small volume was irradiated with high dose. Locations of hot spots within OARs may also change every treatment day owing to day-to-day variations in OARs' positions and shapes.

The PTV margins in our clinical protocol for SBRT of liver patients presume treatment with daily CT guidance (10). In this study we have found that the applied procedure is instrumental to ensure adequate TV dose delivery. Obviously the tight stereotactic dose distributions do not, in general tolerate TV displacements. Without setup corrections, PTV margins should have been enlarged to minimize the risk of underdosing the tumor.

On average, OAR dose distribution parameters were also close to planning, but the spread was much bigger than for the TV (compare Figs. 2 and 6a). OAR parameters could both be (substantially) higher and lower than planned. In strong contrast with the TV, the mean impact of setup corrections on OAR dose distribution parameters was virtually zero. Corrections could both positively and negatively (strongly) impact the OAR parameters, with comparable frequencies and magnitudes. Moreover, the dosimetric impact of corrections was independent from the magnitude of the setup error (Fig. 6b). Obviously, setup corrections are needed to ensure target coverage, and may fail to reduce OAR doses higher than planned, or may even (further) enhance these doses, owing to day-to-day anatomy deformations and/or rotations.

In this study, we did not account for dose variations caused by (residual) respiratory organ motion in the SBF. However, the expected impact of respiratory effects is very limited as reported by Wu *et al*. (22), because the breathing motion was reduced to ≤ 5mm by means of abdominal compression. With a single-slice, spiral CT scanner, breathing motion may result in imaging artifacts, as discussed in a previous article (10), and may therefore contribute to setup error measurements based on CT. To reduce imaging artifacts, we acquire respiratory-correlated CT scans in our current liver SBRT practice. From this, we conclude that the magnitudes of daily setup errors found in this study are realistic and inherent to a SBRT treatment in an SBF.

With the 14 patients in the study we were able to convincingly demonstrate that daily setup verification and correction can prevent severe TV underdosage in some of the patients and that these setup corrections have a mixed impact on doses in OAR. To more precisely assess frequency distributions, this study should be extended with more patients.

Several approaches could potentially result in safer dose delivery, with better controlled-sparing of OARs. For treatment planning, OAR planning volumes could be designed, using the information on organ changes sampled from previously treated patients. International Commission on Radiation Units and Measurements Report 62 (1999) stressed the fact that movement and changes in shape and/or size of OARs, should be considered together with the setup uncertainties (23). It was advised to add a margin to compensate for these variations and uncertainties, which led to the concept of the OAR planning volume. However, neither dose criteria nor suggestions to calculate these margins for the different types of OARs were supplied. A few groups

have attempted to give a margin recipe, but limitations have been found, especially for parallel OARs (24, 25). A second solution could be a change in the current image-guidance procedure by explicitly including OARs in the on-line image analyses. As a first step, before dose delivery, one could first establish the required tumor setup correction, followed by a dose calculation for the treatment CT scan, taking into account the setup correction. Accurate and fast evaluation of the simulated treatment dose distribution would however require segmented OARs in the treatment scan. Because manual delineation would be too time consuming, some sort of autosegmentation would be needed. In case of unacceptable OAR doses, one could ideally replan on line to adapt the planning to the patient anatomy of the day, (*e.g*. using a system for automated beam angle and weight optimization) (26). Until such a system for fast, on-line replanning is clinically available, occurrence of observed unacceptable OAR doses in the simulated treatment dose distribution could be a reason not to treat on the particular day. Optimal dose delivery could be achieved with an adaptive treatment strategy, based on added fraction doses, assessed with a reliable nonrigid image registration technique (27). Ideally, nonrigid registration should be part of an on-line procedure, but also off-line application could improve dose delivery. In the latter, prior to each fraction, a new treatment plan could be designed, taking into account the added dose distributions delivered in the previous fractions.

CONCLUSIONS

With the tight dose distributions applied in liver SBRT, daily tumor setup correction is required to ensure coverage of the TV according to planning. OAR dose distribution parameters were on average close to planning, but showed a large variability in observed deviations. In contrast with the target, and caused by day-to-day anatomical variations, the mean impact setup corrections on OAR dose distributions was virtually zero, with large occasional positive and negative deviations. Moreover, for OARs, the dosimetric impact of corrections was independent from the magnitude of the setup error. Especially for dose-escalation protocols, development of adaptive treatment techniques and daily (on-line) replanning is warranted.

REFERENCES

1. Hoyer M, Roed H, Traberg HA, *et al.* Phase II study on stereotactic body radiotherapy of colorectal metastases. *Acta Oncol* 2006; 45:823-830.
2. Kavanagh BD, Schefter TE, Cardenes HR, *et al.* Interim analysis of a prospective phase I/II trial of SBRT for liver metastases. *Acta Oncol* 2006; 45:848-855.
3. Méndez Romero A, Wunderink W, Hussain SM, *et al.* Stereotactic body radiation therapy for primary and metastatic liver tumors: A single institution phase i-ii study. *Acta Oncol* 2006; 45:831-837.
4. Tse RV, Hawkins M, Lockwood G, *et al.* Phase I study of individualized stereotactic body radiotherapy for hepatocellular carcinoma and intrahepatic cholangiocarcinoma. *J Clin Oncol* 2008; 26:657-664.
5. Wulf J, Guckenberger M, Haedinger U, *et al.* Stereotactic radiotherapy of primary liver cancer and hepatic metastases. *Acta Oncol* 2006; 45:838-847.
6. Goitein M. Organ and tumor motion: an overview. *Semin Radiat Oncol* 2004; 14:2-9.
7. Wunderink W, Méndez Romero A, de Kruijf W, *et al.* Reduction of respiratory liver tumor motion by abdominal compression in stereotactic body frame, analyzed by tracking fiducial markers implanted in liver. *Int J Radiat Oncol Biol Phys* 2008; 71:907-915.
8. Eccles C, Brock KK, Bissonnette JP, *et al.* Reproducibility of liver position using active breathing coordinator for liver cancer radiotherapy. *Int J Radiat Oncol Biol Phys* 2006; 64:751-759.
9. Hansen AT, Petersen JB, Hoyer M. Internal movement, set-up accuracy and margins for stereotactic body radiotherapy using a stereotactic body frame. *Acta Oncol* 2006; 45:948-952.
10. Wunderink W, Méndez Romero A, Vasquez Osorio EM, *et al.* Target coverage in image-guided stereotactic body radiotherapy of liver tumors. *Int J Radiat Oncol Biol Phys* 2007; 68:282-290.
11. Dawson LA, Brock KK, Kazanjian S, *et al.* The reproducibility of organ position using active breathing control (ABC) during liver radiotherapy. *Int J Radiat Oncol Biol Phys* 2001; 51:1410-1421.
12. Heinzerling JH, Anderson JF, Papiez L, *et al.* Four-dimensional computed tomography scan analysis of tumor and organ motion at varying levels of abdominal compression during stereotactic treatment of lung and liver. *Int J Radiat Oncol Biol Phys* 2008; 70:1571-1578.
13. Lax I, Blomgren H, Naslund I, *et al.* Stereotactic radiotherapy of malignancies in the abdomen. Methodological aspects. *Acta Oncol* 1994; 33:677-683.
14. Seppenwoolde Y, Berbeco RI, Nishioka S, *et al.* Accuracy of tumor motion compensation algorithm from a robotic respiratory tracking system: a simulation study. *Med Phys* 2007; 34:2774-2784.
15. Wulf J, Hadinger U, Oppitz U, *et al.* Stereotactic radiotherapy of targets in the lung and liver. *Strahlenther Onkol* 2001; 177:645-655.
16. de Pooter JA, Wunderink W, Méndez Romero A, *et al.* PTV dose prescription strategies for SBRT of metastatic liver tumours. *Radiother Oncol* 2007; 85:260-266.
17. Heijmen B, de Pooter JA, Méndez Romero A, *et al.* Computer generation of fully non-coplanar treatment plans of liver tumours based on gEUD optimisation. Proc. of the XVth International Conference on the Use of Computers in Radiation Therapy, Toronto, Canada, 333-337. 7-4-2007.
18. Niemierko A. A generalized concept of equivalent dose (EUD). *Med.Phys.* 2600, 1100. 1999.

19. Thomas E, Chapet O, Kessler ML, *et al.* Benefit of using biologic parameters (EUD and NTCP) in IMRT optimization for treatment of intrahepatic tumors. *Int J Radiat Oncol Biol Phys* 2005; 62:571-578.
20. Pieters BR, van de Kamer JB, van Herten YR, *et al.* Comparison of biologically equivalent dose-volume parameters for the treatment of prostate cancer with concomitant boost IMRT versus IMRT combined with brachytherapy. *Radiother Oncol* 2008;88:46-52.
21. Steel GG. Basic Clinical Radiobiology. Second ed. Bath: Arnold, 1997.
22. Wu QJ, Thongphiew D, Wang Z, *et al.* The impact of respiratory motion and treatment technique on stereotactic body radiation for liver cancer. *Medical Physics* 2008; 35:1440-1451.
23. International Commission on Radiation Units and Measurements. ICRU Report 62: Prescribing, recording, and reporting photon beam therapy (Supplement to ICRU Report 50). Bethesda MD: ICRU Publications; 1999.
24. McKenzie A, van Herk M, Mijnheer B. Margins for geometric uncertainty around organs at risk in radiotherapy. *Radiother Oncol* 2002; 62:299-307.
25. Stroom JC, Heijmen BJ. Limitations of the planning organ at risk volume (PRV) concept. *Int J Radiat Oncol Biol Phys* 2006; 66:279-286.
26. de Pooter JA, Méndez Romero A, Jansen WP, *et al.* Computer optimization of noncoplanar beam setups improves stereotactic treatment of liver tumors. *Int J Radiat Oncol Biol Phys* 2006; 66:913-922.
27. Brock KK, Dawson LA, Sharpe MB, *et al.* Feasibility of a novel deformable image registration technique to facilitate classification, targeting, and monitoring of tumor and normal tissue. *Int J Radiat Oncol Biol Phys* 2006; 64:1245-1254.

6

STEREOTACTIC BODY RADIATION THERAPY FOR COLORECTAL LIVER METASTASES

A. E. M. van der Pool, A. Méndez Romero, W. Wunderink,
B. J. M. Heijmen, P. C. Levendag, C. Verhoef, and J. N. M. IJzermans

British Journal of Surgery 2010; 97: 377–382

ABSTRACT

Background: Stereotactic body radiation therapy (SBRT) is a treatment option for colorectal liver metastases. Local control, patient survival and toxicity were assessed in an experience of SBRT for colorectal liver metastases.

Methods: SBRT was delivered with curative intent to 20 consecutively treated patients with colorectal hepatic metastases who were candidates for neither resection nor radiofrequency ablation (RFA). The median number of metastases was 1 (range 1–3) and median size was 2.3 (range 0.7–6.2) cm. Toxicity was scored according to the Common Toxicity Criteria version 3.0. Local control rates were derived on tumour-based analysis.

Results: Median follow-up was 26 (range 6–57) months. Local failure was observed in nine of 31 lesions after a median interval of 22 (range 12–52) months. Actuarial 2-year local control and survival rates were 74 and 83 per cent respectively. Hepatic toxicity grade 2 or less was reported in 18 patients. Two patients had an episode of hepatic toxicity grade 3.

Conclusion: SRBT is a treatment option for patients with colorectal liver metastases, who are not candidates for resection or RFA.

INTRODUCTION

Colorectal cancer is a common malignancy and the second leading cause of cancer-related death in the USA and Europe (1). Liver metastases develop in 50–70 per cent of patients with colorectal cancer during the course of the disease (2). Resection of colorectal liver metastases is still the 'gold standard' treatment, with 5-year survival rates ranging from 35 to 60 per cent in highly selected patients (3). Unfortunately, most patients are not eligible for surgery because of unfavourable tumour factors or poor general condition. Other local treatment techniques, among which radio-frequency ablation (RFA) is the most widely used, offer a high rate of local control in inoperable patients with liver metastases (4, 5). However, RFA is preferably carried out for metastases that are smaller than 3 cm and not located in the proximity of major blood vessels, the main biliary tract or gallbladder, or just beneath the diaphragm (4).

Traditionally, radiotherapy has had a limited role in the treatment of intrahepatic malignancies owing to the low tolerance of the whole liver to irradiation. However, since the 1990s, groups from the Karolinska Hospital and Michigan Medical School (Ann Arbor) have demonstrated that large doses of conformal radiation can be delivered safely to localized targets in the liver (6, 7).

Stereotactic body radiation therapy (SBRT) is a non-invasive technique that delivers very large doses of radiation in a few fractions (8). Advances in tumour imaging, motion management, radiotherapy planning and dose delivery have allowed safe use of high-dose conformal radiation therapy in liver tumours (9). Several papers have reported outcomes after SBRT for liver metastases from various primary tumours (10–13). This study assessed local control, survival and toxicity after SBRT in a cohort of 20 patients with 31 liver metastases only from colorectal origin only.

METHODS

Patients with colorectal liver metastases who fulfilled the following criteria were included in this study. Patients were evaluated by the Erasmus University MC Liver Board, which comprises hepatobiliary surgeons, medical oncologists, hepatologists, (interventional) radiologists and radiation oncologists, and were judged not eligible for surgery owing to unresectable metastases or poor general condition. Metastases were not suitable for RFA because of their proximity to vessels, bile ducts or the diaphragm. The Karnofsky index was at least 80 per cent. Maximum lesion size was 6 cm and a maximum of three lesions was acceptable. Of patients with extrahepatic disease, only those with metastases eligible for curative treatment were eligible.

Radiotherapy

Patients were positioned in a stereotactic body frame (Elekta Oncology Systems, Stockholm, Sweden) with maximum tolerated abdominal compression to reduce respiratory tumour motion for planning and treatment purposes (14). Three computed tomographies (CT) scans per patient were acquired: two contrast-enhanced scans in the arterial and venous phases for tumour definition and one large-volume scan for dose planning. The border of contrast enhancement was taken as the boundary of the metastasis. The tumour delineations were reviewed by an experienced radiologist. The tumour volume was then expanded with safety margins to compensate for the residual breathing motion and other uncertainties in tumour position, resulting in the planning target volume (PTV). Initially, equal safety margins were selected for all patients based on the Karolinska experience (5 mm in the left–right and anterior–posterior directions, and 10 mm in the craniocaudal direction) (14). Later, the margin was individualized in all three directions by measuring the residual motion of fiducials implanted around the tumour using video fluoroscopy registrations.

Up to June 2006, patients received three fractions of SBRT starting at 12.5 Gy, according to a phase I–II design (15). Thereafter, doses were escalated based on published data (16). Treatment plans were generated with the CadPlan treatment planning system (Varian Oncology Systems, Palo Alto, California, USA) with a median of 7 (4–10) beams. The dose was prescribed in such a way that at least 95 per cent of the PTV received a dose of 12.5 Gy (15 Gy in two patients). The length of the treatment course was 5–6 days and the dose was delivered in fractions every other day.

Follow-up

Treatment results and side-effects were evaluated prospectively by clinical and laboratory examination and CT or magnetic resonance imaging at 1 and 3 months after irradiation, followed by further examinations every 3 months during the first 2 years, and every 6 months thereafter. Toxicity was evaluated with the Common Toxicity Criteria (CTC), version 3.0, of the National Cancer Institute (http://ctep.cancer.gov). Local failure was defined as an increase in tumour size or tumour regrowth, with rates calculated on a tumour basis. Patients were monitored for local control even if distant or new liver metastases developed. Progressive disease included any intrahepatic or extrahepatic disease progression. If local failure or progressive disease was diagnosed, the date of recurrence was defined as the first date on which an abnormality was recognized on CT.

Statistical analysis

To assess local control and survival, Kaplan–Meier analyses were generated using SPSS® version 15.0 software (SPSS, Chicago, Illinois, USA). The log rank test was used to identify variables associated with local control.

RESULTS

Between December 2002 and July 2008, SBRT was administered to 20 consecutively treated patients with 31 lesions. In 19 patients the metastases were not amenable to resection or RFA owing to an unfavourable location and/or limited liver remnant. One patient had cardiac co-morbidity and non-invasive treatment was preferred.

One patient received radiotherapy three times for recurrent lesions, first elsewhere and the second and third times at this centre. Characteristics of the 31 metastases treated with SBRT are shown in Table 1. The median number of metastases was 1 (range 1–3) and median size was 2.3 (range 0.7–6.2) cm.

Table 1. Patient, target and treatment characteristics of 20 patients with 31 hepatic metastases

Patients	20
Sex ratio (M : F)	15 : 5
Median (range) age (years)	72 (45–81)
Location of primary tumour	
Rectum	5
Colon	15
Metastases	31
Site (Couinaud segments)	
I	3
II	0
III	1
IV	3
IV/V	1
V	3
VI	1
VI/VII	1
VII	5
VIII	13
Dose fractionation	
3 × 12.5 Gy	29
3 × 15 Gy	2

Local control

Thirteen patients had SBRT as a second-line treatment after resection, isolated hepatic perfusion, RFA or SBRT elsewhere. None of the 20 patients received adjuvant chemotherapy after SBRT. Fourteen patients had complete local control of all 22 lesions. Size of metastases was not a predictive factor of outcome. Local failure occurred in nine lesions in six patients after a median interval of 22 (range 12–52) months. One

patient who had two local failures in two lesions received chemotherapy, with an excellent response. This allowed extended liver surgery with curative intent. Three patients received palliative chemotherapy and died, and a further two patients were still receiving chemotherapy at the time of writing. Actuarial 1- and 2-year local control rates were 100 and 74 per cent respectively (Fig. 1a).

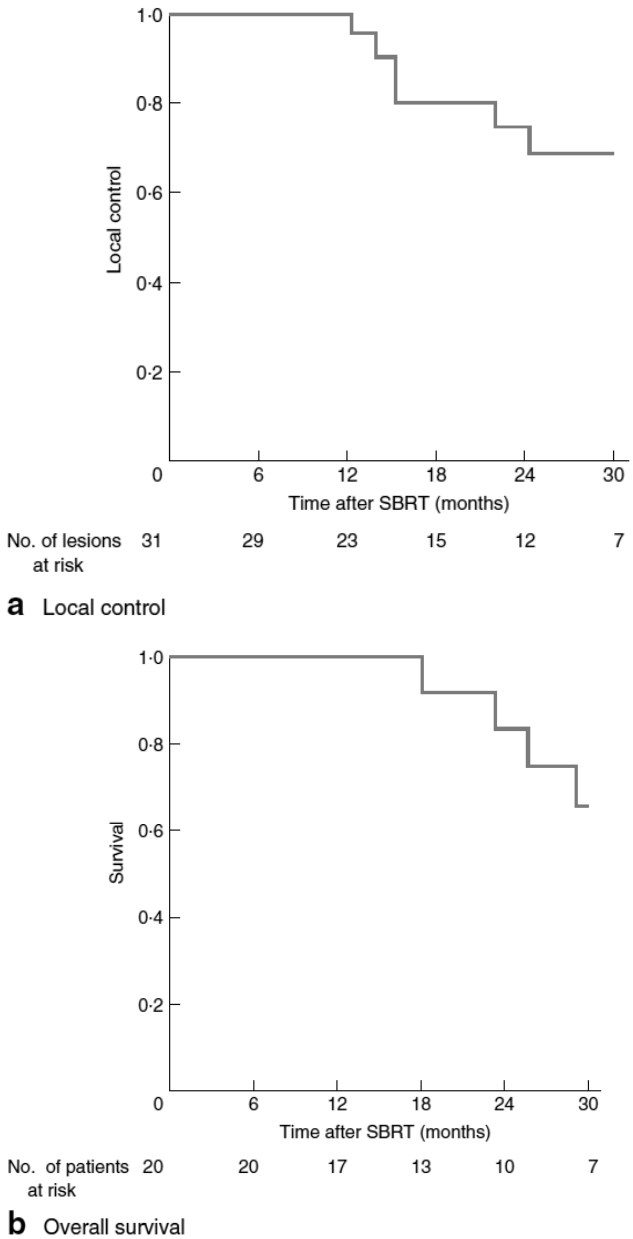

Fig. 1. a Local control rate and **b** overall survival after stereotactic body radiation therapy (SBRT).

Overall survival

Nine patients had died after a median follow-up of 26 (range 6–57) months. Median time to progression of disease was 11 (range 1–52) months. Median overall survival was 34 months, and actuarial 1- and 2-year survival rates were 100 and 83 per cent respectively (Fig. 1b).

Toxicity

Eighteen patients had hepatic toxicity of grade 2 or less, whereas two patients had grade 3 toxicity (CTC version 3.0) with an increase in -glutamyl transferase level. One patient showed no changes in liver function parameters but developed portal hypertension syndrome with oesophageal varices (grade 1 toxicity) with one episode of melaena, and was treated conservatively. After the second radiation treatment this patient presented with hepatic toxicity and ascites (both grade 2), which responded well to temporary diuretic medication. Oesophageal bleeding evidenced by melaena occurred again, and the varices were treated with endoscopic band ligation. One patient became physically weak (grade 3) during the first month after treatment but recovered spontaneously during the second month. Grade 2 pain owing to rib fractures occurred in one patient 10 months after irradiation of a subcapsular liver metastasis located in the vicinity of the ribs. No grade 4 or 5 (death), or stomach, bowel, kidney or spinal cord toxicity was found.

DISCUSSION

The present study has shown that SBRT for colorectal liver metastases can achieve 2-year local control and survival rates of 74 and 83 per cent respectively with acceptable toxicity in patients who are not eligible for surgery or RFA. Three patients developed CTC toxicity grade 3, and late toxicity of grade 1 and 2 was reported in two patients.

Resection should be regarded as the standard curative treatment in patients with hepatic metastases from colorectal cancer. However, only a minority of patients are suitable for liver resection (17). RFA has certain advantages over hepatic resection, such as a shorter hospital stay and a lower complication rate (5, 18), although the authors do not advocate it as an alternative to hepatic resection as it is associated with a higher local recurrence rate, with median time to local tumour progression between 4 and 9 months (19). RFA should be reserved for those in whom resection of all metastases is not possible (20). SBRT has been used for liver metastases that are unsuitable for or refractory to liver resection or RFA in an attempt to control disease locally.

SBRT involves the precise delivery of large doses of highly conformal radiation to extracranial targets using a small number of fractions. This treatment has several advantages over RFA. Owing to the heat-sink effect of large vessels, tissue close to the vessels is not amenable to RFA and major bile ducts are at increased risk of heat injury during ablation (18). To avoid these problems, centrally located liver lesions and metastases near large vessels may be treated with SBRT instead of RFA. SBRT is non-invasive and can be offered to patients who are not eligible for invasive or minimal invasive interventions; it is also feasible in the outpatient setting, with no requirement for hospitalization or general anaesthesia. SBRT may be as effective as RFA for small tumours but may be less suitable for multiple tumours.

Herfarth and Debus (10) reported poorer local control of colorectal metastases than of tumours with other histology (45 *versus* 91 per cent after 18 months). This is in line with other studies that showed a lower local control or survival rate in patients with metastases from colorectal cancer compared with metastases from other primary tumours (12, 21). In contrast, Rusthoven and co-workers (22) reported an improved median survival of 32 months after treatment of liver metastases from favourable primaries (breast, colorectal, renal, carcinoid, gastrointestinal stromal tumour and sarcoma), compared with the median survival of 12 months for those from unfavourable primary sites (primary tumours of the lung, ovary and non-colorectal gastrointestinal malignancies). This raises the question of whether it is justified to group liver metastases from primary colorectal cancer together with those from other primary cancers when evaluating the results of SBRT. Therefore, the present study focused on colorectal metastases only.

A 2-year local control rate of 74 per cent was achieved for colorectal metastases generally treated with 3 × 12.5 Gy, with a median survival of 34 months. Previous studies describing the outcomes of SBRT for colorectal liver metastases are summarized in Table 2. Hoyer and colleagues (23) achieved a 2-year local control rate of 86 per cent after SBRT with 3 × 15 Gy for colorectal metastases in the liver, lung or suprarenal lymph nodes, or at two of these sites; median follow-up was 4.3 years. When liver metastases were analysed separately, a 2-year local control rate of 78 per cent was noted (M. Hoyer, personal communication). This is in line with the present results, probably because the dose was similar in the two studies and median follow-up was adequate (more than 2 years). Rusthoven and co-workers (22) reported a 2-year local control rate of 92 per cent in liver metastases from a variety of primary tumours treated with 36–60 Gy. This clinical experience is consistent with the knowledge that escalated doses of radiation are associated with improved local control and survival (21, 24). Dose escalation in the present cohort was limited owing to the small functional liver remnant because most patients had already undergone several partial liver resections and RFA procedures before SBRT. However, it is generally difficult to compare studies

Table 2. Reported local control rates after treatment of colorectal liver metastases with stereotactic body radiation therapy

Reference	No. of patients	No. of liver lesions	Dose fractionation scheme	Median follow-up (months)	Actuarial local control(%)		Actuarial survival(%)	
					1 year	2 years	1 year	2 years
10	35	–	1×20–26Gy (80)	15*	–	45†	–	–
13	–	23	3–4×7–12,5Gy (65) or 1×26Gy (80)	15	88‡	56‡	–	–
11	20	–	7–20×2–6Gy (80)	15	–	–	80‡	26‡
12	40	–	6×4.6–10 (–)	11	–	–	63	–
Present series	20	31	3×12.5–15Gy (65)	26	100	74	100	83

Values in parenthesis are percentage isodose. *Mean. †Eighteen month. ‡Data from figures.

on SBRT for liver tumours. Conflicting results regarding patient outcome might be explained by differences in patient selection criteria, site of metastases, dose prescription, assessments of local failure or control, and duration of follow-up. In the present series median follow-up was 26 months and the median time to local failure was 22 (range 12–52) months. Median follow-up in the series of Rusthoven *et al*. (22) was only 16 months, which may be too short to allow reliable estimation of local control.

Only a minority of patients with colorectal liver metastases in this clinic were treated with SBRT. The 20 patients in this study represent a negative selection as they were not eligible for surgery and/or RFA because of tumour size and/or location. Lesions were centrally located or near to biliary ducts and vessels. In this respect, these patients represent a group with a poor prognosis.

Median survival of patients with stage IV colorectal cancer is about 24 months with modern chemotherapy (25, 26). In the present series, median survival was 34 months after SBRT; no serious acute toxicity was encountered in keeping with previous reports (10, 27, 28); and none of the patients received adjuvant chemotherapy. The low toxicity after SBRT, and at least comparable survival to that after systemic chemotherapy, may justify its use in this patient group. The median time to disease progression after SBRT was 11 months, similar to that after liver resection in the authors' experience (29). The lower median survival of 34 months after SBRT, compared with 44 months after partial liver resection, can be explained by the generally poorer prognosis of the cohort.

Further research is needed to define the role of SBRT within the treatment armamentarium for colorectal liver metastases. A phase III trial has been proposed by this centre among others (International Liver Group) to compare SBRT in three fractions with RFA for the treatment of unresectable colorectal liver metastases up to 4 cm in diameter. Combined treatment with radiation sensitizers should be pursued in addition to randomized trials of SBRT for colorectal liver metastases. It has already been hypothesized that the combination of radiotherapy and angiogenesis inhibitors may

have a synergistic effect (30). Proper selection of patients for this treatment in high-volume hepatobiliary centres with a multidisciplinary team is advocated.

In conclusion, SBRT is indicated in patients with unresectable colorectal liver metastases or as a second-line therapy for recurrence after liver surgery (31). SBRT achieves adequate local control, and appears to be safe with respect to both acute and late toxicity in selected patients if normal tissue dose restrictions are respected.

ACKNOWLEDGEMENTS

C.V. and J.N.M.IJ. both qualify as last authors and contributed equally to this work. The authors declare no conflict of interest.

REFERENCES

1. Jemal A, Siegel R, Ward E, Murray T, Xu J, Thun MJ. Cancer statistics, 2007. *CA Cancer J Clin* 2007; 57: 43–66.
2. Khatri VP, Petrelli NJ, Belghiti J. Extending the frontiers of surgical therapy for hepatic colorectal metastases: is there a limit? *J Clin Oncol* 2005; 23: 8490–8499.
3. Rees M, Tekkis PP, Welsh FK, O'Rourke T, John TG. Evaluation of long-term survival after hepatic resection for metastatic colorectal cancer: a multifactorial model of 929 patients. *Ann Surg* 2008; 247: 125–135.
4. de Meijer VE, Verhoef C, Kuiper JW, Alwayn IP, Kazemier G, IJzermans JN. Radiofrequency ablation in patients with primary and secondary hepatic malignancies. *J Gastrointest Surg* 2006; 10: 960–973.
5. Gillams AR, Lees WR. Five-year survival in 309 patients with colorectal liver metastases treated with radiofrequency ablation. *Eur Radiol* 2009; 19: 1206–1213.
6. Blomgren H, Lax I, Göranson H, Krsgmaeligpelien T, Nilsson B, Näslund I *et al.* Radiosurgery for tumors in the body: clinical experience using a new method. *J Radiosurg* 1998; 1: 63–74.
7. McGinn CJ, Ten Haken RK, Ensminger WD, Walker S, Wang S, Lawrence TS. Treatment of intrahepatic cancers with radiation doses based on a normal tissue complication probability model. *J Clin Oncol* 1998; 16: 2246–2252.
8. Timmerman R, Papiez L, McGarry R, Likes L, DesRosiers C, Frost S *et al.* Extracranial stereotactic radioablation: results of a phase I study in medically inoperable stage I non-small cell lung cancer. *Chest* 2003; 124: 1946–1955.
9. Dawson LA, Lawrence TS. The role of radiotherapy in the treatment of liver metastases. *Cancer J* 2004; 10: 139–144.
10. Herfarth KK, Debus J. [Stereotactic radiation therapy for liver metastases.] Chirurg 2005; 76: 564–569.
11. Katz AW, Carey-Sampson M, Muhs AG, Milano MT, Schell MC, Okunieff P. Hypofractionated stereotactic body radiation therapy (SBRT) for limited hepatic metastases. *Int J Radiat Oncol Biol Phys* 2007; 67: 793–798.
12. Lee MT, Kim JJ, Dinniwell R, Brierley J, Lockwood G, Wong R *et al.* Phase I study of individualized stereotactic body radiotherapy of liver metastases. *J Clin Oncol* 2009; 27: 1585–1591.
13. Wulf J, Guckenberger M, Haedinger U, Oppitz U, Mueller G, Baier K *et al.* Stereotactic radiotherapy of primary liver cancer and hepatic metastases. *Acta Oncol* 2006; 45: 838–847.
14. Lax I, Blomgren H, Näslund I, Svanträm R. Stereotactic radiotherapy of malignancies in the abdomen. Methodological aspects. *Acta Oncol* 1994; 33: 677–683.
15. Méndez Romero A, Wunderink W, Hussain SM, De Pooter JA, Heijmen BJ, Nowak PC *et al.* Stereotactic body radiation therapy for primary and metastatic liver tumors: a single institution phase i–ii study. *Acta Oncol* 2006; 45: 831–837.
16. Kavanagh BD, Schefter TE, Cardenes HR, Stieber VW, Raben D, Timmerman RD *et al.* Interim analysis of a prospective phase I/II trial of SBRT for liver metastases. Acta Oncol 2006; 45: 848–855.
17. Cummings LC, Payes JD, Cooper GS. Survival after hepatic resection in metastatic colorectal cancer: a population-based study. *Cancer* 2007; 109: 718–726.
18. Wood TF, Rose DM, Chung M, Allegra DP, Foshag LJ, Bilchik AJ. Radiofrequency ablation of 231 unresectable hepatic tumors: indications, limitations, and complications. *Ann Surg Oncol* 2000; 7: 593–600.

19. Stang A, Fischbach R, Teichmann W, Bokemeyer C, Braumann D. A systematic review on the clinical benefit and role of radiofrequency ablation as treatment of colorectal liver metastases. *Eur J Cancer* 2009; 45: 1748–1756.
20. Aloia TA, Vauthey JN, Loyer EM, Ribero D, Pawlik TM, Wei SH *et al.* Solitary colorectal liver metastasis: resection determines outcome. *Arch Surg* 2006; 141: 460–466.
21. Milano MT, Katz AW, Schell MC, Philip A, Okunieff P. Descriptive analysis of oligometastatic lesions treated with curative-intent stereotactic body radiotherapy. *Int J Radiat Oncol Biol Phys* 2008; 72: 1516–1522.
22. Rusthoven KE, Kavanagh BD, Burri SH, Chen C, Cardenes H, Chidel MA *et al.* Multi-institutional phase I/II trial of stereotactic body radiation therapy for lung metastases. *J Clin Oncol* 2009; 27: 1579–1584.
23. Hoyer M, Roed H, Traberg Hansen A, Ohlhuis L, Petersen J, Nellemann H *et al.* Phase II study on stereotactic body radiotherapy of colorectal metastases. *Acta Oncol* 2006; 45: 823–830.
24. Dawson LA, McGinn CJ, Normolle D, Ten Haken RK, Walker S, Ensminger W *et al.* Escalated focal liver radiation and concurrent hepatic artery fluorodeoxyuridine for unresectable intrahepatic malignancies. *J Clin Oncol* 2000; 18: 2210–2218.
25. Falcone A, Ricci S, Brunetti I, Pfanner E, Allegrini G, Barbara C *et al.* Phase III trial of infusional fluorouracil, leucovorin, oxaliplatin, and irinotecan (FOLFOXIRI) compared with infusional fluorouracil, leucovorin, and irinotecan (FOLFIRI) as first-line treatment for metastatic colorectal cancer: the Gruppo Oncologico Nord Ovest. *J Clin Oncol* 2007; 25: 1670–1676.
26. Tournigand C, André T, Achille E, Lledo G, Flesh M, Mery-Mignard D *et al.* FOLFIRI followed by FOLFOX6 or the reverse sequence in advanced colorectal cancer: a randomized GERCOR study. *J Clin Oncol* 2004; 22: 229–237.
27. Schefter TE, Kavanagh BD, Timmerman RD, Cardenes HR, Baron A, Gaspar LE. A phase I trial of stereotactic body radiation therapy (SBRT) for liver metastases. *Int J Radiat Oncol Biol Phys* 2005; 62: 1371–1378.
28. Wulf J, Hädinger U, Oppitz U, Thiele W, Ness-Dourdoumas R, Flentje M. Stereotactic radiotherapy of targets in the lung and liver. Strahlenther Onkol 2001; 177: 645–655.
29. Dols LF, Verhoef C, Eskens FA, Schouten O, Nonner J, Hop WC *et al.* [Improvement of 5 year survival rate after liver resection for colorectal metastases between 1984 and 2006.] *Ned Tijdschr Geneeskd* 2009; 153: 490–495.
30. Verhoef C, de Wilt JH, Verheul HM. Angiogenesis inhibitors: perspectives for medical, surgical and radiation oncology. *Curr Pharm Des* 2006; 12: 2623–2630.
31. van der Pool AE, Lalmahomed ZS, de Wilt JH, Eggermont AM, Ijzermans JM, Verhoef C. Local treatment for recurrent colorectal hepatic metastases after partial hepatectomy. *J Gastrointest Surg* 2009; 13: 890–895.

7

COMPARISON OF MACROSCOPIC PATHOLOGY MEASUREMENTS WITH MAGNETIC RESONANCE IMAGING AND ASSESSMENT OF MICROSCOPIC PATHOLOGY EXTENSION FOR COLORECTAL LIVER METASTASES

Alejandra Méndez Romero, Joanne Verheij, Roy S. Dwarkasing,
Yvette Seppenwoolde, William K. Redekop, Pieter E. Zondervan,
Peter J. C. M. Nowak, Jan N. M. IJzermans, Peter C. Levendag,
Ben J. M. Heijmen, and Cornelis Verhoef

Int. J. Radiation Oncology Biol. Phys: In press December 2010

ABSTRACT

Purpose: To compare pathology macroscopic tumor dimensions with magnetic resonance imaging (MRI) measurements, and to establish the microscopic tumor extension of colorectal liver metastases.

Methods and Materials: In a prospective pilot study we included patients with colorectal liver metastases planned for surgery and eligible for MRI. A liver MRI was performed within 48 hours before surgery. Directly after surgery, an MRI of the specimen was acquired to measure the degree of tumor shrinkage. The specimen was fixed in formalin for 48 hours, and another MRI was performed to assess the specimen/tumor shrinkage. All MRI sequences were imported into our radiotherapy treatment planning system, where the tumor and the specimen were delineated. For the macroscopic pathology analyses photographs of the sliced specimens were used to delineate and reconstruct the tumor and the specimen volumes. Microscopic pathology analyses were conducted to assess the infiltration depth of tumor cell nests.

Results: Between February 2009 and January 2010 we included 13 patients for analysis with 21 colorectal liver metastases. Specimen and tumor shrinkage after resection and fixation was negligible. The best tumor volume correlations between MRI and pathology were found for T1-weighted (w) echo gradient sequence (r_s=0.99, slope=1.06), and the T2-w fast spin echo (FSE) single shot sequence (r_s=0.99, slope=1.08), followed by the T2-w FSE fat saturation sequence (r_s=0.99, slope=1.23), and the T1-w gadolinium-enhanced sequence (r_s=0.98, slope=1.24). We observed 39 tumor cell nests beyond the tumor border in 12 metastases. Microscopic extension was found between 0.2 and 10 mm from the main tumor, with 90% of the cases within 6mm.

Conclusions: MRI tumor dimensions showed a good agreement with the macroscopic pathology suggesting that MRI can be used for accurate tumor delineation. However, microscopic extensions found beyond the tumor border indicate that caution is needed in selecting appropriate tumor margins.

Acknowledgements: The authors thank Rob van Os, M.Sc., Anne van der Pool, M.D., Wouter Wunderink M.Sc., Paulette Prins, PhD, and Hans Joosten for their contributions.

INTRODUCTION

Colorectal cancer is one of the leading causes of cancer-related mortality in men and women each year (1). During follow-up as many as 50 to 70% of patients diagnosed with colorectal cancer present liver involvement, which in half of these patients is the only site of recurrence (2).

Surgery is nowadays accepted as curative treatment option for colorectal liver metastases, but the majority of patients are not eligible for resection due to technical or medical reasons (2). When resection is not possible, radiofrequency ablation (RFA) is currently the most widely used treatment method (3). However, the location of metastases close to the large vessels, the main bile ducts, or the gallbladder poses a problem for adequate delivery of RFA.

Over the past 20 years, stereotactic body radiation therapy (SBRT) has evolved as another local treatment option for primary and metastatic liver tumors. Local control rates have been increased by dose escalation protocols while acceptable levels of toxicity have been maintained (4,5). Nevertheless, to further optimize the treatment, the definition of the target volume should be improved. It is agreed that in SBRT for liver metastases, a safety margin should be added to the tumor visible in computed tomography (CT) and/or magnetic resonance imaging (MRI) to compensate for residual respiratory tumor motion and setup inaccuracies. However, there is still debate about the need for an extra margin to compensate for microscopic extension (ME), and a range of margins between 0 and 10 mm have been described in the literature (4-8). Neither has it been decided whether pre-treatment with chemotherapy might influence the ME of the metastases. Similarly, to precisely define the limits of the target volume, the correlation between macroscopic tumor dimensions visible in medical images and pathology should be evaluated. To our knowledge, literature reports on these subjects are scarce (9-12).

The aims of this prospective study were to correlate pathology macroscopic tumor dimensions with MRI measurements, and to establish the microscopic tumor extension in a cohort of 20 colorectal liver metastases.

METHODS AND MATERIALS

Study design

Candidates for this prospective cohort study were diagnosed with colorectal liver metastases planned for surgery, and eligible to undergo an MRI scan. Patients with an insufficient renal function or estimated creatinine clearance <50ml/min were excluded. In total 20 colorectal liver metastases were estimated to be included in a period of approximately one year, 10 treated preoperatively with chemotherapy and

10 not. The study was approved by the Ethical Commission of Erasmus MC. Written informed consent was required.

Imaging

MRI was selected above CT as imaging modality because it is superior for the assessment of malignant focal liver lesions (13,14).

Preoperative procedure

Within 48 hours before surgery, and preferably the day before, an MRI of the liver was performed with a 1.5T MR scanner (Signa HDxt, General Electrics, WI). This preoperative MRI included a T2-weighted (w) fast spin echo (FSE) single shot (SS) sequence, a T1-w gradient echo (GE) sequence, a T1-w dynamic multiphasic gadolinium-enhanced (DMGE) sequence, and a T2-w FSE fat saturation (FS) sequence (Fig. 1A-D). The T1-w sequences and T2-w FSE SS sequences were carried out in breath hold (exhale). The T2-w FSE FS sequences were performed with the system triggered in expiration. The slice thickness for T1-w GE sequences and T2-w sequences was 8 mm, and for T1-w DMGE sequence it was 5 mm.

Surgery

No deviations were requested from the surgical approach decided up front, unless unexpected new lesions were observed, in which case the surgery was adapted to treat all lesions.

Directly after surgery

Once the specimen containing the tumor had been resected, it was sent to the radiology department with a proper indication of the orientation in the body (superior/inferior, left/right, and anterior/posterior) by three labeled small plastic tacks that were sewed into relevant positions of the specimen.

An MRI examination of the specimen was carried out directly after the resection and before fixation. The aim was to investigate the possible shrinkage of the tumor directly after the specimen had been separated from the rest of the liver. The MRI equipment was the same as the one used to acquire the preoperative imaging. A combination of a T1-w GE sequence and a T2-w FSE FS sequence of the liver specimen was acquired with dedicated small field of view (Fig. 1E-F). The slice thickness was 2 to 4 mm. After acquisition of MRI sequences, the specimen was fixed in formalin.

Forty-eight hours after surgery

After 48 hours of fixation, a second MRI of the resected specimen was performed with the same scanner and the same protocol as previously described. Figures 1G-H provide

sample images. The required acquisition of an MRI after 48 hours of fixation restricted the possibility of receiving specimens to Mondays, Tuesdays and Wednesdays (until midday).

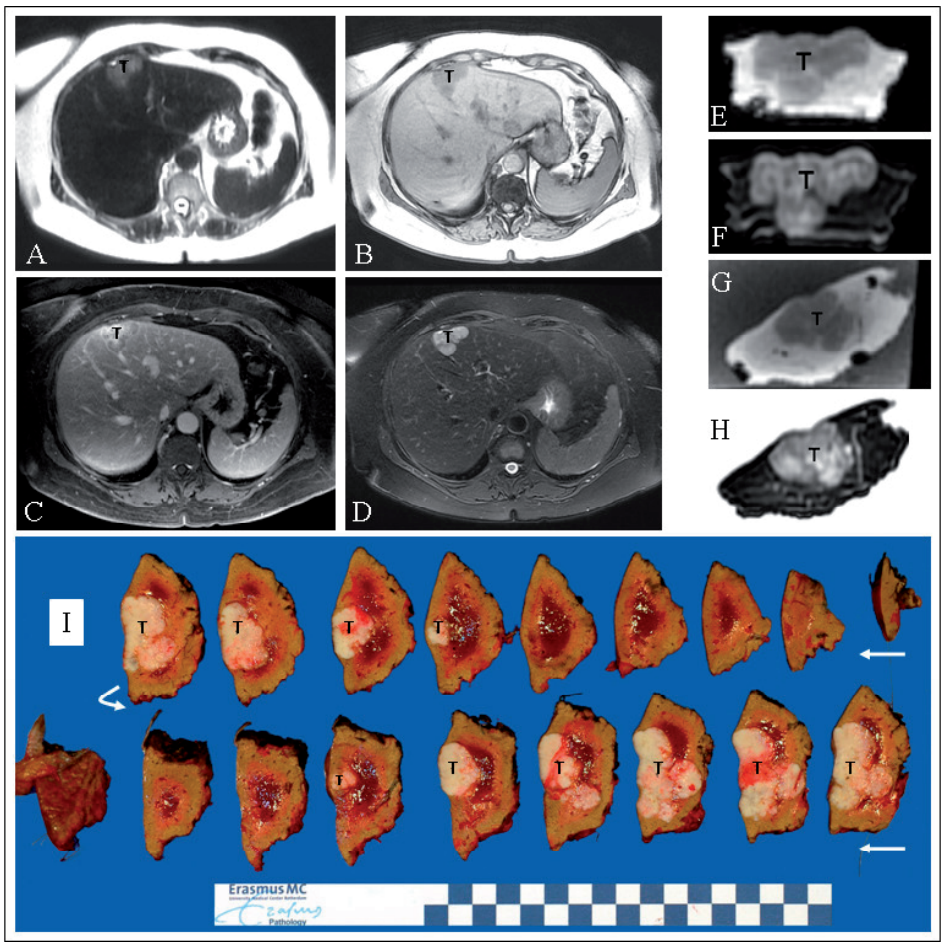

Fig. 1. Magnetic resonance imaging series and macroscopic pathology corresponding to a patient with a colorectal liver metastasis located in segment 4. Tumor is represented by T.
A: Preoperative T2-weighted fast spin echo (FSE) single shot sequence.
B: Preoperative T1-weighted gradient echo sequence.
C: Preoperative T1-weighted dynamic multiphasic gadolinium-enhanced sequence.
D: Preoperative T2-weighted FSE fat saturation sequence.
E: Postoperative T1-weighted gradient echo sequence.
F: Postoperative T2-weighted FSE fat saturation sequence.
G: Post-formalin T1-weighted gradient echo sequence.
H: Post-formalin T2-weighted FSE fat saturation sequence.
I: Sliced specimen.

Macroscopic pathology analysis

On the same day of the postformalin MRI acquisition, we carried out an axial sectioning of the specimen in slices of approximately 5 mm thickness, using a knife equipped with a sharp blade. Maximal diameters of the tumor and the specimen were measured together with the specimen weight. The specimen and later the consecutive sections were laid out for digital photography (Fig. 1I). The images were imported in MatLab (The MathWorks, Natick, MA) for further analysis. Establishment of the macroscopic pathologic tumor volume required delineated tumor contours and exact slice thicknesses. However, due to imperfections in sectioning of the specimen, the slice thickness needed for volume calculation was not exactly known and had to be estimated. For this purpose we divided the dimension of the specimen along which the slices were cut by the total number of slices. This procedure was validated in a subgroup of specimens by comparing the volume obtained from delineated specimen contours and the estimated slice thickness with the volume calculated from the measured weight of the specimen after applying a weight-to-volume correcting factor of 1.05 (average CT density of liver).

Microscopic pathology analysis

Slices of the tumor and the surrounding liver parenchyma were taken for further microscopic analysis at the level of the percentiles 25, 50 and 75 of the superior/inferior axis, regardless of tumor size. After cutting, slices were further fixed in formalin because the impact of the previous fixation was limited to mainly the superficial areas of the specimen. Correction for potential additional shrinkage could not be quantified. Later, the slices were embedded in paraffin and cut with a microtome in 4 µm sections, and stained with hematoxylin and eosin. Experienced hepatopathologists (JV, PEZ) evaluated the ME by light microscopy. If the main tumor was completely or partially surrounded by a fibrous pseudocapsule, the ME was considered to be the maximum distance from the outer border of the pseudocapsule to the outer boundary of the visible nests of tumor cells (15). If a fibrous pseudocapsule surrounding the main tumor was absent, we defined the tumor mass as the area where none or almost none of liver parenchyma interposed between tumor cells could be seen. The tumor border was defined as the line where liver tissue and nests of tumor cells interchanged. The ME was defined in this case as the distance from the main tumor border to the outer boundary of the visible nests of tumor cells (16).

Volume assessment of tumor and specimen in MRI

Preoperative MRI series together with preformalin and postformalin sequences were imported into our radiotherapy planning system (FocalSim, version 4.3.3, CMS Inc, Maryland Heights, MO). Axial slices were used to contour and assess the volume of

the gross tumor/specimen in the image sets. Tumor contours were reviewed by an experienced liver radiologist (RSD).

Calculation of shrinkage factor

The aim was to investigate the possible shrinkage of the tumor and when available the specimen, after the separation of the tumor/specimen from the rest of the liver, and after the fixation of tumor/specimen in formalin. To calculate the shrinkage factors we assumed that the tumors were ellipsoids, and that the shrinkage was uniform in all three directions, resulting in the formula:

$$\text{Axis shrinkage factor} = (\text{Volume}_2/\text{Volume}_1)^{(1/3)} \quad (1)$$

Comparison of preoperative MRI with macroscopic pathology

For each of the four preoperative MRI sequences, delineated gross tumor volumes were compared with macroscopic pathology. Moreover, established MRI and pathology volumes were converted into effective tumor radii, assuming the tumors were spherical.

Statistics

Descriptive statistics of variables were calculated (mean, standard deviation, minimum and maximum values). Linear regression analyses were performed to calculate the Spearman correlation coefficient (r_s) and the regression coefficient, slope (s), of the assumed linear relationship between preoperative MRI and pathology volumes and effective radii. Correlation analyses using several independent variables were also carried out to establish the presence and degree of correlation between pathology results and characteristics of the patient and the tumor. All other analyses were performed using non-parametric tests (signed-rank test and Kruskal-Wallis test).

RESULTS

Study population

Between February 2009 and January 2010 we enrolled 16 patients with colorectal liver metastases. Three patients were excluded from the analyses; two due to the lack of specimen photographs, and one due to a too thick slicing of the specimen. Patient characteristics of the 13 remaining patients with 21 metastases are presented in Table1.

The chemotherapy regimen administered as treatment before surgery included oxaliplatin, capecitabine and bevacizumab.

Table 1. Patient and tumor characteristics

	Patients	
Gender		
Male	8	
Female	5	
Age (years) Mean (Min-Max)	63.9 (46-80)	
Timing of developing metastases	Patients	Metastases
Synchronous	3	5
Metachronous	10	16
Preoperative chemotherapy	Patients	Metastases
Yes	5	10
No	8	11
Type of surgery	Patients	Metastases
Hemihepatectomy	4	6
Segmentectomy	9	15

For all 21 metastases preoperative imaging was obtained without deviations in the protocol. For one small lesion (10 mm) in one patient, the tumor boundary could not be defined with certainty in three sequences of the preoperative MRI (T1-w EG, T2-w FSE SS and T2-w FSE FS). For another metastasis (30 mm) in another patient, the limits of the tumor could not be identified properly in one sequence (T2-w FSE SS).

In four metastases in two patients there were deviations from the protocol regarding postoperative imaging. In these two patients the operation was concluded in the evening. This circumstance made it impossible to scan the specimens directly after surgery. For one patient, with two metastases, the specimen was scanned at the start of the next day, before fixation in formalin. For the two specimens of the other patient, imaging before fixation was not performed due to logistic reasons.

Postformalin imaging was available for all 21 metastases, although two metastases of one patient were not scanned on a Friday 48 hours after fixation but on Monday morning because of a technical problem with the MRI scanner.

The pathology volume was not assessed in four metastases of two patients. All of these metastases had been pretreated with chemotherapy. Two of them were so small (6 mm and 10 mm diameter) that they were only present in one slice of the hemihepatectomy making a volume calculation impossible. For the other two, it was extremely difficult to differentiate between tumor and normal liver parenchyma. Later these two metastases were described in the pathology report as mostly being composed of necrotic tissue.

Descriptive statistics of the metastases volumes assessed by means of imaging and pathology are presented in Table 2.

Table 2. Tumor volumes assessed by means of preoperative MRI and macroscopic pathology

	N	Mean (cc)	SD (cc)	Minimum (cc)	Maximum (cc)
T1-w gradient echo	20	17.81	22.50	1	82
T2-w FSE single shot	19	18.59	23.5	1	84.80
T1-w gadolinium enhanced	21	20.22	26.12	1.2	95.40
T2-w FSE fat saturation	20	20.79	26.13	1.2	95.60
Pathology	17	18.35	22.15	0.5	76.90

w: weighted. FSE: fast spin echo.

Shrinkage factors

Calculation of the shrinkage factors was based on the T1-w EG sequence. Table 3 presents an overview of the descriptive statistics for the calculated shrinkage factors of the tumor and the specimen volumes. Eighteen tumors and ten specimens (out of seventeen) were available for shrinkage factor calculations. One tumor could not be properly defined on the preoperative T1-w EG sequence. Two tumors/specimens had no postoperative imaging. Five specimens were not fully scanned beyond the tumor area. For both tumors and specimens shrinkage was very small (maximum 2%) and was neglected in further analyses.

Table 3. Tumor and specimen shrinkage factors from stage to stage

	Tumor				Specimen			
	N	Mean	SD	P	N	Mean	SD	P
Preoperative / Postoperative	18	0.98	0.03	0.03	N.A	N.A.	N.A.	N.A.
Postoperative / Post-formalin	18	1.00	0.01	0.22	10	1.00	0.01	0.23

N.A.: not applicable. SD: standard deviation.
P-values resulting from the signed-rank test calculation are presented.

Volume comparison

The mean differences between the tumor volumes measured in each of the four preoperative sequences and the volumes obtained by the macroscopic pathology are presented in Table 4. For all MRI sequences, the increase in mean volume compared to pathology was statistically significant. The smallest mean difference was found for the T1-w EG sequence. As also presented in Table 4, the slope of the fit-line between the volumes measured in this sequence and pathology was closest to one (s = 1.06). All MRI sequences correlated well with the pathology ($r_s \geq 0.98$, Table 4). As shown in Table 5, differences between MRI and pathology in effective tumor radii were very small, especially for T1-w EG and T2-w FSE SS sequences with mean differences of 0.06 and 0.07 cm respectively, and slope in both of 1.01. In Figure 2A, correlations between MRI- and pathology volumes are compared with the ideal correlation (slope = 1). Figure 2B shows similar data for effective tumor radii.

Table 4. Mean differences between pre-operative MRI tumor volumes and corresponding macroscopic pathology

Difference	N	Mean (cc)	SD (cc)	P	r_s	s
T1-w gradient echo - pathology	17	1.98	2.55	0.02	0.99	1.06
T2-w FSE single shot -pathology	16	2.38	2.94	0.01	0.99	1.08
T1-w gadolinium enhanced - pathology	17	5.92	6.18	<0.01	0.98	1.24
T2-w FSE fat saturation - pathology	17	5.39	5.92	<0.01	0.99	1.23

w: weighted. FSE: fast spin echo.
Standard deviations (SD) and P-values obtained from signed-rank tests. Spearman's rank correlation coefficients (r_s) and slopes (s) are also represented.

Table 5. Mean differences between pre-operative MRI tumor volumes and corresponding macroscopic pathology

Difference	N	Mean (cc)	SD (cc)	P	rs	s
T1-w gradient echo - pathology	17	1.98	2.55	0.02	0.99	1.06
T2-w FSE single shot -pathology	16	2.38	2.94	0.01	0.99	1.08
T1-w gadolinium enhanced - pathology	17	5.92	6.18	<0.01	0.98	1.24
T2-w FSE fat saturation - pathology	17	5.39	5.92	<0.01	0.99	1.23

w: weighted. FSE: fast spin echo.
Standard deviations (SD) and P-values obtained from signed-rank tests. Spearman's rank correlation coefficients (rs) and slopes (s) are also represented.

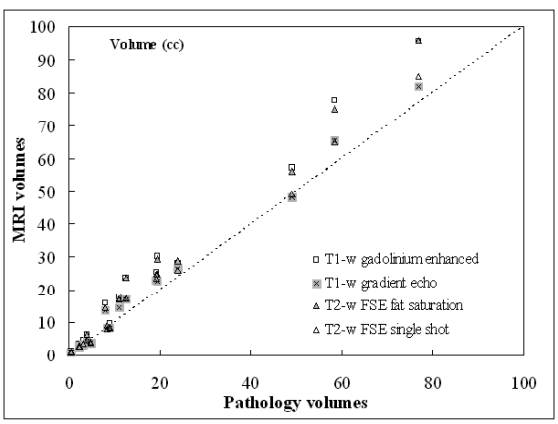

(A)

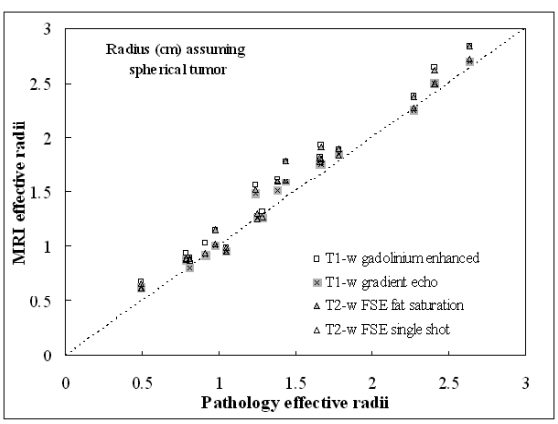

(B)

Fig. 2. Measured correlations between MRI and pathology tumor dimensions compared to the ideal correlation (dotted line).
(A): Tumor volumes.
(B): Effective tumor radii, assuming a spherical tumor shape.

Microscopic extension

A total of 39 tumor nests from 12 macroscopic metastases (57%) were found. Five of these metastases had been previously treated with chemotherapy and seven had not. Mean maximum infiltration depth for the 39 tumor nests was 2.2 mm (range 0.2-10). For almost 80% of the tumor nests the maximum infiltration depth was found within 3 mm, and in almost 90% within 6 mm. Figure 3 shows a frequency histogram of tumor nests observed at various distances from the main tumor border. An example of a metastasis with two tumor nests is presented in Figures 4A and B. No significant relationship was found between preoperative tumor volume and a deeper ME ($p = 0.74$, $r_s = 0.11$). Neither could we find a significant relationship between patient or tumor characteristics, including preoperative chemotherapy, and presence or frequency of ME.

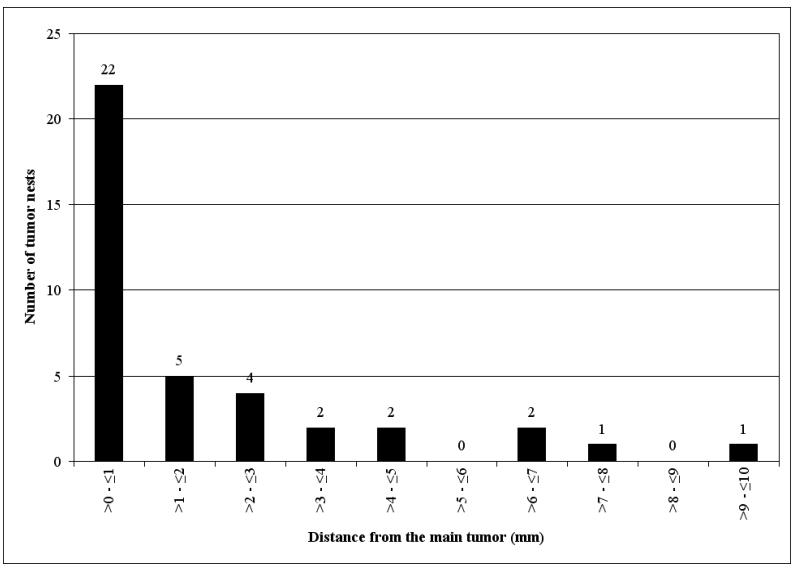

Fig. 3. Microscopic extension. Presented are the observed numbers of tumor nests as a function of the distance measured from the main tumor to the outer border of the tumor nest.

DISCUSSION

SBRT applied to unresectable colorectal liver metastases has demonstrated a good local control rate (17). To further optimize the treatment, we designed this study to compare pathology macroscopic tumor dimensions with MRI measurements, and to establish the microscopic tumor extension. MRI volumes and effective radii correlated well with macroscopic pathology (correlation close to 1 for all sequences). However, mean MRI volumes and effective tumor radii were statistically significant enlarged compared to pathology for all sequences. Although statistically significant,

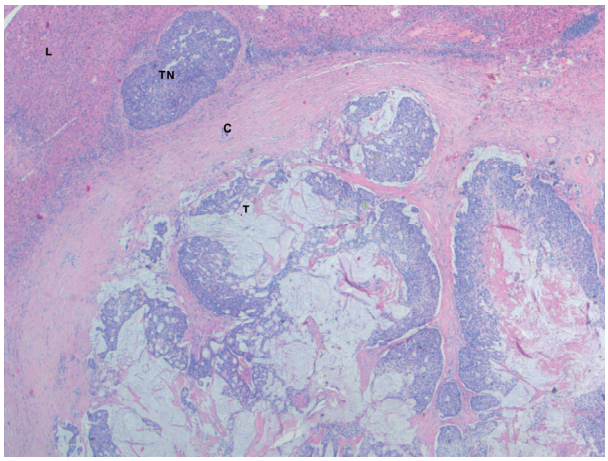

(A)

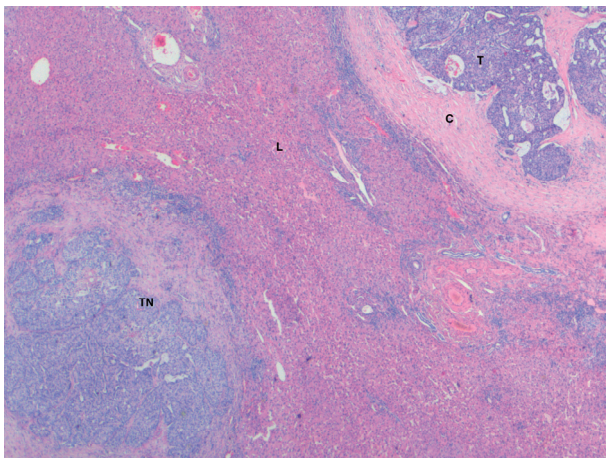

(B)

Fig. 4. Microscopic extension evaluated using a light microscope (objective x 20).
(A): Tumor nest (TN) found adjacent to the capsule (C) that surrounds the main tumor (T). Liver parenchyma represented as L.
(B): Tumor nest (TN) found at 3.5 mm from the capsule (C) that surrounds the main tumor (T). Liver parenchyma represented as L.

the enlargements were small, especially for the T1-weighted (w) gradient echo (GE) and the T2-w fast spin echo (FSE) single shot (SS) sequences. The difference was larger for the T2-w FSE fat saturation (FS) and for the T1-w dynamic multiphasic gadolinium-enhanced (DMGE) sequences. Probably we have included in our delineated tumor volumes some perilesional changes that are better depicted with these sequences (12,18). Semelka *et al* have correlated the presence of perilesional enhancement on gadolinium-enhanced MR images with pathology findings for seven liver metastases (five colorectal) (12). They found a difference of 10-13 mm in diameter between the precontrast and postcontrast series in three metastases (all colorectal), with the postcontrast series showing larger tumor dimensions due to prominent perilesional enhancement. Histopathologic analysis revealed the presence of a thick tumor border containing a combination of peritumoral desmoplastic reaction, peritumoral inflammation, and vascular proliferation. However, the area with increased enhancement was systematically larger than the tumor border, suggesting that the enhancement

extends beyond the tumor border into the surrounding liver. The authors presumed that this might have been caused by the inflammatory effect around the tumor border which increases perfusion in the adjacent zone of hepatic parenchyma by releasing local factors that stimulate angiogenesis. This increases vascularity surrounding the tumor which will accumulate the contrast media (gadolinium) and thus demonstrate enhancement beyond the tumor. The same holds for the T2-w FSE FS sequence with demonstration of high signal intensity of the zone of increased vasculature surrounding the tumor. We detected a very small shrinkage of the tissue after the preoperative MRI measurement (2%) that might have increased the differences between preoperative MRI and pathology results slightly. Although we did not correct for this factor, its impact on the present results is limited because the degree of shrinkage is less than the differences found between the MRI and the pathology results.

In a prospective study published in abstract format, Dawson *et al* compared the volumes in 4 patients with liver metastases assessed by preoperative (within 4 weeks of resection) CT, MRI, and positron emission tomography with macroscopic pathology (9). As in our study, the pathology gross target volume (GTV) was smaller than the imaging GTV in most of the patients (3 of 4). As well, in agreement with our results, the authors reported that pathology GTV correlated best with unenhanced MRI compared to venous enhanced for all patients.

In a retrospective study published in abstract format, Gandhi *et al* compared the clinical tumor sizes in 27 patients with 36 colorectal liver metastases, assessed by preoperative CT or MRI, with the pathology size (10). The median number of days between imaging and surgery was 29 days. In 53% of tumors the pathology size was larger than the radiographic size, and smaller or equal in 47%. A possible explanation for this result might be tumor growth in the time between imaging and surgery.

As discussed above, nonenhanced MRI sequences showed the best correlation with the macroscopic pathology, and therefore they seem more adequate for tumor delineation, especially the T1-w EG sequence. Even though the T2-w FSE SS sequence showed a very high correlation between MRI and macroscopic pathology, the tumor boundary was easier to delineate in the other three series. Probably this observation is inherent to the image quality resulting from this sequence (18). In the liver MRI protocol at our institution this sequence serves mainly as a localizer and to characterize lesions as solid vs. nonsolid. The other series of our protocol are used to detect and further characterize liver lesions. The T2-w FSE FS and the postcontrast T1-w DMGE sequences may facilitate the tumor delineation but they may unnecessarily overestimate the tumor volume by including other effects like peritumoral inflammation or vascular proliferation. This may compensate for limited ME (a few millimeters) but it may not always be enough for the largest microscopic extension found in this study.

The frequency and infiltration depths of ME observed in the present study are in agreement with results reported in the literature. Prospective and retrospective surgical reports describe the presence of ME, although with a large variation in occurrence (2-58%) and in distance of infiltration (0.15-38 mm) (19-22). In agreement with our results, Wakai *et al* reported that ME occurred more frequently (95% of the tumor nests) in the close zone (<1cm) than in the distant zone (≥1cm) of the gross tumor (22). Dawson *et al* (as mentioned above) also analyzed the ME beyond the GTV in 4 patients (9). They found an extension of <1 mm for all cases. No frequency was reported. In agreement with these results, Gandhi *et al* (see above) also found measurable microscopic disease (mean 1.25 mm) in 7 of 24 (29%) analyzed tumors (10). No range was reported. The authors concluded that liver metastases from colorectal cancer do not seem to exhibit significant ME. Both publications are in agreement with our results of finding ME, but our maximum and mean infiltration depths were larger, even though most of the tumor nests that we found -almost 60%- were located within ≤1 mm from the tumor border. Ricke *et al*. described two categories of colorectal liver metastases: round, with a regular margin, and oligonodular with an irregular margin (23). The latter included radiologically visible satellite lesions and showed an impaired local control after CT-guided brachytherapy. In general, all the metastases included in the present study showed a rather irregular shape, which made it difficult to establish a relationship between a more irregular tumor shape and a more frequent or deeper ME.

This study was designed as a prospective pilot study to establish all the procedures needed to obtain a good clinicopathologic correlation and to measure the ME. As well, we tried to determine all factors that could negatively influence the accuracy of the measured results. The first factor was the uncertainty of estimating the specimen slice thicknesses to reconstruct the tumor/specimen macroscopic pathology. To validate the procedure we used the data from a subgroup of specimens. Even though not all the specimens could be used for analysis, the correlation between the weight-corrected volume and the estimated volume of the specimen was good. The second factor was the unfeasibility of quantifying the potential additional shrinkage after cutting the specimen and taking slices for microscopic analysis. Hence, the ME measured in millimeters could therefore be underestimated. The third factor was the impossibility of excluding entirely that some of our tumor nests (observed in a two dimensional microscopic field) were not in reality attached to the main tumor at another level, as some of the colorectal metastases demonstrated a very irregular border. We tried to correct to a maximum for this factor by inspecting thoroughly the slices located just above and beneath the one in which we observed the ME. The fourth factor was the limitation in the number of slices that we used for analyses (percentiles 25, 50 and 75 of the superior/inferior axis). The ideal situation would have been to analyze

the whole liver tissue surrounding the main metastasis but because of the workload involved this was unfeasible in our study. However at the selected levels we examined the complete tumor border, irrespective of the size of the metastasis. Therefore, we conclude that the number of detected tumor nests is a lower limit of the real number. When converted into a histogram with relative frequencies, the histogram shown in Figure 3 may be considered as an estimate of the real relative histogram.

In a practical context our results could be considered as a prescription for extension of the high dose area around the main tumor, depending on the risk of error accepted (24). With a risk error of 10%, for example, it would be necessary to extend the high dose area by 6 mm, and with a risk error of 20 % an extension of 3 mm would be required. However, in part because of the size limitations, this study does not allow definitive and precise conclusions to be drawn about the need for or extent of an extra margin in SBRT planning to compensate for ME. The need for an extension of the high dose volume beyond the GTV does also not necessarily imply the need for an enhanced planning margin. Even with the most conformal techniques, there is often unavoidable delivery of a high dose beyond the gross tumor borders. Goitein *et al* reported on strategies for treating possible tumor extensions and which dose should be delivered (25). These authors suggested that when there is a low, but nonzero probability of disease in a particular region, then the delivery of a lower dose than that given to the GTV could be advantageous. Seidensticker *et al* published a proposal for a safety margin in brachytherapy for colorectal liver metastases (26). They estimated that to prevent the growth of micrometastases a threshold (single) dose of 15.4 Gy should be delivered. High local control rates have been published after treatment for SBRT of liver metastases with three fractions of 20 Gy, without adding extra margins to compensate for ME (5). Possibly, the limited conformality of external beam dose distributions, even for SBRT, allowed omission of a safety margin for ME. The need for an explicit enhancement of planning margins to cope with ME can also be obscured if generous ("safe") margins are used to account for patient setup errors and tumor mobility. The ongoing developments in increasing treatment precision (adaptive therapy, particle therapy) warrant investigations on ME of liver metastases to fully exploit these techniques for our future patients.

CONCLUSIONS

Our study demonstrated a good agreement between the tumor dimensions measured by MRI and the macroscopic pathology, suggesting that MRI can be used for accurate tumor delineation. However, microscopic extensions found beyond the tumor border indicate that caution is needed in selecting appropriate tumor margins.

REFERENCES

1. http://www.who.int.
2. Poston GJ. Surgical strategies for colorectal liver metastases. *Surg Oncol* 2004; 13:125-136.
3. Stang A, Fischbach R, Teichmann W, *et al.* A systematic review on the clinical benefit and role of radiofrequency ablation as treatment of colorectal liver metastases. *Eur J Cancer* 2009; 45:1748-1756.
4. Lee MT, Kim JJ, Dinniwell R, *et al.* Phase I study of individualized stereotactic body radiotherapy of liver metastases. *J Clin Oncol* 2009; 27:1585-1591.
5. Rusthoven KE, Kavanagh BD, Cardenes H, *et al.* Multi-institutional phase I/II trial of stereotactic body radiation therapy for liver metastases. *J Clin Oncol* 2009; 27:1572-1578.
6. Ben-Josef E, Normolle D, Ensminger WD, *et al.* Phase II trial of high-dose conformal radiation therapy with concurrent hepatic artery floxuridine for unresectable intrahepatic malignancies. *J Clin Oncol* 2005; 23:8739-8747.
7. Méndez Romero A, Wunderink W, Hussain SM, *et al.* Stereotactic body radiation therapy for primary and metastatic liver tumors: A single institution phase i-ii study. *Acta Oncol* 2006; 45:831-837.
8. Wulf J, Guckenberger M, Haedinger U, *et al.* Stereotactic radiotherapy of primary liver cancer and hepatic metastases. *Acta Oncol* 2006; 45:838-847.
9. Dawson LA, Brock KK, Moulton C, *et al.* Comparison of Liver Metastases Volumes on CT, MR and FDG PET Imaging to Pathological Resection Using Deformable Image Registration [Abstract]. *Int J Radiat Oncol Biol Phys* 2007; 69, Number 3, (Suppl. 1):68.
10 Ghandi D, Mitchell KA, Miick R, *et al.* Clinicopathologic Analysis of Gross Tumor Size and Microscopic Extension in Liver Metastases from Colorectal Cancer (CRC): Implications for Stereotactic Body Radiotherapy (SBRT) [Abstract]. *Int J Radiat Oncol Biol Phys* 2009; 75, Number 3, (Suppl. 1):29.
11. Outwater E, Tomaszewski JE, Daly JM, *et al.* Hepatic colorectal metastases: correlation of MR imaging and pathologic appearance. *Radiology* 1991; 180:327-332.
12. Semelka RC, Hussain SM, Marcos HB, *et al.* Perilesional enhancement of hepatic metastases: correlation between MR imaging and histopathologic findings-initial observations. *Radiology* 2000; 215:89-94.
13. Balci NC, Befeler AS, Leiva P, *et al.* Imaging of liver disease: comparison between quadruple-phase multidetector computed tomography and magnetic resonance imaging. *J Gastroenterol Hepatol* 2008; 23:1520-1527.
14. Cantwell CP, Setty BN, Holalkere N, *et al.* Liver lesion detection and characterization in patients with colorectal cancer: a comparison of low radiation dose non-enhanced PET/CT, contrast-enhanced PET/CT, and liver MRI. J *Comput Assist Tomogr* 2008; 32:738-744.
15. Okano K, Yamamoto J, Kosuge T, *et al.* Fibrous pseudocapsule of metastatic liver tumors from colorectal carcinoma. Clinicopathologic study of 152 first resection cases. *Cancer* 2000; 89:267-275.
16. Baumert BG, Rutten I, hing-Oberije C, *et al.* A pathology-based substrate for target definition in radiosurgery of brain metastases. *Int J Radiat Oncol Biol Phys* 2006; 66:187-194.
17. van der Pool AE, Méndez Romero A, Wunderink W, *et al.* Stereotactic body radiation therapy for colorectal liver metastases. Br J Surg 2010; 97:377-382.
18. Semelka RC, Chew W, Hricak H, *et al.* Fat-saturation MR imaging of the upper abdomen. *AJR Am J Roentgenol* 1990; 155:1111-1116.

19. Ambiru S, Miyazaki M, Isono T, *et al.* Hepatic resection for colorectal metastases: analysis of prognostic factors. *Dis Colon Rectum* 1999; 42:632-639.
20. Kokudo N, Miki Y, Sugai S, *et al.* Genetic and histological assessment of surgical margins in resected liver metastases from colorectal carcinoma: minimum surgical margins for successful resection. *Arch Surg* 2002; 137:833-840.
21. Nanko M, Shimada H, Yamaoka H, *et al.* Micrometastatic colorectal cancer lesions in the liver. *Surg Today* 1998; 28:707-713.
22. Wakai T, Shirai Y, Sakata J, *et al.* Appraisal of 1 cm hepatectomy margins for intrahepatic micrometastases in patients with colorectal carcinoma liver metastasis. *Ann Surg Oncol* 2008; 15(9):2472-2481.
23. Ricke J, Mohnike K, Pech M, *et al.* Local response and impact on survival after local ablation of liver metastases from colorectal carcinoma by computed tomography-guided high-dose-rate brachytherapy. *Int J Radiat Oncol Biol Phys* 2010; 78:479-485.
24. Giraud P, Antoine M, Larrouy A, *et al.* Evaluation of microscopic tumor extension in non-small-cell lung cancer for three-dimensional conformal radiotherapy planning. *Int J Radiat Oncol Biol Phys* 2000; 48:1015-1024.
25. Goitein M, Schultheiss TE. Strategies for treating possible tumor extension: some theoretical considerations. *Int J Radiat Oncol Biol Phys* 1985; 11:1519-1528.
26. Seidensticker M, Wust P, Ruhl R, *et al.* Safety margin in irradiation of colorectal liver metastases: assessment of the control dose of micrometastases. *Radiat Oncol* 2010; 5:24.

8

GENERAL DISCUSSION AND FUTURE DIRECTIONS

GENERAL DICUSSION AND FUTURE DIRECTIONS

Stereotactic body radiation therapy (SBRT) is a new cancer-treatment strategy that has evolved over the last twenty years. Unlike conventional external beam radiotherapy, which is usually delivered in 20-40 daily fractions of 1.8-2 Gy, SBRT applies high doses per fraction, generally around 6-20 Gy in a course of 1-6 fractions. In the past, such doses were impossible due to limitations in the dose delivery technology and to the potential toxicity associated with exposing large volumes of normal tissue to such doses.

Recent technical developments in precise radiotherapy have made it possible to safely deliver high doses per fraction to tumors in different locations in the body (1). With SBRT we intentionally create hotspots within the radiation dose distribution, of up to - and even beyond - 50% or more of the prescribed dose. The purpose is to intensify the radiation dose inside the tumor while establishing a steep gradient of dose falloff at the interface between tumor and normal tissues (2).

Four essential characteristics of SBRT are secure immobilization, accurate repositioning, proper accounting for internal organ motion, and an extremely conformal dosimetry. This therapy is used to treat well demarcated visible tumors in the liver, generally those up to 6 cm in diameter. Its intention is to totally disrupt the clonogenicity and the cellular functioning of the target tissues (3).

The specific aim of this thesis is to assess the clinical outcomes of SBRT for liver tumors at our institution, to investigate the quality of SBRT, and to identify potential methods for its improvement.

In 2001, working on the basis of positive results reported by other groups, we developed a study protocol on SBRT for patients with liver metastases and hepatocellular carcinoma (HCC) that were not eligible for surgery or RFA (4-6). The aim was to build up our experience and to assess the feasibility, toxicity, local control, and quality of life associated with this treatment.

In Chapter 2 we report the outcomes of feasibility, toxicity and local control from this phase I-II trial. The prescribed doses used in this study were selected on the basis of the experience of Wulf *et al.* and Blomgren *et al.* We demonstrated that, although this treatment, was both resources-intensive and time consuming, it was feasible at our institution. In agreement with other studies, we showed that we could achieve an encouraging local control rate of 86% at two years for liver metastases and of 75% for HCC.

The lower tumor control achieved in the HCC group was probably a consequence of the low dose (5 x 5 Gy) delivered to those patients with cirrhosis and large tumors; in contrast, all HCC treated with 3 x 12.5 Gy remained locally controlled. A clear dose relationship for HCC had already been established by Dawson *et al.* and Park *et al*. (7, 8).

A recent SBRT study has demonstrated excellent local control rates and good clinical tolerance at high radiation doses (3 x 12-16 Gy) in patients with HCC and Child-Pugh A cirrhosis (9). Other SBRT studies have also reported high rates of local control for HCC with acceptable toxicity (10-13).

A point of concern in our study was the hepatic toxicity associated with SBRT in the presence of cirrhosis Child-Pugh grade B. Various authors including Cheng *et al*. and Liang *et al*. showed that cirrhosis Child-Pugh grade B was associated with a higher susceptibility to radiation-induced liver disease (RILD) (14-16). Other authors have also encountered limiting toxicity within this patient group (9). Because liver function is substantially deteriorated in these patients, it may not be acceptable in this population to use dose parameters that could influence the development of RILD modelled by the group from Michigan, whose patient population did not include patients with substantial alteration of the liver function (17).

After the closure and analysis of the phase I-II study in 2006 we decided to treat only HCC patients with Child-Pugh grade A cirrhosis. Using the Michigan group parameters, we started calculating the normal tissue complication probability (NTCP) associated with the treatment, allowing for a maximum value of less than 5%. On the basis of this value, and independently of the tumor size, we now deliver 3 x 12.5 Gy at the 65% isodose or 6 x 8-9 Gy at the 80% isodose. Since the NTCP model is sensitive to high dose values that are enhanced by hypofractionation, we choose the latter fractionation scheme when the NTCP value is ≥5%, with the treatment consisting of three fractions. Options for raising the dose in this patient group have been reported and should be validated in our own population in future trials.

Promising clinical benefits might be obtained through concomitant or sequential combinations of SBRT and Sorafenib for non-resectable HCC (18). Study protocols have been developed and trials have been open for inclusion of patients (19, 20). A systematic review and meta-analysis showed that the combination of transarterial chemoembolisation (TACE) with 3D conformal radiotherapy had greater therapeutic benefits than TACE alone (21). These encouraging results have led to the design of several studies to further explore the association of TACE with high biological doses delivered by SBRT (22).

While we observed limited hepatic toxicity within the metastases group during our phase I-II study, even lower toxicity rates were reported by the Colorado group from a phase I-II trial which proposed that at least 700 ml of normal liver should receive a total dose of less than 15 Gy (23, 24). Our own constraint was that 50% of the liver (including CTV) should receive a dose of 15 Gy or less. Additional review of patients with hepatic toxicity showed that sparing even more than 50% of the liver did not always correspond with at least 700 ml, but with a smaller volume. The 700ml constraint may be more suited to preserving enough functional organ parenchyma

and to preventing toxicity, particularly in small livers. Since 2006 we have introduced this value as our new liver constraint.

Dose-escalation studies in this patient group have shown that local control was higher with a delivered higher dose (7, 25, 26). On the basis of these findings, we have raised the treatment doses for liver metastases at our institution to 3x12.5-16.75 Gy at the 67% isodose. This prescription isodose was chosen between different European institutions involved in organizing a treatment protocol for a phase III randomized trial to compare SBRT with RFA for colorectal liver metastases (Karolinska Hospital, Aarhus University Hospital, and Erasmus MC).

Quality of life is an important health parameter that provides clinicians and patients with useful information about a treatment's impact on health status. In Chapter 3 we analyze the impact of SBRT on the quality of life of patients included in the phase I-II trial. In addition to a disease-specific questionnaire, the European Organization for Research and Treatment of Cancer Core Quality of Life Questionnaire (EORTC QLQ C-30), we used two generic quality of life instruments, Euro-QoL-5D (EQ-5D) and the EuroQoL-Visual Analogue Scale (EQ-5D VAS). On the basis of the model proposed by Wilson and Cleary we analyzed quality of life at three levels: general health perceptions, functioning, and symptoms (27). General health perceptions were measured by using the EQ-5D health state index, EQ-5D VAS score, and QLQ-C30 global health status index. Functional and symptom status were evaluated using the EORTC C-30 functional and symptom domains, respectively.

Although the mean values obtained at baseline were lower than those in the general Dutch population, general health perceptions remained quite stable after treatment. Compared to baseline, mean values corresponding to functional domains were also stable after treatment. Mean values corresponding to symptom domains were slightly higher after treatment although only fatigue at one month resulted in a significant difference compared with baseline. This fact did not affect the subjective evaluation of quality of life.

Although there have been few clinical studies on the impact of local liver treatments, we tested the robustness of our results by comparing our findings with the literature. Wietzke-Braun, who used the EORTC QLQ C-30 questionnaire to analyze the impact of ultrasound-guided interstitial thermotherapy on quality of life in patients with unresectable colorectal liver metastases, detected a significant increase in symptoms regarding pain at one week but also at six months after treatment (28). They suggested this might be related to the local incision and insertion of the catheter.

Langenhoff *et al*. analyzed quality of life after surgical treatment in three groups of patients with colorectal liver metastases (29). The first group had undergone the planned resection of metastases, or, if resection alone was not possible, had been treated with local tumor ablation. The second group turned out to have inoperable

disease at laparotomy and had undergone exploratory laparotomy only, as no resection or local ablative therapy with curative intent was possible. The third group consisted of patients who had been referred for surgery, but had been judged to have inoperable disease and therefore not scheduled for surgery.

Although the EQ-5D baseline was more or less similar to that in our group, the researchers found, unlike us, that EORTC scales were comparable to norm scores obtained from the general population; it was suggested that these high scores might be due to a reframing process. A potential explanation for the different finding may be that, regardless of a reframing process, the outcome reflects the fact that the patients referred to SBRT had already experienced an extensive variety of treatments, including one or more liver resections or RFA procedures, as well as different chemotherapy schemes.

Another remarkable difference is that, unlike the third group of Langenhoff *et al*., whose scores at 6 months without treatment were lower than at baseline, we found no significant decrease in quality of life domains six months after treatment with SBRT. This suggests that SBRT, like surgery or RFA, may help to maintain a patient's quality of life. In a paper published later than ours, Shun *et al.* reported that, in agreement with our findings, quality of life was stable in liver cancer patients treated with SBRT for the first six weeks after SBRT relative to quality of life at baseline (pretreatment) (30).

New studies including a large number of patients are necessary to validate our findings and are already in preparation (RAS study) (22).

Over recent years, the EORTC QLQ-C30 has been supplemented by additional two disease-specific questionnaires for liver tumors: one for liver metastases from colorectal cancer (EORTC QLQ-LMC 21), and one for primary liver cancer (EORTC QLQ-HCC 18). As these questionnaires are intended to provide us with valuable information about specific symptoms and psychosocial issues not included in the EORTC QLQ-C30, they should be utilized in future clinical trials.

In Chapter 4 we investigate the benefit of computer-optimized noncoplanar beam setups for the stereotactic treatment of liver tumors using Cycle, an automated system developed in house for beam orientation and weight selection. This system was used to generate coplanar and noncoplanar plans to be compared with manually generated clinical plans. The main objective of using Cycle was to maximize the minimum dose in the planning target volume (PTV) measured by means of the $D_{PTV,99\%}$ or the dose delivered to 99% of the PTV, without exceeding the clinically delivered mean liver dose and without violating the clinical constraints.

Automatically optimized beam selection resulted in higher $D_{PTV,99\%}$ values than the clinical plan for the same isocenter and mean normal liver doses, without violating the clinical constraints. Automatically selected noncoplanar beam setups also had a higher dose gradient between the PTV and the surrounding normal tissue region than the

automatically selected coplanar beam setups did. On average, the OARs were better spared with the optimized noncoplanar plan than with the optimized coplanar plan and with the clinical plan.

Although Thomas *et al.* have reported that the use of noncoplanar beams for the treatment of liver tumors was favorable only where the PTV incorporated another OAR besides the liver, our study showed that applying non coplanar directions in the beam setup for every case had a clear advantage (31). One reason for these different observations might be that, in our case, the noncoplanar beam directions were computer optimized for each individual patient.

Cycle was clinically introduced for the treatment of liver tumors in early 2009. Since then several modifications have been performed to make the system faster and more flexible and user friendly. Depending on the difficulty of the case, the generation of a new plan by Cycle now takes 15-30 minutes. Later, the technician imports the plan file generated by Cycle into our current planning system XIO (CMS). In the worst-case scenario this procedure will take an additional two to six hours. For the time being, we have limited the maximum number of beams to 20. Cycle represents an important step forward for our department in the stereotactic radiotherapy treatment of liver tumors not only because it helps us to improve the quality of the plans but also because it reduces the workload during the treatment planning process.

Because SBRT delivers large radiation doses in a few fractions, high precision is required in tumor volume definition, daily setup and dose delivery to guarantee accurate targeting and low toxicity. Because day-to-day changes in the position of the liver may impair target coverage in SBRT, the tumor position is daily verified using computed tomography (CT)-guided treatment procedures to adjust the treatment setup before dose delivery (32-34).

Even in image-guided treatments, however, optimal sparing of organs at risk (OARs) according to the treatment plan is not guaranteed, as the translational setup corrections are based fully on the tumor displacements measured, while motion of the OARs may be different due to anatomy deformations. In chapter 5 we investigate the effects of the daily setup corrections and day-to-day anatomy variations on the dose distribution of the target volume (TV) and the OARs.

For this study we included the CT data sets corresponding to the planning and three treatment fractions of a group of treated patients. For each treatment scan, two dose distributions were calculated, one using the planned setup for the body frame, and one using the clinically applied setup derived from the tumor displacements measured. These two dose distributions were compared, and the clinically delivered dose distribution was compared with the planned dose distribution.

We observed that setup corrections prevented underdosage of the TV during treatment: without setup corrections, the mean target coverage would have decreased by

6.8% with respect to planning. After applying setup corrections, the mean difference was reduced to 1.7%. Although there were large positive and negative deviations in the OARs doses relative to planning, the tumor based setup corrections had on average no impact on these doses.

Several approaches could potentially result in safer dose delivery to the OARs. For treatment planning, the planning volumes of the OARs could be designed taking in account the information on organ changes sampled from patients treated previously. ICRU Report 62 (1999) stressed that movement and changes in the shape and/or size of OARs should be considered together with the setup uncertainties (35). It was recommended that a margin should be added to compensate for these variations and uncertainties, which led to the concept of the planning organ at risk volume (PRV). However, the report supplied neither dose criteria nor suggestions for calculating these margins for the different types of OARs, with the consequence that the concept of planning volume of the OARs became of limited use.

A second solution might be to change the current image-guidance procedure by including not only the target but also the OARs in the on-line image analysis. As a first step, one could establish, before dose delivery, which tumor setup correction was required, and then calculate the dose distribution for the treatment CT scan. However, accurate and fast evaluation of the simulated treatment dose distribution would require segmented OARs in the treatment scan. As manual delineation would be too time consuming, some sort of auto-segmentation would be needed. In case of unacceptable OAR doses, one could ideally re-plan on-line to adapt the planning to the patient anatomy of the day, for example by using a system for automated beam angle and weight optimization (36). Optimal dose delivery could be achieved with an adaptive treatment strategy based on added fraction dose distributions, assessed with a reliable non-rigid image registration technique (37). Ideally, non-rigid registration should be part of an on-line procedure, but off-line application could also improve dose delivery. In the latter, a new treatment plan could be designed prior to each fraction taking account of the added dose distributions delivered in the previous fractions.

Currently several projects are under investigation at our institution in order to achieve a truly adaptive treatment for liver tumors. Three research areas deserve special mention: a system for automated body-anatomy segmentation, a non-rigid image registration method, and a fast system for beam selection and optimization that would allow for daily on-line planning.

Chapter 5 presents long term clinical outcomes of SBRT for colorectal liver metastases. This retrospective study was the first published report on SBRT and liver metastases of only colorectal origin.

We included for analysis 20 patients who had been treated between December 2002 and July 2008 with 31 metastases that were not eligible for surgery or RFA.

Up to June 2006 patients had received three fractions of 12.5 Gy, according to our phase I-II study. Thereafter, doses were escalated based on published data from the University of Colorado (23, 24). Median follow-up was 26 months.

Our results showed that SBRT can achieve a two year local control and survival rate of 74% and 83%, with acceptable toxicity. In a personal communication, Hoyer *et al.* reported a two year local control rate of 78% after SBRT with 3x15 Gy at the isocenter for colorectal liver metastases. This was in line with our own results, and probably reflects the rather similar doses used in the two studies and the median follow up of more than two years.

Among other authors, Herfarth and Debus reported a significantly poorer local control of liver metastases from colorectal cancer than of tumors from other histologies, especially for patients treated previously with systemic therapy (38, 39). A possible explanation is that chemotherapy might select radioresistant cells. Wulf *et al.* also found worse two year local control from colorectal cancer than from other primaries (56% vs.74%) although in this case it was not significant (26). More recently, another publication evaluated the role of frameless robotic radiosurgery for colorectal liver metastases showing a two year local control of 55% (40). In this study, pretreatment with chemotherapy was preferred although not required. Rusthoven *et al*. reported a two year local control of 92% after a median follow up of 16 months from a variety of primaries treated with 36-60 Gy (41). This clinical experience is consistent with the knowledge that escalated doses of radiation are associated with improved local control (7, 25, 26, 42).

Median survival in our study was 34 months and two year survival was 83%. Lee *et al.* reported that patients with primary colorectal cancer may have poorer survival, although non significant in univariate analysis, than other primaries such as breast (two year survival 59% vs. 38%) (43). In contrast, Rusthoven *et al.* found a significantly better median survival of 32 months after treatment of liver metastases from favorable primaries (breast, colorectal, renal, carcinoid, GIST and sarcoma), against 12 months for those from unfavorable primaries (lung, ovary, non-colorectal gastrointestinal malignancies) (41). This raises the question of whether it is justified to group for analysis metastases from primary colorectal cancer with those from other primaries. The differences observed in survival between studies may also be the result of patient selection criteria based on the presence of a more or less extended intrahepatic and extrahepatic disease.

With a median survival of 44 months, resection should be regarded as the standard curative treatment option in patients with hepatic metastases from colorectal cancer (44). However, only a minority of patients are eligible for resection. For those with unresectable liver metastases, RFA is the most widely used treatment technique, with median overall survival in this patient group of 35 months (range 24-59 months)

(45). With modern chemotherapy, median survival rates for patients with hepatic metastases are 24 months. In our study, however, median overall survival of patients with colorectal liver metastases not eligible for resection, nor for RFA, was 34 months after SBRT without serious toxicity. The lower median survival relative to surgery can be explained by the generally poor prognosis in our cohort of patients.

Further research is needed to better define the role of SBRT within the treatment options for unresectable colorectal liver metastases. A phase III trial to compare RFA with SBRT has been proposed by various centers, including ours (22). The trial has been already open at Karolinska Hospital. Accrual of patients in this study will be further increase most likely by Aarhus University Hospital and Erasmus MC.

In order to further optimize the treatment of colorectal liver metastases with SBRT, the target volume definition needed to be improved. It is generally agreed that to compensate for residual respiratory tumor motion and setup inaccuracies, a safety margin should be added to the tumor visible in CT or magnetic resonance imaging (MRI). However, there is some debate on the need for an extra margin to compensate for microscopic extension (26, 41, 43, 46).

Similarly, to precisely define the limits of the target volume, it was necessary to evaluate the correlation between macroscopic tumor dimensions visible in medical images and pathology. For this purpose, we organized a prospective pilot study to correlate pathologic macroscopic tumor dimensions with MRI measurements, and to establish the microscopic extension in colorectal liver metastases. The results of this study are presented in Chapter 7. MRI was selected as imaging modality rather than CT, as it is superior for assessing malignant focal liver lesions (47).

Sixteen patients with 21 colorectal metastases were analyzed. MRI volumes correlated well with microscopic pathology with a correlation factor (r_s) of 0.99 for the T1-weighted echo gradient sequence, the T2-weighted fast spin echo (FSE) single shot sequence, and the T2-weighted FSE fat saturation sequence. The correlation for the T1-weighted dynamic multiphasic gadolinium-enhanced sequence was 0.98. Although statistically significant, the mean differences between MRI and pathology volumes were small, especially for the T1-weighted echo gradient sequence (1.98 cc) and the T2-weighted FSE single shot sequence (2.38 cc). The mean differences were larger for the T2-weighted FSE fat saturation sequence (5.39 cc) and for the T1-weighted dynamic multiphasic gadolinium-enhanced sequence (5.92 cc). Probably, we have included in our delineated tumor volumes some perilesional changes such as peritumoral inflammation and vascular proliferation, which are better depicted with these sequences (48, 49). In agreement with our results, Dawson *et al*. reported that because pathology gross target volumes (GTV) correlated better with the unenhanced MRI than with the venous enhanced sequences, they seem more suitable for tumor delineation, especially the T1-weighted echo gradient sequence (50). Even though

the T2-weighted FSE single shot sequence also showed a very high correlation between MRI and macroscopic pathology, the tumor boundary was easier to delineate in the other three series. This observation is probably inherent to the image quality resulting from this sequence (48). Although the T2-weighted FSE fat saturation and the postcontrast T1-weighted gadolinium-enhanced sequences may facilitate tumor delineation, they may unnecessarily overestimate tumor volume by including other effects stated above.

The second aim of the study was to assess the microscopic extension of colorectal liver metastases. We found a total of 39 tumor nests (microscopic extension) outside 12 out of 21 metastases (57%). The mean maximum infiltration depth was 2.2 mm (0.2-10 mm), almost 80% of the tumor nests being found within 3 mm. While our results about frequency and range of infiltration depths were within the range of other results reported in the literature, our limitation in the number of slices used for analysis probably means that the number of tumor nests found in our study was a lower limit of the real number (50-54). Therefore, this study did not enable us to draw definitive and precise conclusions about the need for or extent of an extra margin in SBRT planning to compensate for microscopic extension.

Neither does the need for an extension of the high dose volume beyond the GTV necessarily imply that an enhanced planning margin is needed. Even with the most conformal techniques, there is often unavoidable delivery of a high dose beyond the gross tumor borders. Moreover, the need for an explicit enhancement of planning margins to cope with microscopic extension can also be obscured when generous ("safe") margins are used to account for patient setup errors and tumor mobility.

The on-going developments in increasing treatment precision (adaptive therapy, particle therapy) warrant investigations on the microscopic extension of liver metastases to fully exploit these techniques for our future patients. Greater accuracy in target definition is also essential for improving treatment precision. Systems to allow the incorporation of two other imaging modalities, MRI and PET-CT, into our current delineation procedure are of extreme importance and therefore under development.

REFERENCES

1. Timmerman RD, Kavanagh BD. Stereotactic body radiation therapy. *Curr Probl Cancer* 2005; 29:120-157.
2. Lax I, Blomgren H, Larson D*, et al.* Extracranial Stereotactic Radiosurgery of Localized Targets. *Journal of Radiosurgery* 1998; 1:135-148.
3. Timmerman R, Galvin J, Michalski J*, et al.* Accreditation and quality assurance for Radiation Therapy Oncology Group: Multicenter clinical trials using Stereotactic Body Radiation Therapy in lung cancer. *Acta Oncol* 2006; 45(7):779-786.
4. Blomgren H, Lax I, Göranson H*, et al.* Radiosurgery for Tumors in the Body: Clinical Experience Using a New Method. *Journal of Radiosurgery* 1998; 1:63-74.
5. Herfarth KK, Debus J, Lohr F*, et al.* Stereotactic single-dose radiation therapy of liver tumors: results of a phase I/II trial. *J Clin Oncol* 2001; 19:164-170.
6. Wulf J, Hadinger U, Oppitz U*, et al.* Stereotactic radiotherapy of targets in the lung and liver. *Strahlenther Onkol* 2001; 177:645-655.
7. Dawson LA, McGinn CJ, Normolle D*, et al.* Escalated focal liver radiation and concurrent hepatic artery fluorodeoxyuridine for unresectable intrahepatic malignancies. *J Clin Oncol* 2000; 18:2210-2218.
8. Park HC, Seong J, Han KH*, et al.* Dose-response relationship in local radiotherapy for hepatocellular carcinoma. *Int J Radiat Oncol Biol Phys* 2002; 54:150-155.
9. Cardenes HR, Price TR, Perkins SM*, et al.* Phase I feasibility trial of stereotactic body radiation therapy for primary hepatocellular carcinoma. *Clin Transl Oncol* 2010; 12:218-225.
10. Kwon JH, Bae SH, Kim JY*, et al.* Long-term effect of stereotactic body radiation therapy for primary hepatocellular carcinoma ineligible for local ablation therapy or surgical resection. Stereotactic radiotherapy for liver cancer. *BMC Cancer* 2010; 10:475.
11. Louis C, Dewas S, Mirabel X*, et al.* Stereotactic radiotherapy of hepatocellular carcinoma: preliminary results. *Technol Cancer Res Treat* 2010; 9:479-487.
12. Takeda A, Takahashi M, Kunieda E*, et al.* Hypofractionated stereotactic radiotherapy with and without transarterial chemoembolization for small hepatocellular carcinoma not eligible for other ablation therapies: Preliminary results for efficacy and toxicity. *Hepatol Res* 2008; 38:60-69.
13. Tse RV, Hawkins M, Lockwood G*, et al.* Phase I study of individualized stereotactic body radiotherapy for hepatocellular carcinoma and intrahepatic cholangiocarcinoma. *J Clin Oncol* 2008; 26:657-664.
14. Cheng JC, Wu JK, Lee PC*, et al.* Biologic susceptibility of hepatocellular carcinoma patients treated with radiotherapy to radiation-induced liver disease. *Int J Radiat Oncol Biol Phys* 2004; 60:1502-1509.
15. Jiang GL, Liang SX, Zhu XD*, et al.* Radiation-Induced Liver Disease in Three-Dimensional Conformal Radiotherapy for Primary Liver Carcinoma. *Abstract* 2004; 60 (supplement 1):S 413.
16. Liang SX, Zhu XD, Xu ZY*, et al.* Radiation-induced liver disease in three-dimensional conformal radiation therapy for primary liver carcinoma: the risk factors and hepatic radiation tolerance. *Int J Radiat Oncol Biol Phys* 2006; 65:426-434.
17. Dawson LA, Normolle D, Balter JM*, et al.* Analysis of radiation-induced liver disease using the Lyman NTCP model. *Int J Radiat Oncol Biol Phys* 2002; 53:810-821.
18. Hsieh CH, Jeng KS, Lin CC*, et al.* Combination of sorafenib and intensity modulated radiotherapy for unresectable hepatocellular carcinoma. *Clin Drug Investig* 2009; 29(1):65-71.

19. Horgan AM, Dawson LA, Swaminath A, *et al.* Sorafenib and Radiation Therapy for the Treatment of Advanced Hepatocellular Carcinoma. *J Gastrointest Cancer* 2010.
20. Zhao JD, Liu J, Ren ZG, *et al.* Maintenance of Sorafenib following combined therapy of three-dimensional conformal radiation therapy/intensity-modulated radiation therapy and transcatheter arterial chemoembolization in patients with locally advanced hepatocellular carcinoma: a phase I/II study. *Radiat Oncol* 2010; 5:12.
21. Meng MB, Cui YL, Lu Y, *et al.* Transcatheter arterial chemoembolization in combination with radiotherapy for unresectable hepatocellular carcinoma: a systematic review and meta-analysis. *Radiother Oncol* 2009; 92:184-194.
22. http://clinicaltrials.gov/.
23. Kavanagh BD, Schefter TE, Cardenes HR, *et al.* Interim analysis of a prospective phase I/II trial of SBRT for liver metastases. *Acta Oncol* 2006; 45:848-855.
24. Schefter TE, Kavanagh BD, Timmerman RD, *et al.* A phase I trial of stereotactic body radiation therapy (SBRT) for liver metastases. *Int J Radiat Oncol Biol Phys* 2005; 62:1371-1378.
25. McCammon R, Schefter TE, Gaspar LE, *et al.* Observation of a dose-control relationship for lung and liver tumors after stereotactic body radiation therapy. *Int J Radiat Oncol Biol Phys* 2009; 73:112-118.
26. Wulf J, Guckenberger M, Haedinger U, *et al.* Stereotactic radiotherapy of primary liver cancer and hepatic metastases. *Acta Oncol* 2006; 45(7):838-847.
27. Wilson IB, Cleary PD. Linking clinical variables with health-related quality of life. A conceptual model of patient outcomes. *JAMA* 1995; 273:59-65.
28. Wietzke-Braun P, Schindler C, Raddatz D, *et al.* Quality of life and outcome of ultrasound-guided laser interstitial thermo-therapy for non-resectable liver metastases of colorectal cancer. *Eur J Gastroenterol Hepatol* 2004; 16:389-395.
29. Langenhoff BS, Krabbe PF, Peerenboom L, *et al.* Quality of life after surgical treatment of colorectal liver metastases. *Br J Surg* 2006; 93(8):1007-1014.
30. Shun SC, Chiou JF, Lai YH, *et al.* Changes in quality of life and its related factors in liver cancer patients receiving stereotactic radiation therapy. *Support Care Cancer* 2008; 16:1059-1065.
31. Thomas E, Chapet O, Kessler ML, *et al.* Benefit of using biologic parameters (EUD and NTCP) in IMRT optimization for treatment of intrahepatic tumors. *Int J Radiat Oncol Biol Phys* 2005; 62:571-578.
32. Eccles C, Brock KK, Bissonnette JP, *et al.* Reproducibility of liver position using active breathing coordinator for liver cancer radiotherapy. *Int J Radiat Oncol Biol Phys* 2006; 64(3):751-759.
33. Wulf J, Hadinger U, Oppitz U, *et al.* Impact of target reproducibility on tumor dose in stereotactic radiotherapy of targets in the lung and liver. *Radiother Oncol* 2003; 66:141-150.
34. Wunderink W, Méndez Romero A, Vasquez Osorio EM, *et al.* Target coverage in image-guided stereotactic body radiotherapy of liver tumors. *Int J Radiat Oncol Biol Phys* 2007; 68:282-290.
35. International Commission on Radiation Units and Measurements. ICRU Report 62: Prescribing, recording, and reporting photon beam therapy (Supplement to ICRU Report 50). Bethesda MD: ICRU Publications; 1999.
36. de Pooter JA, Méndez Romero A, Jansen WP, *et al.* Computer optimization of noncoplanar beam setups improves stereotactic treatment of liver tumors. *Int J Radiat Oncol Biol Phys* 2006; 66:913-922.
37. Brock KK, Dawson LA, Sharpe MB, *et al.* Feasibility of a novel deformable image registration technique to facilitate classification, targeting, and monitoring of tumor and normal tissue. *Int J Radiat Oncol Biol Phys* 2006; 64:1245-1254.

38. Herfarth KK, Debus J. [Stereotactic radiation therapy for liver metastases]. *Chirurg* 2005; 76:564-569.
39. Milano MT, Katz AW, Schell MC, *et al.* Descriptive analysis of oligometastatic lesions treated with curative-intent stereotactic body radiotherapy. *Int J Radiat Oncol Biol Phys* 2008; 72:1516-1522.
40. Stintzing S, Hoffmann RT, Heinemann V, *et al.* Frameless single-session robotic radiosurgery of liver metastases in colorectal cancer patients. *Eur J Cancer* 2010; 46:1026-1032.
41. Rusthoven KE, Kavanagh BD, Cardenes H, *et al.* Multi-institutional phase I/II trial of stereotactic body radiation therapy for liver metastases. *J Clin Oncol* 2009; 27:1572-1578.
42. Rule W, Timmerman R, Tong L, *et al.* Phase I Dose-Escalation Study of Stereotactic Body Radiotherapy in Patients With Hepatic Metastases. *Ann Surg Oncol* 2010.
43. Lee MT, Kim JJ, Dinniwell R, *et al.* Phase I study of individualized stereotactic body radiotherapy of liver metastases. *J Clin Oncol* 2009; 27:1585-1591.
44. van der Pool AE, Lalmahomed ZS, Ozbay Y, *et al.* "Staged" liver resection in synchronous and metachronous colorectal hepatic metastases; differences in clinicopathological features and outcome. *Colorectal Dis* 2009.
45. Stang A, Fischbach R, Teichmann W, *et al.* A systematic review on the clinical benefit and role of radiofrequency ablation as treatment of colorectal liver metastases. *Eur J Cancer* 2009; 45:1748-1756.
46. Ben-Josef E, Normolle D, Ensminger WD, *et al.* Phase II trial of high-dose conformal radiation therapy with concurrent hepatic artery floxuridine for unresectable intrahepatic malignancies. *J Clin Oncol* 2005; 23:8739-8747.
47. Balci NC, Befeler AS, Leiva P, *et al.* Imaging of liver disease: comparison between quadruple-phase multidetector computed tomography and magnetic resonance imaging. *J Gastroenterol Hepatol* 2008; 23:1520-1527.
48. Semelka RC, Chew W, Hricak H, *et al.* Fat-saturation MR imaging of the upper abdomen. *AJR Am J Roentgenol* 1990; 155:1111-1116.
49. Semelka RC, Hussain SM, Marcos HB, *et al.* Perilesional enhancement of hepatic metastases: correlation between MR imaging and histopathologic findings-initial observations. *Radiology* 2000; 215:89-94.
50. Dawson LA, Brock KK, Moulton C, *et al.* Comparison of Liver Metastases Volumes on CT, MR and FDG PET Imaging to Pathological Resection Using Deformable Image Registration [Abstract]. *Int J Radiat Oncol Biol Phys* 2007; 69, Number 3, (Suppl. 1):68.
51. Ambiru S, Miyazaki M, Isono T, *et al.* Hepatic resection for colorectal metastases: analysis of prognostic factors. *Dis Colon Rectum* 1999; 42:632-639.
52. Kokudo N, Miki Y, Sugai S, *et al.* Genetic and histological assessment of surgical margins in resected liver metastases from colorectal carcinoma: minimum surgical margins for successful resection. *Arch Surg* 2002; 137:833-840.
53. Nanko M, Shimada H, Yamaoka H, *et al.* Micrometastatic colorectal cancer lesions in the liver. *Surg Today* 1998; 28:707-713.
54. Wakai T, Shirai Y, Sakata J, *et al.* Appraisal of 1 cm hepatectomy margins for intrahepatic micrometastases in patients with colorectal carcinoma liver metastasis. *Ann Surg Oncol* 2008; 15:2472-2481.

9

SUMMARY / SAMENVATTING

SUMMARY

This thesis describes the clinical outcomes of stereotactic body radiation therapy (SBRT) for liver tumors at our institution; it investigates both the quality of SBRT and potential methods for its improvement.

Chapters 2 and 3 present the clinical results on toxicity, local control, and quality of life in a group of patients included in a phase I-II study. Patients who were considered to be candidates for SBRT had been diagnosed with hepatocellular carcinoma or liver metastases that were not eligible for other local treatments, including surgery or radiofrequency ablation (RFA). Patients with cirrhosis Child-Pugh grade A and B were included.

Local control rates were encouraging, with rates for the whole group of 94% at one year and 82% at two years. Four patients had acute toxicity ≥ 3. Three patients with liver metastases presented acute toxicity grade 3; two of these had an asymptomatic elevation of gamma glutamyl transpherase, and one had asthenia. One patient with Child Pugh grade B had hepatic toxicity grade 5, indicating that caution is needed in patients with cirrhosis due to a preexisting deteriorated liver function and consequently an increased risk of toxicity.

Chapter 3 reports the impact of SBRT on the quality of life of the patients included in the phase I-II study. Assessment was based on two generic questionnaires and one cancer specific questionnaire. Points of measurement were directly before treatment and one, three, and six months afterwards. We found that on average SBRT was associated with no significant change in the patient's quality of life.

Chapter 4 investigates the use of Cycle, an automated system developed in house for beam orientation and weight selection, to improve the stereotactic treatment of liver tumors. In a group of 8 patients we showed that computer-optimized noncoplanar beam setups resulted in plans that were more favorable not only than the optimized coplanar beam setups but also than the clinical plans. Sparing of the organs at risk was better, and the dose received by the 99% of the planning target volume ($D_{PTV,99\%}$) was higher, while maintaining the same isocenter dose. The automation enabled us to reduce the planning workload relative to the clinical plans.

Chapter 5 assesses the impact of daily translational setup corrections and the day-to-day anatomic variations on dose in target and organs at risk (OARs). For this study we included the computed tomography (CT) data sets corresponding to the planning and the three treatment fractions of 24 patients. For each treatment scan, two dose distributions were calculated, one using the planned setup for the body frame, and one using the clinically applied setup derived from tumor displacements. We showed that to obtain proper target coverage, daily correction of the treatment setup is necessary. Due to day-to-day anatomy deformations, there were large deviations in the

OARs dose distributions that occurred with respect to the planning. On average, the clinical setup corrections had no impact on these doses.

Chapter 6 presents a clinical report of 20 patients with 31 colorectal liver metastases treated with SBRT. Actuarial local control and survival at two years were 74% and 83%, indicating that SBRT can offer an adequate local control and survival in patients not eligible for resection or RFA. Three episodes of toxicity grade 3 were observed, two asymptomatic elevation of gamma glutamyl transpherase, and one asthenia, suggesting that the toxicity rate was acceptable. Two of these three patients with toxicity had been included previously in our phase I-II study.

Chapter 7 compares tumor measurements determined by magnetic resonance imaging (MRI) and by macroscopic pathology, and assesses of microscopic extension for a group of 21 colorectal liver metastases. MRI and pathology were highly correlated (correlation factor 0.98-0.99), particularly for the non enhanced sequences (0.99), suggesting that MRI can be used for accurate tumor delineation. We found 39 tumor cell nests in 12 metastases located between 0.2 and 10mm beyond the main tumor, with 90% of the cases within 6 mm. This indicates that caution is needed in selecting appropriate tumor margins.

SAMENVATTING

Dit proefschrift beschrijft de klinische uitkomsten van stereotactische radiotherapie (SRT) voor levertumoren in ons instituut; zowel de kwaliteit van SRT en potentiële methoden voor verbeteringen van de techniek werden onderzocht.

De hoofdstukken 2 en 3 presenteren de klinische resultaten van toxiciteit, lokale controle en de kwaliteit van leven in een groep van patiënten geïncludeerd in een fase I-II studie. Deze patiënten waren gediagnosticeerd met hepatocellulair carcinoom of levermetastasen die niet in aanmerking kwamen voor andere lokale behandeling opties, zoals chirurgie of "radiofrequentie ablatie" (RFA). Patiënten met cirrose Child-Pugh grade A en B waren geïncludeerd.

De lokale controle was bemoedigend, met getallen voor de hele groep voor een jaar van 94% en voor twee jaar 82%. Vier patiënten hadden acute complicaties graad 3 of hoger. Drie patiënten met levermetastasen vertoonden acute graad 3 complicaties; twee van hen hadden een asymptomatische verhoging van de gamma glutamyl transpherase en één had vermoeidheid. Eén patient met Child Pugh grade B had hepatische toxiciteit graad 5. Dit betekent dat voorzichtigheid is geboden bij patiënten met levercirrose omdat een verslechterde leverfunctie een verhoogde kans op complicaties geeft.

Hoofdstuk 3 rapporteert de invloed van SRT op de kwaliteit van leven van de patienten in deze fase I-II studie.

De beoordeling was gebaseerd op twee algemene vragenlijsten en een kankerspecifieke vragenlijst. De lijsten werden ingevuld: direct voor de behandeling en een, drie en zes maanden na afloop. Met SRT bleef de kwaliteit van leven van de patiënten onveranderd.

Hoofdstuk 4 onderzoekt de meerwaarde van een zelfontwikkeld programma (Cycle) voor computeroptimalisatie van bundelhoeken en gewichten. In een groep van 8 patiënten bleken de computergeoptimaliseerde niet-coplanaire plannen superieur aan geoptimaliseerde coplanaire plannen en de klinische plannen. Het sparen van risico-organen was beter en de afgegeven dosis aan 99% van het planning target volume ($D_{PTV,99\%}$) was hoger bij dezelfde dosis in het isocentrum. De automatisering van de procedure reduceerde de werklast bij het maken van klinische planningen.

Hoofdstuk 5 bestudeert de invloed van dagelijkse translationele correcties van gemeten fouten in de positionering van de tumor ten opzichte van de bestralingsbundels en van anatomie deformaties op de dosis in het doelgebied en de risico-organen. Voor elk van de 24 patiënten is gebruik gemaakt van de planning computertomografie (CT) scan en van de scans gemaakt op de drie behandeldagen. Retrospectief werden voor elke behandeldag twee dosisverdelingen berekend, één voor de geplande positionering van het stereotactische frame en de ander voor de klinisch toegepaste gecorrigeerde

positionering, zoals afgeleid van de gemeten tumor verplaatsing. Aangetond werd dat dagelijkse positioneringcorrecties onvermijdelijk zijn om bij de toegepaste krappe marges tumoronderdosering te voorkomen. Als gevolg van optredende deformaties in de anatomie van patiënten werden in de risico-organen soms grote afwijkingen van de geplande dosisverdeling gezien. Gemiddeld genomen hadden de translationele positiecorrecties geen invloed hierop, positief noch negatief.

Hoofdstuk 6 presenteert de klinische resultaten van 20 patiënten met 31 colorectale levermetastasen behandeld met SRT. De actuariële lokale controle en overleving op twee jaar waren 74% en 83% dat aangeeft dat SRT een adequate lokale controle en overleving geeft voor patiënten die niet in aanmerking komen voor chirurgie of RFA. Slechts drie graad 3 complicaties werden gezien, tweemaal een asymptomatische verhoging van de glutamyl transpherase en één casus van vermoeidheid. Twee van deze drie patiënten met complicaties zijn eerder in onze fase I-II studie geïncludeerd.

Hoofdstuk 7 vergelijkt tumor volumes gemeten met magnetische resonantiebeldvorming (MRI) met macroscopische pathologie en bepaalt verder de microscopische uitbreiding voor 21 colorectale levermetastasen. MRI en pathologie waren sterk met elkaar gecorreleerd (correlatiefactor: 0.98-0.99), in het bijzonder de "non enhanced" sequenties (0.99). Dit suggereert dat MRI gebruikt kan worden voor nauwkeurige tumor intekening. We vonden 39 tumorcelnesten rond 12 metastasen op afstanden variërend van 0.2 tot 10mm. In 90% van de gevallen was de afstand kleiner of gelijk aan 6mm. Voorzichtigheid is geboden bij het kiezen van de tumormarge, zeker bij dosisverdelingen die de tumoren nauw omsluiten en een sterke dosisafval richting de gezonde weefsels hebben.

LIST OF PUBLICATIONS

1. Méndez Romero A, Verheij J, Dwarkasing RS*, et al.* Comparison of Macroscopic Pathology Measurements with Magnetic Resonance Imaging and Assessment of Microscopic Pathology Extension for Colorectal Liver Metastases. *Int J Radiat Oncol Biol Phys* 2010.
2. Wolbers JG, Méndez Romero A, van Linge A*, et al.* [The most efficient intervention for vestibular schwannoma]. *Ned Tijdschr Geneeskd* 2010; 154:A714.
3. Wunderink W, Méndez Romero A, Seppenwoolde Y*, et al.* Potentials and limitations of guiding liver stereotactic body radiation therapy set-up on liver-implanted fiducial markers. *Int J Radiat Oncol Biol Phys* 2010; 77:1573-1583.
4. van der Pool AE, Méndez Romero A, Wunderink W*, et al.* Stereotactic body radiation therapy for colorectal liver metastases. *Br J Surg* 2010; 97:377-382.
5. Dols LF, Verhoef C, Eskens FA*, et al.* [Improvement of 5 year survival rate after liver resection for colorectal metastases between 1984-2006]. *Ned Tijdschr Geneeskd* 2009; 153:490-495.
6. Méndez Romero A, Zinkstok RT, Wunderink W*, et al.* Stereotactic body radiation therapy for liver tumors: impact of daily setup corrections and day-to-day anatomic variations on dose in target and organs at risk. *Int J Radiat Oncol Biol Phys* 2009; 75:1201-1208.
7. de Pooter JA, Méndez Romero A, Wunderink W*, et al.* Automated non-coplanar beam direction optimization improves IMRT in SBRT of liver metastasis. *Radiother Oncol* 2008; 88:376-381.
8. Wunderink W, Méndez Romero A, de Kruijf W*, et al.* Reduction of respiratory liver tumor motion by abdominal compression in stereotactic body frame, analyzed by tracking fiducial markers implanted in liver. *Int J Radiat Oncol Biol Phys* 2008; 71:907-915.
9. Molinelli S, de Pooter JA, Méndez Romero A*, et al.* Simultaneous tumour dose escalation and liver sparing in Stereotactic Body Radiation Therapy (SBRT) for liver tumours due to CTV-to-PTV margin reduction. *Radiother Oncol* 2008; 87:432-438.
10. Méndez Romero A, Wunderink W, van Os RM*, et al.* Quality of life after stereotactic body radiation therapy for primary and metastatic liver tumors. *Int J Radiat Oncol Biol Phys* 2008; 70:1447-1452.
11. de Pooter JA, Wunderink W, Méndez Romero A*, et al.* PTV dose prescription strategies for SBRT of metastatic liver tumours. *Radiother Oncol* 2007; 85:260-266.

12. Wunderink W, Méndez Romero A, Vasquez Osorio EM*, et al.* Target coverage in image-guided stereotactic body radiotherapy of liver tumors. *Int J Radiat Oncol Biol Phys* 2007; 68:282-290.
13. de Pooter JA, Méndez Romero A, Jansen WP*, et al.* Computer optimization of noncoplanar beam setups improves stereotactic treatment of liver tumors. *Int J Radiat Oncol Biol Phys* 2006; 66:913-922.
14. Méndez Romero A, Wunderink W, Hussain SM*, et al.* Stereotactic body radiation therapy for primary and metastatic liver tumors: A single institution phase i-ii study. *Acta Oncol* 2006; 45:831-837.

ACKNOWLEDGEMENTS

Prof. Levendag, promotor: Dear Peter, thank you for giving me the opportunity to be part of this department. You initiated this work, and with your support we could use all the resources we needed to develop the treatment and make this project successful.

Prof. Heijmen, promotor: Dear Ben, thank you for your commitment to this project. You made it possible to work as a team and to learn how we could complement each other with our different clinical and technical insights. Thank you for your scientific and personal support. Also thanks for your intensive work to improve every single paper, not only during working hours but also during weekends and holidays. Your sense of humor and personal touch were highly appreciated – and still are.

Dr. Verhoef, copromotor: Dear Kees, thank you for the confidence you always have shown in this novel treatment. You have been open-minded and supportive with all the new ideas I presented for new studies. I hope our fruitful collaboration will continue.

Prof. van Saase, thank you for accepting the not easy task of being the secretary of the inner doctoral committee. It is an honor for me that the chairman of the board of education in Erasmus MC has been involved in the evaluation of my thesis.

Prof. Høyer and Prof. Dawson, members of the inner doctoral committee: Dear Morten and Laura, I'm honored that such experts in liver stereotactic radiotherapy have evaluated my thesis and will be present at my defense. Prof. Kavanagh and Prof. Lax: Dear Brian and Ingmar, thank you for your participation on this big day. I could not think of four guests who are more qualified to show us both the state of the art and the future development of this treatment.

Prof. IJzermans, chairman of the hepatobiliary board: Dear Jan, thank you for taking part of the plenary doctoral committee and for your support during these years. You have been a pioneer, accepting the role of stereotactic radiotherapy to treat liver tumors, showing your confidence in this technique, and making it possible for me to participate in the tumor board.

Prof. Pattynama, thank you for participating in the plenary doctoral committee. Your contribution as an expert in interventional radiology, together with Dr. Leertower, was essential to developing our current protocol for marker implantation.

Dr. Kazemier, liver transplantation surgeon: Dear Geert, thank you for your participation in the plenary doctoral committee and in our symposium. It has always been a pleasure to discuss surgical and radiotherapy approaches for our common patients.

Dr. Dwarkasing, chief liver radiologist: Dear Roy, thank you for your patience and the time you have spent over the years reviewing my delineations of every single patient. You have made an essential contribution to the quality of our treatment. Thanks, too, for your collaboration in studies and for the ways you made it possible for me to develop new protocols focused on my special radiotherapy needs.

Dr. Verheij and Dr. Zondervan, hepatopathologists: Dear Joanne and Piet, thank you for the ideas and time you have invested to make our common article possible. In our discussions of different diagnoses under the microscope, you opened a fascinating new world for me. Joanne, I will miss our talks between the train station and the hospital.

Dr. de Man, hepatologist and Dr. Eskens, internal oncologist, prominent members of the hepatobiliary board: Dear Rob and Ferry thank you for your prompt and educative answers to my many questions about cirrhosis, liver function, and chemotherapy.

W. Wunderink, physicist: Dear Wouter, it has been a pleasure to share these arduous years with you. Thanks to you, I became wiser in all the technical aspects of the treatment. The telephone line was always open when I needed to discuss patient or research issues. I really enjoyed our long calls, day or night, about our favorite topic, liver SBRT. It's easy to understand that recently, at extremely busy times, Eliana requested us to limit the duration of our calls to no more than half an hour. I'm sure a bright carrier is waiting for you as a medical physicist.

Y. Seppenwoolde and E. Woudstra, medical physicists: Dear Yvette and Evert, your contribution to the research and the liver treatments has been essential. With the new matching procedure before treatment delivery, CT and XVI marker studies, and by introducing Cycle in the clinic, we have made important steps forward. I hope our future collaboration will continue to be so fruitful and successful. Evert, I'm honored that you agreed to be my paranymph. I hope we can enjoy this day as much as we enjoy our discussions about liver plans.

J. de Pooter, physicist: Dear Jacco, thank you for your contribution to improving this research line with such interesting papers on SBRT planning for liver tumors. R. Zinkstok, medical physicist: Dear Roel, thank you for your work on the organ at risk article.

Dr. A. van der Pool, surgeon: Dear Anne, thank you for your collaboration on analyzing and writing our results on SBRT for colorectal liver metastases. Our different backgrounds contributed positively to our ability to achieve a successful result.

Dr. A. Devos, radiologist and paranymph: Dear Annick, thank you for accompanying me on this important day. When this thesis has been finalized, I hope we can find the time to enjoy a nice coup of tea together. Thank you for your welcoming attitude every time Rob and I visit the de Graaff family. We always return home in a good mood after all the laughing and the talks with you, Arnoud, and young Silke and Seppe.

R. van Os, MSc in Medical Informatics: Dear Rob, thank you for the statistical analyses you have performed for me over the years. Thanks, too, for all the long, constructive discussions in the development phase of each study, which often went on for whole days at a time including many holiday periods. Your experience in data bases has been invaluable. Thank you for your unconditional support and your immense patience. An invitation to a Michelin three-star restaurant is waiting for you.

Dr. Nowak: Dear Peter, it has been a pleasure to work with you over almost ten years. I have learned a lot about intracranial stereotactic radiotherapy - not only from our collaboration, but also from our discussions and disagreements.

I want to thank all my colleagues radiation oncologists for their support over the years. I would like to thank Dr Joost Nuyttens for replacing me the times I could not be present for the liver treatments, and for the time invested in "constraints" discussions. Dr. Margreet Baaijens deserves a special thank for her good advice. And in a special way I want to remember Dr. Ineke van Mierlo, with whom I often talked about this thesis and this big day. Unfortunately for us all, she can be present only in our memory.

Prof. Redekop and Prof. Stolk: Dear Ken and Ellie, thank you for your statistical support and your methodological contribution to improving the papers. Ken, I could not thank you enough for your availability to discuss any statistical problem at any time, including weekends or holidays.

P. Wielopolsky, physicist and expert in MRI technology: Dear Piotr, thank you for your bright ideas and stimulating discussions about liver MRI.

The technicians involved in this liver treatment have played an important role in the success of this project. In their order of appearance during the liver treatments, I would like to thank the members of the CT team: Hans Joosten, Marja Verbeek, Marja ten Kleij, Ingrid Lokken, Lijanne Vollaard, and Teresia van Battum; the members

of the planning team, Zaida Adams, Henrie van der Est, and Koos Sterkenburg, and the members of the linac team, between others, Lies Joosten, Hetty Rutten, Glen Dhawtal, Leonie Gaakeer-Schipper, Vincent Ouwerkerk, Lisanne Polderman, Marliene Vreugdenhil and Marjolein van Os.

Yvonne Anomtaroeno, from the patient logistics section: Dear Yvonne, you have accomplished with excellence the almost impossible mission of organizing all the appointments for the liver patients I have requested. I want to thank you and your colleagues for the excellent job you have all done for our liver patients.

Astrid Shippers-Mertens, Jolanda van Buuren-Visser, Linda Koffijberg-Visser and Sevcan Gungormus-Tas, secretaries of the radiotherapy department: Dear ladies, I can not thank you enough for all the work that you have done for me and for Wouter over recent months. You have organized all the events around the defense of the thesis, and I'm sure everything will be perfect. Thank you, too, for your daily support making my work and my life easier. Special thanks to Jacqueline van der Valk and Jolanda Jacobs-van den Heuvel, secretaries of the physics division: Dear ladies thank you for your support organizing and scheduling our liver meetings - not an easy task. Thank you, too, to Jeannette Nicolaas-Schilperoord and Jessica Vrolijk for all the letters, e-mails and appointments you have organized for me in recent months.

David Alexander, lecturer in biomedical English: Dear David, thank you for your intensive work improving the readability of the manuscript. Also thank you for your kind and personal approach.

Thank you to the people who have had a special influence in my development as a radiation oncologist: the members of the departments of radiation oncology at Hospital de la Santa Creu i Sant Pau in Barcelona, Hospital Duran i Reinalds (ICO) in Barcelona, and Academic Medical Center in Amsterdam.

A mis hermanos, Cris y Tono nunca les podré agradecer todo el apoyo que me ofrecen día a día. Gracias por acompañarme en esta ocasión. Para mi tío Paco y para Marta mi agradecimiento por su presencia.

To all the persons who have contributed to this thesis and have not been mentioned, THANK YOU!

CURRICULUM VITAE

Alejandra Méndez Romero was born on 25 May 1968 in Melide (La Coruña), Spain. From 1986 to 1992 she studied medicine at the University of Santiago de Compostela. In 2000 she completed her training as a radiation oncologist at Hospital de la Santa Creu i Sant Pau (University of Barcelona). She spent 2001 as a fellow in radiation oncology at Amsterdam Academic Medical Center, under the supervision of Prof. D. González González. In 2002 she started working at the department of radiation oncology at Erasmus MC-Daniel den Hoed Cancer Center. Her main areas of interest are intracranial and extracranial stereotactic radiotherapy.

PHD PORTFOLIO SUMMARY

Summary of PhD and training activities

Name PhD student: Alejandra Méndez Romero
Erasmus MC department: Radiation oncology
PhD period: 1/2006-1/2011
Promotors: Prof. P. C. Levendag, Prof. B. J. M. Heijmen
Copromotor: Dr. C. Verhoef

Presentations:
Stereotactic body radiation therapy for primary and metastatic liver tumors.
3rd Acta Oncologica Symposium on Stereotactic Body Radiation Therapy, Aarhus, Denmark, 2006.
Award Acta Oncologica travel grant spent in Princess Margaret Hospital, Toronto (Ontario), Canada, and Aurora Cancer Center, Denver (Colorado), USA.

Quality of life after stereotactic body radiation therapy for primary and metastatic liver tumors.
8th Congress of the International Stereotactic Radiosurgery Society, San Francisco (California) USA, 2007.

Stereotactic body radiation therapy for liver tumors: Impact of daily setup corrections and anatomic variations in target and organs at risk.
27th ESTRO Meeting, Goteborg, Sweden, 2008.

Stereotactic body radiation therapy for colorectal liver metastases.
European Colorectal Congress, St Gallen, Switzerland, 2010.

Comparison of macroscopic pathology measurements with magnetic resonance imaging and assessment of microscopic pathology extension for colorectal liver metastases.
52nd ASTRO Meeting, San Diego, California, USA, 2010.